Finite Element Analysis and Passive Vibration Control of the Timoshenko Beam Traversed by a Moving Vehicle Using an Optimized Tuned Mass Damper

Mahsa Moghaddas

A Thesis
in
The Department
of
Mechanical and Industrial Engineering

Presented in Partial Fulfillment of the Requirements
for the Degree of Master of Applied Science at
Concordia University
Montreal, Quebec, Canada.

March 2008

Library and
Archives Canada

Published Heritage
Branch

395 Wellington Street
Ottawa ON K1A 0N4
Canada

Bibliothèque et
Archives Canada

Direction du
Patrimoine de l'édition

395, rue Wellington
Ottawa ON K1A 0N4
Canada

Your file Votre référence
ISBN: 978-0-494-40913-8
Our file Notre référence
ISBN: 978-0-494-40913-8

Abstract

In the present work, the behavior of a combined bridge-vehicle system in which, the bridge is modeled as a Timoshenko beam and the vehicle is considered as a half car model has been investigated using the finite element method. Responses of the beam and the vehicle model have been obtained and then validated with those reported in literature. The limitation of considering the vehicle as a quarter car model and also the effect of taking into account the rotatory inertia and shear deformation i.e. using the Timoshenko beam model has also been investigated.

The finite element formulation of the Timoshenko with the attached Tuned Mass Dampers (TMDs) has been derived. Then the general equation of motion of a Timoshenko beam element with the attached TMDs traversed by a moving half car model has been obtained by the combination of two previously derived finite element equations of motion; for the beam with attached TMDs and the beam under the moving vehicle.

Finally, a design optimization algorithm has been developed in which the derived finite element analysis module has been combined with the optimization procedure. The algorithm is based on the Sequential Programming Technique (SQP), to determine the optimum values of the parameters (frequency and damping ratios) of one TMD, for minimization of the maximum frequency response of the beam midspan under the moving vehicle.

The obtained results show that by adding an optimally tuned mass damper to the system a significant faster damping can be achieved.

Acknowledgements

First of all, I would like to express my appreciation to my supervisors Dr. Ramin Sedaghati and Dr. Ebrahim Esmailzadeh for their precious technical guidance and support in my research. I would also like to extend my gratitude to Dr. Peyman Khosravi for his valuable advice and also his benevolent encouragements during my work.

I am also grateful to Dr. Ahmed and Dr. Haghighat for reviewing my work and attending my examination committee.

I dedicate this thesis to my dear father for his kindness and devotion in all my life and to the memory of my beloved mother.

Table of Contents

Nomenclatures

A	*Cross-sectional area of the beam*
b_1 & b_2	*Distance between the center of gravity of the vehicle body and the contact point of the first and the second tires, respectively*
c	*Damping coefficient of the beam*
c_1 & c_2	*Damping coefficient of the vehicle un*sprung *and sprung masses in quarter car model*
C_1 & C_2	*Damping coefficient of the first and second suspension systems, respectively*
C_{t1} & C_{t2}	*Damping coefficient of the first and second tires of the vehicle, respectively*
C_{p1} & C_{p2}	*Damping coefficient of the driver and the passenger, respectively*
C_{TMD}	*Damping coefficient of TMD*
d_1 & d_2	*Distance between the center of gravity of the vehicle body and the driver and the passenger, respectively*
E	*Beam elastic modulus*
f_g	*Effect of vehicle weight acting on the beam*
f_{TMD}	*Frequency ratio of TMD*
g	*Acceleration due to gravity*
G	*Beam shear modulus*
$H(x)$	*Heaviside function*
I	*Second moment of inertia of the beam*
J	*Rotational mass moment of inertia of the vehicle body*
k_1 & k_2	*Stiffness of the vehicle unsprung mass and sprung mass in the quarter car model*
K_1 & K_2	*Stiffness of the first and second suspension systems of the vehicle, respectively*
K_{t1} & K_{t2}	*Stiffness of the first and second tires of the vehicle, respectively*
K_{p1} & K_{p2}	*Stiffness of the driver and the passenger, respectively*
K_s	*Beam shear coefficient*
K_{TMD}	*Stiffness of TMD*

l	*Beam element length*
L	*Total beam length*
m_s	*Vehicle body mass*
m_{t1} & m_{t2}	*Vehicle first and second wheel mass, respectively*
m_{p1} & m_{p2}	*Driver and passenger mass, respectively*
M_1 & M_2	*Vehicle unsprung mass and sprung mass in the quarter car model*
M	*Beam bending moment*
$Q(t)$	*Vector of variables*
t	*Time*
T	*Total kinetic energy of the system*
$u(t)$	*Position of the center of gravity of the vehicle body*
U	*Total potential energy of the system*
V	*Shear force*
w	*Weighting function*
W_{nc}	*Virtual work of non-conservative forces of the system*
y	*Transversal deflection of the beam*
β & γ	*Newmark's constants*
δ^*	*Dirac delta function*
ξ_1 & ξ_2	*Locations of the contact point of the front and rear tires with the bridge surface, respectively*
ξ_{TMD}	*Damping ratio of TMD*
μ_{TMD}	*Mass ratio of TMD*
υ	*Beam Poisson's ratio*
ρ	*Linear density of the beam*
φ	*Lagrange shape function*
ψ	*Beam rotation*
ω	*Natural frequency of the beam*

List of Figures

List of Tables

Chapter 1: INTRODUCTION

1.1 Motivation and Objectives

In general, transportation infrastructure is a significant factor affecting the development of a national economy. The vibration of a bridge caused by passage of vehicles is one of the most imperative considerations in the design of a bridge as a common sort of transportation structure, and has been a topic of interest for over a century. The problem came up from the observations that as a bridge structure is subjected to moving vehicles and trains, the dynamic transversal deflection as well as the stresses could become considerably greater than those for the static loads. With the great increase in the proportion of heavy and articulated trucks and high-speed vehicles in highway and railway traffic, the study of interaction between vehicles and bridge structures has become extremely important. Large deflections and vibration induced by heavy and high-speed vehicles affect significantly the safety and efficiency of bridges. As a result, vibration control of the bridge is essential to enhance its structural assurance and sturdiness and also increase of passengers' comfort.

While utilization of active vibration suppression techniques in structures is flexible and effective, they are complicated and cost greatly due to large power consumption. Instead, due to low expenditure of passive vibration damping treatments and their simple configuration, they are still widely applied in different sort of structures such as beams. One of the simplest and most economic passive methods to control the vibration of a beam structure is to make use of the tuned mass damper (TMD), which is a single mass

attached to the beam by viscoelastic material or other mechanisms of similar effect, and can be modeled as a simple mass-spring-dashpot system. The natural frequency of TMD is tuned in resonance with the one of the modes of the beam, so that a large amount of the structural vibrating energy is transferred to the TMD and then dissipated by the damping as the primary structure is subjected to external disturbances.

Although extensive research has been conducted to formulate and study the behavior of beams under moving vehicles and control their vibration in this situation, the use of tuned mass dampers in vibration attenuation of these structures has not received appropriate attention. Furthermore, finite element method which is one of the most versatile numerical methods in engineering has not been intensely used in simulation of these types of problems.

In this study, the finite element formulation for the dynamics of a bridge modeled as Timoshenko beam traversed by a half car model moving vehicle with six degrees of freedom is presented. The finite element formulation is then expanded to model the combined bridge-mass damper systems. Finally, optimization technique is utilized to find the appropriate parameters of the tuned mass damper, to minimize the vertical deflection of the bridge traversed by the moving vehicle.

1.2 Overview and Literature Survey (State of the Art)

As the present work includes three main aspects, this section is divided into three parts:

In the first part an overview of the Timoshenko beam model and the finite element analysis of Timoshenko beam are presented.

The second part includes the review of the research done on the beams under moving vehicle. The survey starts from the primary simple models and subsequently, explores more complicated simulations. Moreover, the literature on the finite element analysis of beams under moving vehicles is represented latterly.

The third and last part relates to the review of the vibration suppression of beams by tuned mass dampers. Finally, the research on vibration control of beams under moving vehicles by means of TMDs is presented.

1.2.1 Finite Element Analysis of Timoshenko Beam

There has always been a powerful connection between transportation infrastructure and the growth of economy in a society. Bridges are one of the most essential constructed structures in the field of transportation. Usually bridge structures are modeled in the form of beams. A *beam* is a structural member that resists forces applied laterally or transversely to its axes[1].

It was recognized by the early researchers that the bending effect is the single most important factor in a transversely vibrating beam. The Euler-Bernoulli beam theory, sometimes called the classical beam theory, is the most commonly used theory to formulate the differential equation of motion of a vibrating beam. It is simple to use and provides reasonable engineering approximations for many problems. This theory is based on the assumption that plane cross-sections remain plane and perpendicular to the neutral axis after bending, which implies that all transverse shear strains are zero. The

development of this model dates back to the 18th century and was developed by Jacob Bernoulli, Daniel Bernoulli, and Leonhard Euler[2].

Although this theory is the most straightforward and often used theory, it tends to slightly overestimate the natural frequencies. This problem is exacerbated for the natural frequencies of the higher modes. There were some improvements by presentation of the Rayleigh beam theory[3] by including the effect of rotation of the cross-section and shear model[4,5]which adds shear distortion to the Euler-Bernoulli model. Timoshenko[6] proposed a beam theory which adds the effect of shear as well as the effect of rotation to the Euler-Bernoulli beam. Whilst shear and rotary inertia lead to small corrections to the Euler-Bernoulli theory for the lowest modes of long, thin beams, significant errors may occur if they are not taken into account for thick beams or for the higher modes of any beam.

Sutherland and Goodman[7,8] as well as Huang[8,9] presented the solution of Timoshenko equations for a cantilever beam of rectangular cross section. Several methods of solution have been applied to this problem. Anderson[10] and Dolph[11] provided a general solution and complete analysis of a simply supported uniform beam. Ritz and Galerkin methods were used by Huang[12] to obtain the frequency and normal mode equations for flexural vibrations for common types of simple, finite beams.

A significant number of Timoshenko beam finite elements for use in vibration problems have been proposed. They differ from each other in the preference of interpolation functions applied for the transverse deflection and rotation, or in the weak form utilized to form the finite element model. In an investigative review of many of the uniform straight beam elements[13] it was shown that the elements could be categorized as

a simple, having two degrees of freedom at each two nodes, or complex, with additional degrees of freedom. Furthermore, It was concluded that the simple element[14,15,16] is the most suitable for general purpose use. Despite its good performance, a complex element[17,18,19,20]can perform better if selected properly. On the other hand, choosing an incorrect complex element may result in poorer accuracy than using the simple element. Also, additional degrees of freedom can induce complications for the user in application in intricate situations[21]. In this study the simple elements were used in simulation of the beam.

However, a problem can arise in using the linear interpolation function for both deflection and rotation in Timoshenko beam finite element: If constant strain is assumed, the numerical solution based on the exact integration exhibits *shear locking*[22,23]. Distinctively, this numerical scheme predicts the incorrect result that the beam becomes infinitely stiff as its thickness reduces to zero. In other words, in the thin beam element limit, i.e. as the length-to-thickness ratio becomes large (about 100), the numerical model severely overestimates the stiffness of the beam. This problem has been studied extensively.

Using the *reduced integration*[24] is the primitive and most prevalent method of overcoming shear locking. This has been justified by taking into account the number of constraints imposed by the integration scheme and showing that under reduced integration, unlike when using full integration, the number of imposed constraints is less than the number of degrees of freedom[25]. Another justification argues that the shear part of the stiffness matrix should be singular for a thin beam, and then shows that this is the

case when using reduced integration[26] . In this study, the reduced integration element is used for the structural finite element analysis.

Aside from reduced integration, other solutions for shear locking have been proposed such as using the mode decomposition or projection technique[27], changing the shear correction factor for thin beams[28], or using B-Spline approximation[29] . The other common approach is using a consistent interpolation for the deflection and rotation so that the degree of the polynomial representing the rotation is one less than the degree of the deflection-polynomial[23]. In this way locking simply does not happen.

1.2.2 Beam under Moving Vehicle

The dynamic behavior of beam structures under moving loads or masses has been an area of interest for more than a century. Attentiveness to this problem initiated in civil engineering for the design of bridges and railway tracks, and in mechanical engineering, for machining processes and also trolleys of overhead cranes moving on their girders. It was observed that as vehicles or trains move on a bridge structure, the dynamic transversal deflection as well as the stresses in the bridge could become notably greater than those for the static loads, and this drew more consideration on the topic.

Vehicle-Bridge interaction is an intricate dynamic phenomenon depending on many parameters, such as the type of the bridge and its natural frequencies of vibration, vehicle weight and velocity, number of vehicles on the bridge, the damping characteristics of vehicle and the bridge, etc. The research on this issue can be classified into three main models of simulation:

In early studies *a constant moving load model* was used in which the inertia of the vehicle was neglected, and the interaction between the vehicle and the bridge was ignored.

Where the inertia of the vehicle can not be considered negligible, *a moving-mass model* can be adopted instead, which takes into account the inertia of the vehicle. However this model suffers from inability to consider the bouncing effect of the moving mass.

In the last group of models, which are more inclusive, the vehicle is modeled as a *series of mass-spring-damper dynamic system*, providing detailed consideration of the vehicle-bridge dynamic interaction.[30]In this section a literature review on each of these simulation models is presented.

Two early remarkable studies on bridge vibrations induced by moving load belong to Stokes[31] who investigated a pulsating load passing over a beam, and Willis[32] who published a report discussing the reasons for the collapse of the Chester Railway Bridge. Willis was the first who formulated the equations of motion for a railway bridge vibration problem. Timoshenko[33] examined a simply supported beam under a constant moving force using eigenfunctions. He later extended the problem with moving harmonic force.[34]An inclusive clarification of the problem of the dynamic response of a prismatic bar under a constant magnitude load moving with a constant velocity was revealed by Krylov[35]. Inglis[36] presented a comprehensive exposition on the dynamic response of railway bridges traversed by locomotives, using harmonic analysis.

In the case of vehicle-bridge interaction, the modeling ideas started from a single lumped load, moving along a beam at constant speed which were initiated by Frýba[37] and Timoshenko *et al.* [38] who solved the case of a constant velocity concentrated force moving along a beam, neglecting damping forces, and presented an expression for the critical velocity. The same problem was investigated analytically by Warburton[39]. The models used in these studies generally obey the Euler-Bernoulli beam theory. On the other hand several studies have been done concerning Timoshenko beam under moving load. Crandall[40] solved the steady-state response of the Timoshenko beam on an elastic foundation subjected to a moving concentrated load. Florence[41] obtained the short time transit behavior for a semi-infinite Timoshenko beam under a concentrated moving force by Laplace transform method. Steele[42] found the steady-state solution for a semi-infinite Timoshenko beam of an elastic foundation with a step load moving at a constant velocity. Huang[43] solved the problem of moving load on an infinitely long viscoelastic Timoshenko beam with an elastic foundation using the Fourier transform technique, and Mackertich[44] presented an expression for the deflection of a simply supported Timoshenko beam under a traveling concentrated load.

Jeffcott[45] was the first to consider the inertia effect of the vehicle and dealt with the problem of a beam carrying moving masses. Bolotin[46] studied the "moving-force moving-mass" problem for a simply supported beam using Galerkin's variational method, and he considered just the first term of the series. Stanišić and Hardin[47] presented a theory for a simply supported beam carrying arbitrary number of moving masses, based on Fourier technique. Leach and Tabarrok[48] concerned the behavior of a Timoshenko

beam under a moving concentrated mass for different boundary conditions. Using series solutions implicating the Green function, Sadiku and Leipholz[49] compared the solutions for both the "moving-force moving-mass" and the corresponding "moving force" problems and presented an iterative solution process converging to a unique continuous function of space and time. Akin and Mofid[50] presented an analytical–numerical method for verification of the dynamic response of Euler-Bernoulli beams under a moving mass with different boundary conditions. Esmailzadeh and Ghorashi[51] investigated the behavior of an Euler-Bernoulli beam carrying either uniform partially distributed moving masses or forces and evaluated the critical speeds considering the deflection of the midspan of the beam. They later further developed the scope of their study by analyzing the response of the Timoshenko beam traversed by uniform partially distributed moving mass using finite difference based algorithm.[52]

With the considerable growth in the number of heavy and articulated trucks and high-speed vehicle in highway and railway passage, more investigations has been focused on the dynamic interaction between vehicles and bridge structures during the last 60 years. The vehicle models have become more and more complicated which considered the elastic forces in the vehicle model as well as the inertia effect. Wen[53] presented the solution of the problem of a two-axle moving load on a beam by assuming the bridge as a beam of uniform mass and the vehicle as a sprung mass with two axles. Sundara and Jagadish[54] idealize the bridge as an orthotropic plate carrying sprung mass vehicle model. Frýba[37] formulated in his monograph the differential equations of motion of moving one-axle mass- spring-damper vehicle, two-axle mass-spring-damper vehicle, multi-axle

mass-spring-damper vehicle and beam by utilizing the d'Alembert's principle. Hwang *et al.*[55] increased the number of vehicle's degrees of freedom and analyzed the dynamic loads in bridges. Yang *et al* [56] performed a parametric study for various simple and continuous beams traversed by five-axle trucks. Henchi *et al.*[57] proposed a 3D vehicle model for the simulation of the interaction between the bridge and vehicles. Esmailzadeh and Jalili[58] have investigated the dynamics of the vehicle-structure interaction of a bridge traversed by moving vehicles taking into account the passenger dynamics for a more realistic simulation. The vehicle, containing the driver and the passenger, was modeled as a mobile half planer model traveling on a wide span uniform bridge modeled in the form of a simply supported Euler-Bernoulli beam. The response of the beam and the vehicles were studied by modal expansion (Galerkin approximation).

From 1970s, with the expansion of computer technology and the innovation of analysis theory, discrete methods, especially the finite element method, were introduced in structural analysis and became a strong and principal technique for investigation of the bridge dynamics. Thus, it is proper to take a look at the research on the finite element analysis of beams under the moving load or vehicle.

Yoshida and Weaver[59] applied the finite element method to study the problem of Euler-Bernoulli beam carrying moving loads. After that many researchers[60,61,62,63,64] applied this technique to study the dynamic response of a bridge structure under moving loads or vehicles. Lin and Trethewey[65]presented finite element formulation for beams under the arbitrary movement of a spring-mass-damper system. Frýba et al.[66] presented a

stochastic finite element analysis for a beam resting on an elastic foundation, traversed by a constant force moving with constant velocity.

Yang and Lin[67] developed a procedure for the finite element simulation of dynamic response of vehicle-bridge systems using dynamic condensation method. They defined an interaction element consisted of a bridge element and the suspension units of vehicle placed on the element and then using the dynamic condensation method they eliminated all the degrees of freedom correlated with the vehicle bodies. The method was suitable for simulation of bridges with series of vehicle moving at different speeds and/or different directions. However, because of the approximation made in relating the vehicle to the bridge DOFs, this methodology was not capable of computing the vehicle response. This drawback was prevailed by Yang and Yau[68] through the discretization of equations of motion of the vehicle by Newmark's time integration scheme and then condensing them to the bridge elements in contact. In other words, they solved the contact forces in terms of the wheel displacements and then related them to the bridge displacement at contact points. Later, Yang *et al.*[69] extended the previous work by consideration the vehicle's pitching effect via modeling the vehicle as a rigid beam supported by two spring-damper units. Cheng *et al*[70]studied the vibration problem of railway bridges under a moving train using finite element method. They took into consideration the elastic characteristics and the damping properties of track structures, and suggested a new element identified as the bridge-track-vehicle element, which consists of vehicles modeled as mass-spring-damper systems, an upper beam element to model the rails and a lower beam element to model the bridge deck. However, the

element did not consider the pitching effect on the vehicle front and rear wheel. Koh *et al.*[71] described a group of finite elements for dynamic analysis of a train–track system, formulated in a relative co-ordinate system attached to the moving load or vehicle, instead of the fixed co-ordinate system. Hou *et al.*[72] presented a finite element model to simulate an asymmetrical vehicle–track dynamic system. Young and Li[73] investigated the vertical vibration of a vehicle moving on an imperfect track system utilizing the finite element technique. In their study, the car body and sleepers are modeled as Timoshenko beams with finite length and the rail is assumed as an infinite Timoshenko beam with discrete supports in which imperfection of the track system comes from a sleeper lost partial support by the ballast. Lou and Zeng[74] presented an approach for formulating the equations of motion for the vehicle–track–bridge interaction system using the principle of a stationary value of total potential energy of dynamic system, in which the contact forces are considered as internal forces. All the relevant equations were derived for two cases involving different levels of complexity for the vehicle–track–bridge interaction system. They later proposed a finite element-based vehicle–track coupling element for analyzing the vertical dynamic response of the railway track under a moving train, derived by the energy method.[75]Ju *et al.*[76] developed a finite element method combining the moving wheel element, spring-damper element, lumped mass and rigid link effect to simulate complicated vehicles. They validated their model with the solution proposed by Frýba[37] for a simply supported beam under a moving two-axle system through different numerical examples and concluded that the model is accurate.

1.2.3 Vibration Suppression of the Beams Using Tuned Mass Dampers

An efficient method to inaugurate supplementary damping into structures and machinery is via a combined mass-damper system that is tuned to one of the modes of the beam in resonance. This system is called a Tuned Mass Damper (TMD). The resonance generates a relative motion of the damped mass that is enough to enable the damper to extract the necessary vibrating energy from the primary structure.

The idea of reducing dynamic motion by means of a resonating mass is due to Frahm[77] who proposed the use of spring-mass system. The system proposed was without a damper, and it was proposed to just balance the external load exclusive of absorbing energy. Den Hartog and Ormondroyd[78] showed that the introduction of the damper not only dissipated energy, but also increased the frequency interval over which the device is active. Brock[79] proposed a more pragmatic argument for selecting the damping level of the tune mass damper. Den Hartog[80] first proposed an optimal design theory for the TMD for an undamped single-degree-of-freedom structure. Some years earlier, Young[81] investigated the prospect of utilizing TMDs for the continuous systems such as beams. Neubert[82] and Snowdon[83] employed two TMDs to suppress the first two resonances of a bar and a beam. Jacquot[84] developed a technique that gives the optimal dynamic vibration absorber parameters for the elimination of the excessive vibration in sinusoidal forced Euler-Bernoulli beams. The methodology was based on the use of the optimum TMD parameters for an equivalent single-degree-of –freedom system to determine the ones for the beam. Candir and Ozguven[85] determined the optimum parameters of an absorber tuned in the first and second resonance of a cantilever beam. Esmailzadeh and

Jalili[86] studied the design procedure of the optimum vibration absorbers for a damped Timoshenko beam subjected to the distributed harmonic force excitation. They decoupled the differential equations of motions of the Timoshenko beam, and solved each equation, corresponding to one mode, as a single degree of freedom system with one TMD. The method provided flexibility of choosing number of TMDs upon the number of modes to be suppressed. Younesian, Esmailzadeh and Sedaghati[87] used a similar decoupling method to suppress the vibration in a Timoshenko beam subjected to random excitation by evaluating the optimum values of the TMD system.

In 1989, Kajikawa *et al.*[88] utilized a single TMD on highway bridges and concluded that this passive control device was not capable of complete suppression of the traffic induced vibrations since the dynamic responses of a bridge are frequency variant due to the vehicle motion. Later, Kwon *et al.* [89] investigated the vibration control of a high-speed railway continuous bridge modeled as an Euler Bernoulli beam under a simple moving load at constant speed using a single TMD. The parameters of the TMD used in their research were based on Den Hartog[80] scheme. The TMD was tuned to the first dominant vertical mode and was installed in the middle of the beam. The numerical results showed the decrease of about 21% of the vertical free displacement response by using a TMD with mass ratio of 1%. Chen *et al.*[90] analyzed a Timoshenko beam system with TMDs under moving load excitation. A simplified two-degrees-of-freedom system based on the first mode of the Timoshenko beam is used for the design of TMDs. The modal expansion method was used for the beam and some design formulas were derived for identical TMDs for vibration control.

Wang *et al.*[91] studied the applicability of tuned mass dampers in suppression of train-induced vibration on bridge. A railway bridge was modeled as an Euler Bernoulli beam and the train was simulated as series of moving forces, moving masses or moving suspension masses with constant speed to investigate the effect of different vehicle models on the bridge attribute with or without TMD. The modal superposition was used in modeling the beam and the numerical results for a moderate long bridge showed the good performance of TMD in suppression of the vertical displacement and acceleration at the beam midspan, the right end rotation of the beam and also the vertical acceleration of the train. They later studied the applicability of multiple tuned mass dampers (MTMDs) to suppress train-induced vibration on bridges.[92] It was concluded from the numerical results that for a high-speed railway train passing over a bridge with constant speed, its induced excitation frequency content has a narrow bandwidth and could be far away from the bridge's natural frequencies. Thus, an MTMD has good control efficiency only when the train travels at resonant speeds.

1.3 Present Work

As it can be realized, although some research works have been performed on the vibration suppression of Timoshenko beam subjected to a moving vehicle, not much study has been conducted on the use of tuned mass dampers in vibration suppression of these structures. Besides, in most previous works, the continuous beams (representing bridge type structures) were simplified as equivalent single degree of freedom systems and optimal TMD parameters were found based on these equivalent systems. Moreover, not much research has been focused on finite element analysis of a Timoshenko beam

under a moving vehicle with several degrees of freedom with the attached TMDs. Considering this, the main objective of this study is twofold:

1. To develop an efficient finite element model for a Timoshenko beam under a half car model with six degrees of freedom with and without attached TMDs.

2. To develop a design optimization methodology in which the developed finite element model is combined with the formal gradient based optimization technique to evaluate the optimal parameters of the TMD to efficiently suppress the vibration of the beam traversed by moving vehicle.

1.4 Thesis Organization

The present thesis contains five chapters. In the first chapter, an introduction explaining the general goals and important description along with literature survey are presented.

The second chapter presents in detail the finite element formulation of a simply supported Timoshenko beam subjected to a half car model with six degrees of freedom. For the sake of comparison, the formulation of the Timoshenko beam element under a quarter car model with two degrees of freedom is obtained as well. The results based on this method are verified with the results in the literature through a numerical example.

In the third chapter the previous formulation is extended for the situation that one or several TMDs are attached to the beam element.

The optimization of the TMD parameters using the powerful Sequential Programming techniques implemented in MATLAB© environment is the main core of the chapter four. First, the design optimization problem is described and then the vibration of the beam

structure is controlled by minimizing the maximum vertical deflection of the beam as the objective function where the appropriate TMD parameters are found as the optimal design variables.

Finally, chapter five concludes with most important findings and contributions of the present research work and some recommendations are presented for future studies.

Chapter 2: FINITE ELEMENT FORMULATION OF A TIMOSHENKO BEAM TRAVERSED BY A MOVING VEHICLE

2.1 Introduction

In this chapter the finite element formulation of a bridge modeled as simply supported Timoshenko beam traversed by a moving vehicle modeled as the quarter car model and also the half car planner model is presented. First, the governing differential equations of motion for the coupled beam-vehicle system are derived using Hamilton's principle. Then using Galerkin and weak formulation, the governing equations are cast into the finite element form. The mathematical and finite element formulations have been done on both beam-half car model and beam-quarter car model. In the finite Element modeling of the beam, linear beam elements with two degrees of freedom at each node were utilized to model the beam. The entire equations of motion for the system can be obtained by assembling the matrices of all conventional beam elements and the beam element with the moving vehicle on it. The governing finite element equations are solved by direct integration technique using powerful Newmark's method [93,94] to obtain the dynamic response of the Timoshenko beam and the vehicle components. Results are validated through a verification example.

2.2 Equations of Motion for Timoshenko Beam-Half Car Model System

Figure 2-1 shows the suspension system of a 6-degree of freedom half car model moving on a bridge. It is assumed that the vehicle moves with the constant velocity $\dot{u}(t)$, where $u(t)$ is the location of the center of gravity (c.g.) of the vehicle body measured from the left end support of the bridge, and both the front and rear tires remain in contact with the bridge surface constantly.

The vehicle is modeled as a 6 DOF system which consists of a body (sprung mass), two axles (unsprung masses), driver and a passenger. Each of the masses has only vertical oscillation except the body that is considered to have the angular motion (pitch) in addition.

The compliance of the suspension system, the tires and the passenger seats are modeled by combination of linear springs and viscous dampers connected in parallel configurations. The bridge is contemplated initially free of any load or deflection and therefore at the equilibrium under its own weight. The steady state displacements of the vehicle are also measured from their static equilibrium position.

In order to generate the governing equations of motion of the coupled system of beam-half car model, the Hamilton's principle[95] is applied:

$$\int_{t_i}^{t_{ii}} \delta(T-U)dt + \int_{t_i}^{t_{ii}} \delta W_{nc} dt = 0 \tag{2.1}$$

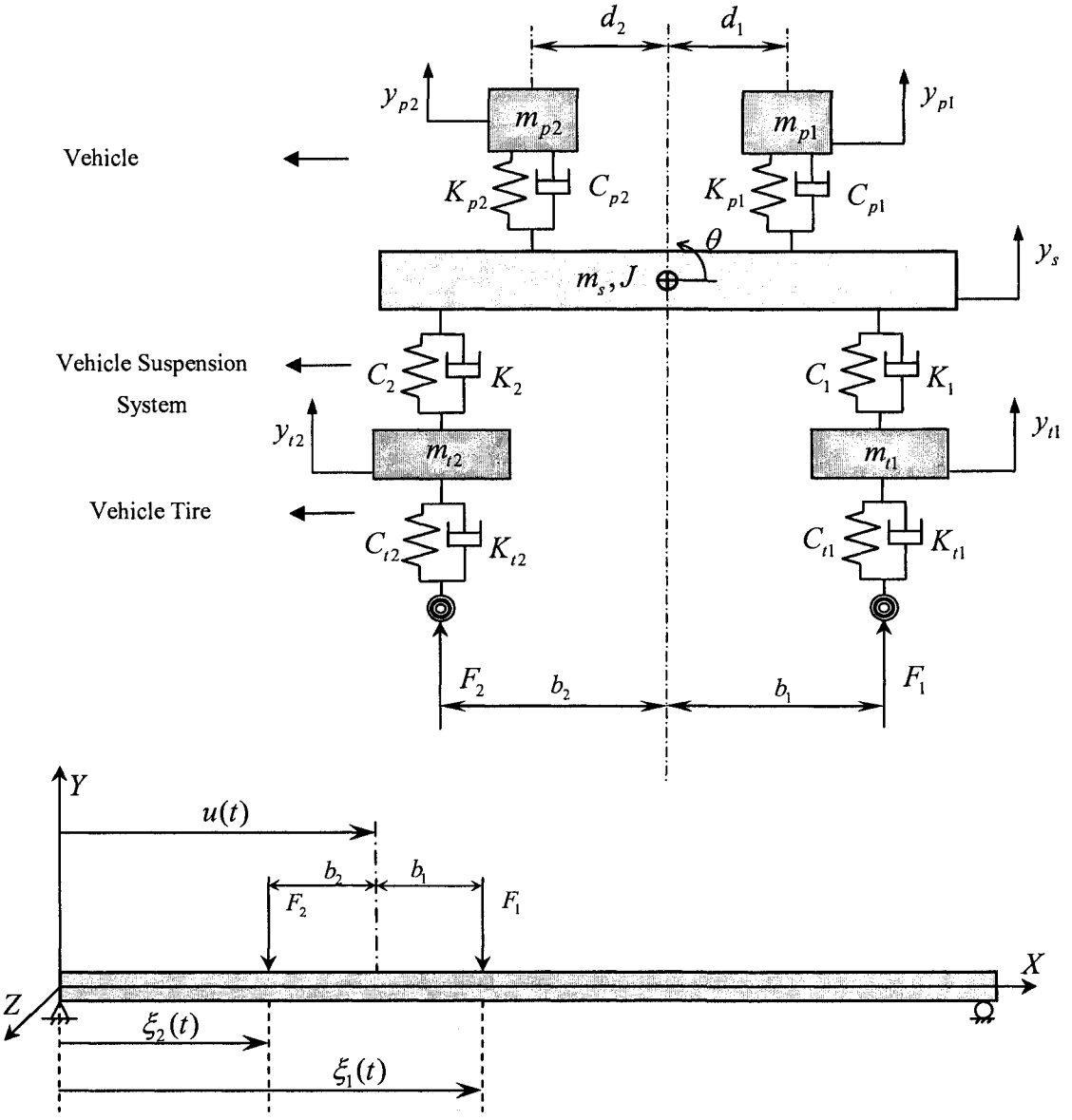

Figure 2-1 Suspension System of a 6 D.O.F Half Car Model Moving on a Bridge

Where δT is the virtual total kinetic energy, δU is the virtual potential energy and δW_{nc} is the virtual work of non-conservative forces of the system in the interval between $t = t_i$ and $t = t_{ii}$.

The total kinetic energy of the system can be defined as:

$$T = \frac{1}{2}\{\int_0^L \rho \dot{y}^2(x,t)dx + \int_0^L \rho I(x)\dot{\psi}^2(x,t)dx + m_s\dot{y}_s^2(t) + J\dot{\theta}^2(t) + m_{p1}\dot{y}_{p1}^2(t) + m_{p2}\dot{y}_{p2}^2(t) + m_{t1}\dot{y}_{t1}^2(t) + m_{t2}\dot{y}_{t2}^2(t)\} \tag{2.2}$$

Thus the virtual kinetic energy of the system can be described as:

$$\delta T = \int_0^L \rho \dot{y}(x,t)\frac{\partial \delta y}{\partial t}dx + \int_0^L \rho I(x)\dot{\psi}(x,t)\frac{\partial \delta \psi}{\partial t}dx + m_s\dot{y}(t)\frac{d\delta y_s}{dt} + J\dot{\theta}(t)\frac{d\delta\theta}{dt} + m_{p1}\dot{y}_{p1}(t)\frac{d\delta y_{p1}}{dt} + m_{p2}\dot{y}_{p2}(t)\frac{d\delta y_{p2}}{dt} + m_{t1}\dot{y}_{t1}(t)\frac{d\delta y_{t1}}{dt} + m_{t2}\dot{y}_{t2}(t)\frac{d\delta y_{t2}}{dt} \tag{2.3}$$

Consequently,

$$\int_{t_i}^{t_{ii}} \delta T dt = -\int_{t_i}^{t_{ii}} \{\int_0^L \rho \ddot{y}(x,t)dx\delta y + \int_0^L \rho I\ddot{\psi}(x,t)dx\delta\psi + m_s\ddot{y}_s\delta y_s + J\ddot{\theta}\delta\theta + m_{p1}\ddot{y}_{p1}\delta y_{p1} + m_{p2}\ddot{y}_{p2}\delta y_{p2} + m_{t1}\ddot{y}_{t1}\delta y_t + m_{t2}\ddot{y}_{t2}\delta y_{t2}\}dt \tag{2.4}$$

The total potential energy of the system can be written as:

$$U = \frac{1}{2}\{\int_0^L EI\left(\frac{\partial \psi}{\delta x}\right)^2 dx + \int_0^L k_s AG\left(\frac{\partial y}{\partial x} + \psi\right)^2 dx + K_{p1}\left[y_s + d_1\theta - y_{p1}\right]^2 + K_{p2}\left[y_s - d_2\theta - y_{p2}\right]^2 + K_1\left[y_s + b_1\theta - y_{t1}\right]^2 + K_2\left[y_s - b_2\theta - y_{t2}\right]^2 + K_{t1}\left[y_{t1} - y(\xi_1,t)\right]^2 H(x-\xi_1) + K_{t2}\left[y_{t2} - y(\xi_2,t)\right]^2 H(x-\xi_2)\} \tag{2.5}$$

where EI represents the flexural rigidity of the beam, and $H(x)$ is the Heaviside function. The locations of the contact point of the front and rear tires with the bridge surface are given by the expressions:

$$\xi_1(t) = u(t) + b_1$$
$$\xi_2(t) = u(t) - b_2 \tag{2.6}$$

It should be noted that the axial strain energy, which contains only the terms of higher order than quadratic in the elastic variables y and ψ has not been included in the potential energy for the consistency of the formulation.

The virtual potential energy of the system can be represented as:

$$\delta U = \int_0^L EI \frac{\partial \psi}{\partial x}\frac{\partial \delta\psi}{\partial x}dx + \int_0^L k_s AG\psi\delta\psi dx + \int_0^L k_s AG\frac{\partial y}{\partial x}\delta\psi dx + \int_0^L k_s AG\frac{\partial \delta y}{\partial x}\psi dx +$$
$$\int_0^L k_s AG\frac{\partial y}{\partial x}\frac{\partial \delta y}{\partial x}dx + K_{p1}S_1\delta S_1 + K_{p2}S_2\delta S_2 + K_1S_3\delta S_3 + K_2S_4\delta S_4 + K_{t1}S_5\delta S_5 H(x-\xi_1) + \tag{2.7}$$
$$K_{t2}S_6\delta S_6 H(x-\xi_2)$$

where

$$\begin{aligned} S_1 &= y_s + d_1\theta - y_{p1} \\ S_2 &= y_s - d_2\theta - y_{p2} \\ S_3 &= y_s + b_1\theta - y_{t1} \\ S_4 &= y_s - b_2\theta - y_{t2} \\ S_5 &= y_{t1} - y(\xi_1, t) \\ S_6 &= y_{t2} - y(\xi_2, t) \end{aligned} \tag{2.8}$$

Therefore,

$$\int_{t_i}^{t_{ii}} \delta U dt = \int_{t_i}^{t_{ii}} \{ \left(\int_0^L -EI\frac{\partial^2\psi}{\partial x^2}dx + \int_0^L k_s AG\left(\psi + \frac{\partial y}{\partial x}\right)dx \right)\delta\psi - \left(\int_0^L k_s AG\left(\frac{\partial^2 y}{\partial x^2} + \frac{\partial \psi}{\partial x}\right)dx \right)\delta y$$
$$+K_{p1}S_1\delta y_s + K_{p1}d_1S_1\delta\theta - K_{p1}S_1\delta y_{p1} + K_{p2}S_2\delta y_s - K_{p2}d_2S_2\delta\theta + K_{p2}S_2\delta y_{p2} + K_1S_3\delta y_s + \tag{2.9}$$
$$+K_1b_1S_3\delta\theta - K_1S_3\delta y_{t1} + K_2S_4\delta y_s - K_2b_2S_4\delta\theta - K_2S_4\delta y_{t2} + K_{t1}S_5\delta y_{t1}H(x-\xi_1) +$$
$$K_{t1}S_5\delta y(\xi_1,t)H(x-\xi_1) + K_{t2}S_6\delta y_{t2}H(x-\xi_2) + K_{t2}S_6\delta y(\xi_2,t)H(x-\xi_2)\}dt$$

The non-conservative virtual work of the system can be written as:

$$\int_{t_i}^{t_{ii}} \delta W_{nc} dt = \int_{t_i}^{t_{ii}} \{ - \int_0^L c\dot{y}(x,t) dx \delta y - C_{p1}\dot{S}_1 \delta S_1 - C_{p2}\dot{S}_2 \delta S_2 - C_1 \dot{S}_3 \delta S_3 - C_2 \dot{S}_4 \delta S_4 - C_{t1}\dot{S}_5 \delta S_5 H(x-\xi_1) - C_{t2}\dot{S}_6 \delta S_6 H(x-\xi_2) + \int_0^L f_g(x,t) dx \delta y \} dt \tag{2.10}$$

in which,

$$\begin{aligned} f_g(x,t) = & -\left(m_{t1} + m_s \frac{b_2}{b_1+b_2} + m_{p1} \frac{b_2+d_1}{b_1+b_2} + m_{p2} \frac{b_2-d_2}{b_1+b_2} \right) gH(x-\xi_1(t)) \\ & -\left(m_{t2} + m_s \frac{b_1}{b_1+b_2} + m_{p1} \frac{b_1-d_1}{b_1+b_2} + m_{p2} \frac{b_1+d_2}{b_1+b_2} \right) gH(x-\xi_2(t)) \\ & = -(f_{g1} H(x-\xi_1(t)) + f_{g2} H(x-\xi_2(t))) \end{aligned} \tag{2.11}$$

is the vehicle weight acting on the bridge.

Now, substituting Eqs. (2.4), (2.9) and (2.10) into Eq. (2.1) yields:

$$\begin{aligned} 0 = & \int_{t_i}^{t_{ii}} \{ - \int_0^L \rho \ddot{y}(x,t) dx \delta y - \int_0^L \rho I \ddot{\psi}(x,t) dx \, \delta\psi - m_s \ddot{y}_s \delta y_s - J\ddot{\theta}\delta\theta - m_{p1}\ddot{y}_{p1}\delta y_{p1} - \\ & m_{p2}\ddot{y}_{p2}\delta y_{p2} - m_{t1}\ddot{y}_{t1}\delta y_t - m_{t2}\ddot{y}_{t2}\delta y_{t2} + \left(\int_0^L EI \frac{\partial^2 \psi}{\partial x^2} dx - \int_0^L k_s AG \left(\psi + \frac{\partial y}{\partial x} \right) dx \right) \delta\psi + \\ & \left(\int_0^L k_s AG \left(\frac{\partial^2 y}{\partial x^2} + \frac{\partial \psi}{\partial x} \right) dx \right) \delta y - K_{p1} S_1 \delta y_s - K_{p1} d_1 S_1 \delta\theta + K_{p1} S_1 \delta y_{p1} - K_{p2} S_2 \delta y_s + \\ & K_{p2} d_2 S_2 \delta\theta + K_2 S_4 \delta y_{t2} + K_1 S_3 \delta y_{t1} - K_1 b_1 S_3 \delta\theta - K_{t1} S_5 \delta y_{t1} H(x-\xi_1) \\ & K_{p2} S_2 \delta y_{p2} - K_1 S_3 \delta y_s - K_2 S_4 \delta y_s + K_2 b_2 S_4 \delta\theta - K_{t2} S_6 \delta y_{t2} H(x-\xi_2) \\ & K_{t1} S_5 \delta y(\xi_1,t) H(x-\xi_1) - K_{t2} S_6 \delta y(\xi_2,t) H(x-\xi_2) - \int_0^L c\dot{y}(x,t) dx \delta y \\ & - C_{p1}\dot{S}_1 \delta S_1 - C_{p2}\dot{S}_2 \delta S_2 - C_1 \dot{S}_3 \delta S_3 - C_2 \dot{S}_4 \delta S_4 - C_{t1}\dot{S}_5 \delta S_5 H(x-\xi_1) \\ & - C_{t2}\dot{S}_6 \delta S_6 H(x-\xi_2) + \int_0^L f_g(x,t) dx \delta y \} dt \end{aligned} \tag{2.12}$$

As $\delta y, \delta\psi, \delta y_s, \delta\theta, \delta y_{p1}, \delta y_{p2}, \delta y_{t1}$ and δy_{t2} are arbitrary virtual variations, their coefficient should be set to zero in order to satisfy Eq. (2.12). This will subsequently leads up to governing equations of motions. The passenger-vehicle model is governed by

six coupled linear second order differential equations of motion, which can be derived in the general form. The equation of the vertical motion (bounce) for the sprung mass (vehicle body) can be written as:

$$\begin{aligned} & m_s\ddot{y}_s(t)+C_1\left[\dot{y}_s(t)+b_1\dot{\theta}(t)-\dot{y}_{t1}(t)\right]+C_{p1}\left[\dot{y}_s(t)+d_1\dot{\theta}(t)-\dot{y}_{p1}(t)\right] \\ & \quad +C_2\left[\dot{y}_s(t)-b_2\dot{\theta}(t)-\dot{y}_{t2}(t)\right]+C_{p2}\left[\dot{y}_s(t)-d_2\dot{\theta}(t)-\dot{y}_{p2}(t)\right] \\ & \quad +K_1\left[y_s(t)+b_1\theta(t)-y_{t1}(t)\right]+K_{p1}\left[y_s(t)+d_1\theta(t)-y_{p1}(t)\right] \\ & \quad +K_2\left[y_s(t)-b_2\theta(t)-y_{t2}(t)\right]+K_{p2}\left[y_s(t)-d_2\theta(t)-y_{p2}(t)\right]=0 \end{aligned} \tag{2.13}$$

The equation of the angular motion (pitch) of the sprung mass has the form of:

$$\begin{aligned} & J\ddot{\theta}(t)+C_1b_1\left[\dot{y}_s(t)+b_1\dot{\theta}(t)-\dot{y}_{t1}(t)\right]+C_{p1}d_1\left[\dot{y}_s(t)+d_1\dot{\theta}(t)-\dot{y}_{p1}(t)\right] \\ & \quad -C_2b_2\left[\dot{y}_s(t)-b_2\dot{\theta}(t)-\dot{y}_{t2}(t)\right]-C_{p2}d_2\left[\dot{y}_s(t)-d_2\dot{\theta}(t)-\dot{y}_{p2}(t)\right] \\ & \quad +K_1b_1\left[y_s(t)+b_1\dot{\theta}(t)-\dot{y}_{t1}(t)\right]+K_{p1}d_1\left[y_s(t)+d_1\theta(t)-y_{p1}(t)\right] \\ & \quad +K_2b_2\left[y_s(t)-b_2\theta(t)-y_{t2}(t)\right]+K_{p2}d_2\left[y_s(t)-d_2\theta(t)-y_{p2}(t)\right]=0 \end{aligned} \tag{2.14}$$

The equation of the vertical motion (bounce) of the driver is described as:

$$m_{p1}\ddot{y}_{p1}(t)+C_{p1}\left[\dot{y}_{p1}(t)-\dot{y}_s(t)-d_1\dot{\theta}(t)\right]+K_{p1}\left[y_{p1}(t)-y_s(t)-d_1\theta(t)\right]=0 \tag{2.15}$$

whereas the vertical motion (bounce) of the passenger is governed by:

$$m_{p2}\ddot{y}_{p2}(t)+C_{p2}\left[\dot{y}_{p2}(t)-\dot{y}_s(t)+d_2\dot{\theta}(t)\right]+K_{p2}\left[y_{p2}(t)-y_s(t)+d_2\theta(t)\right]=0 \tag{2.16}$$

The equation of the vertical motion (bounce) for the front axle is:

$$\begin{aligned} & m_{t1}\ddot{y}_{t1}(t)+C_1\left[\dot{y}_{t1}(t)-\dot{y}_s(t)-b_1\dot{\theta}(t)\right]+C_{t1}\left[\dot{y}_{t1}(t)-\dot{y}(\xi_1(t),t)\right]H(\xi_1(t)-x) \\ & \quad +K_1\left[y_{t1}(t)-y_s(t)-b_1\theta(t)\right]+K_{t1}\left[y_{t1}(t)-y(\xi_1(t),t)\right]H(\xi_1(t)-x)=0 \end{aligned} \tag{2.17}$$

and the vertical motion (bounce) of the rear axle is governed by

$$\begin{aligned} & m_{t2}\ddot{y}_{t2}(t)+C_2\left[\dot{y}_{t2}(t)-\dot{y}_s(t)+b_2\dot{\theta}(t)\right]+C_{t2}\left[\dot{y}_{t2}(t)-\dot{y}(\xi_2(t),t)\right]H(\xi_2(t)-x) \\ & \quad +K_2\left[y_{t2}(t)-y_s(t)+b_2\theta(t)\right]+K_{t2}\left[y_{t2}(t)-y(\xi_2(t),t)\right]H(\xi_2(t)-x)=0 \end{aligned} \tag{2.18}$$

The dynamics of the bridge is described by two coupled equations. The first equation governs the traversed deflection of the beam(y) as:

$$\int_0^L \rho\ddot{y}(x,t)dx - \left(\int_0^L k_s AG\left(\frac{\partial^2 y}{\partial x^2} + \frac{\partial \psi}{\partial x}\right)dx \right) + \int_0^L K_{t1}(y_{t1} - y(\xi_1,t))\delta^*(x-\xi_1)\,dx$$
$$+ \int_0^L K_{t2}(y_{t2} - y(\xi_2,t))\delta^*(x-\xi_2)\,dx + \int_0^L C_{t1}(\dot{y}_{t1} - \dot{y}(\xi_1,t))\delta^*(x-\xi_1)\,dx \qquad (2.19)$$
$$+ \int_0^L C_{t2}(\dot{y}_{t2} - \dot{y}(\xi_2,t))\delta^*(x-\xi_2)\,dx + \int_0^L c\dot{y}(x,t)dx - \int_0^L f_g(x,t)dx = 0$$

and the second equation describes the orientation of the beam cross-section (ψ) around z axis as:

$$\int_0^L \rho I\ddot{\psi}(x,t)dx - \int_0^L EI\frac{\partial^2 \psi}{\partial x^2}dx + \int_0^L k_s AG\left(\psi + \frac{\partial y}{\partial x}\right)dx = 0 \qquad (2.20)$$

2.3 Finite Element Formulation for the Timoshenko Beam-Half Car Model System

In this section the finite element formulation is developed using the Galerkin weak formulation for the coupled beam-vehicle system in which the vehicle is modeled as the half car model.

The weak form is first applied to Eqs. (2-19) and (2-20) for a beam element with length l. Multiplying Eq. (2-19) with a weight function $-w_1$ and integrating over the element will result:

$$\int_0^l -w_1 \times \left\{ \begin{array}{l} \rho \ddot{y}(x,t)\delta y - \left(k_s AG\left(\dfrac{\partial^2 y}{\partial x^2} + \dfrac{\partial \psi}{\partial x} \right) \right) + K_{t1}(y_{t1} - y(\bar{\xi}_1,t))\delta^*(x-\bar{\xi}_1) \\ +K_{t2}(y_{t2} - y(\bar{\xi}_2,t))\delta^*(x-\bar{\xi}_2) + C_{t1}(\dot{y}_{t1} - \dot{y}(\bar{\xi}_1,t))\delta^*(x-\bar{\xi}_1) + \\ C_{t2}(\dot{y}_{t2} - \dot{y}(\bar{\xi}_2,t))\delta^*(x-\bar{\xi}_2) + c\dot{y}(x,t) + \left\{ \begin{array}{l} D_1 f_{g1}\delta^*(x-\bar{\xi}_1) \\ +D_2 f_{g2}\delta^*(x-\bar{\xi}_2) \end{array} \right\} \end{array} \right\} dx = 0 \qquad (2.21)$$

where coefficients D_1 and D_2 depend on the interval of the motion defined by the following four stages:

$$\begin{cases} 0 \le t < t_1, & D_1 = 1, D_2 = 0, \\ t_1 \le t < t_2, & D_1 = 1, D_2 = 1, \\ t_2 \le t < t_3, & D_1 = 0, D_2 = 1, \\ t_3 \le t, & D_1 = 0, D_2 = 0 \end{cases} \qquad (2.22)$$

in which the parameters t_1, t_2 and t_3 are the respective times when the second tire enters the bridge, the first tire leaves the bridge, and the second tire departs from the bridge. Now, multiplying Eq. (2-20) with a weighting function $-w_2$ and integrating over the element will result:

$$\int_0^l -w_2 \times \left\{ \rho I \ddot{\psi}(x,t) - EI\frac{\partial^2 \psi}{\partial x^2} + k_s AG\left(\psi + \frac{\partial y}{\partial x} \right) \right\} dx = 0 \qquad (2.23)$$

Using the integration by parts for each integral in Eq. (2-21) yields:

$$\int_0^l \left\{ \begin{array}{l} -\rho \dfrac{\partial^2 y}{\partial t^2} w_1 + \dfrac{dw_1}{dx} k_s AG\left(\dfrac{dy}{dx} + \psi\right) - w_1 K_{t1}(y_{t1} - y(\bar{\xi}_1, t))\delta^*(x - \bar{\xi}_1) \\ -w_1 K_{t2}(y_{t2} - y(\bar{\xi}_2, t))\delta^*(x - \bar{\xi}_2) - w_1 C_{t1}(\dot{y}_{t1} - \dot{y}(\bar{\xi}_1, t))\delta^*(x - \bar{\xi}_1) \\ -w_1 C_{t2}(\dot{y}_{t2} - \dot{y}(\bar{\xi}_2, t))\delta^*(x - \bar{\xi}_2) - w_1 c\dot{y}(x,t) - w_1 \left\{ \begin{array}{l} D_1 f_{g1}\delta^*(x - \bar{\xi}_1) \\ +D_2 f_{g2}\delta^*(x - \bar{\xi}_2) \end{array} \right\} \end{array} \right\} dx$$

$$-\left[w_1 k_s AG\left(\frac{dy}{dx} + \psi\right) \right]_0^l = 0 \tag{2.24}$$

and for Eq. (2-23), we obtain:

$$\int_0^l \left[\frac{dw_2}{dx} EI \frac{d\psi}{dx} + w_2 K_s AG\left(\frac{dy}{dx} + \psi\right) \right] dx - \left[w_2 EI \frac{d\psi}{dx} \right]_0^l = 0 \tag{2.25}$$

The coefficient of the weighting functions w_1 and w_2 in the boundary integrals are described as:

$$\begin{aligned} K_s AG\left(\frac{dy}{dx} + \varphi\right) &\equiv V \\ EI \frac{d\psi}{dx} &\equiv M \end{aligned} \tag{2.26}$$

where V is the shear force and M is the bending moment.

Here a linear beam element with two nodes has been used. Using similar linear shape function for both vertical deflection y and the rotation about z axis (ψ), one can relate the displacement functions (deflection and rotation) to their associated nodal displacement vectors as:

$$\begin{aligned} y &= \sum_{j=1}^{2} \varphi_j(x) Y_j(t) \\ \psi &= \sum_{j=1}^{2} \varphi_j(x) \Psi_j(t) \end{aligned} \tag{2.27}$$

which φ_1 and φ_2 are the linear Lagrange interpolation functions:

$$\varphi_1(x) = \frac{l-x}{l}$$
$$\varphi_2(x) = \frac{x}{l} \tag{2.28}$$

Using Eqs. (2.27), the discretized form of the Eq. (2-24) can be written as:

$$\int_0^l \rho \frac{\partial^2}{\partial t^2}\left(\sum_{j=1}^{2}\varphi_j Y_j\right) w_1 dx + \left(\int_0^l \frac{dw_1}{dx} k_s AG\left(\frac{\partial}{\partial x}\left(\sum_{j=1}^{2}\varphi_j Y_j\right)+\left(\sum_{j=1}^{2}\varphi_j \Psi_j\right)\right)dx\right)\delta y$$
$$-\int_0^l w_1 K_{t1}(y_{t1}-\left(\sum_{j=1}^{2}\varphi_j Y_j\right))\delta^*(x-\bar{\xi}_1)\,dx - \int_0^l w_1 K_{t2}(y_{t2}-\left(\sum_{j=1}^{2}\varphi_j Y_j\right))\delta^*(x-\bar{\xi}_2)\,dx$$
$$-\int_0^l w_1 C_{t1}(\dot{y}_{t1}-\frac{\partial}{\partial t}\left(\sum_{j=1}^{2}\varphi_j Y_j\right))\delta^*(x-\bar{\xi}_1)\,dx - \int_0^l w_1 C_{t2}(\dot{y}_{t2}-\frac{\partial}{\partial t}\left(\sum_{j=1}^{2}\varphi_j Y_j\right))\delta^*(x-\bar{\xi}_2)\,dx \tag{2.29}$$
$$-\int_0^l w_1 c\frac{\partial}{\partial t}\left(\sum_{j=1}^{2}\varphi_j Y_j\right)dx\delta y - \int_0^l w_1\left\{D_1 f_{g1}\delta^*(x-\bar{\xi}_1)+D_2 f_{g2}\delta^*(x-\bar{\xi}_2)\right\}dx$$
$$+w_1(0)V_0 - w_1(l)V_l = 0$$

similarly for Eq. (2-25), we can write:

$$\int_0^l\left[EI\frac{dw_2}{dx}\frac{\partial}{\partial x}\left(\sum_{j=1}^{2}\varphi_j\Psi_j\right)+K_s AGw_2\left(\left(\sum_{j=1}^{2}\varphi_j\Psi_j\right)+\frac{\partial}{\partial x}\left(\sum_{j=1}^{2}\varphi_j Y_j\right)\right)\right]dx \tag{2.30}$$
$$+w_2(0)M_0 - w_2(l)M_l = 0$$

According to the Galrekin formulation, the weighting functions w_1 and w_2 are replaced by the shape functions. Thus, in Eq. (2. 29), w_1 is replaced first by φ_1 and then by φ_2. Similarly, in Eq. (2.30), w_2 is replaced once by φ_1 and once by φ_2. This will result in the following governing finite element equations:

$$\begin{bmatrix} [M^{11}] & [0] \\ [0] & [M^{22}] \end{bmatrix} \begin{Bmatrix} \{\ddot{Y}\} \\ \{\ddot{\Psi}\} \end{Bmatrix} + \begin{bmatrix} [C^{11}] & [0] \\ [0] & [C^{22}] \end{bmatrix} \begin{Bmatrix} \{\dot{Y}\} \\ \{\dot{\Psi}\} \end{Bmatrix} + \begin{bmatrix} [K^{11}] & [K^{12}] \\ [K^{21}] & [K^{22}] \end{bmatrix} \begin{Bmatrix} Y \\ \Psi \end{Bmatrix} = \begin{Bmatrix} \{F^1\} \\ \{F^2\} \end{Bmatrix} \quad (2.31)$$

where

$$\begin{aligned} M_{ij}^{11} &= \int_0^l \rho A \varphi_i \varphi_j dx \\ M_{ij}^{22} &= \int_0^l \rho I \varphi_i \varphi_j dx \\ C_{ij}^{11} &= \int_0^l c \varphi_i \varphi_j dx \\ K_{ij}^{11} &= \int_0^l K_s AG \frac{d\varphi_i}{dx} \frac{d\varphi_j}{dx} dx \\ K_{ij}^{12} &= \int_0^l K_s AG \frac{d\varphi_i}{dx} \varphi_j dx \\ K_{ij}^{22} &= \int_0^l \left(\left(K_s AG \varphi_i \varphi_j + EI \frac{d\varphi_i}{dx} \frac{d\varphi_j}{dx} \right) \right) dx \end{aligned} \quad (2.32)$$

in which, $i = 1, 2$ and $j = 1, 2$. After integration, the sub mass matrices can be written as:

$$\begin{aligned} [M^{11}] &= \frac{\rho Al}{6} \begin{bmatrix} 2 & 1 \\ 1 & 2 \end{bmatrix} \\ [M^{22}] &= \frac{\rho Il}{6} \begin{bmatrix} 2 & 1 \\ 1 & 2 \end{bmatrix} \end{aligned} \quad (2.33)$$

And

$$[C^{11}] = \frac{cl}{6} \begin{bmatrix} 2 & 1 \\ 1 & 2 \end{bmatrix} \quad (2.34)$$

The element coefficient matrices $[K^{11}]$ and $[K^{12}]$ as well as the first part of $[K^{22}]$ are evaluated exactly, but for the evaluation of the second part of $[K^{22}]$, the reduced

integration was utilized in order to avoid shear locking [22,23]. For constant values of $K_s AG$ and EI, the stiffness sub matrices are evaluated as:

$$\begin{aligned}
\left[K^{11}\right] &= \frac{K_s AG}{l}\begin{bmatrix} 1 & -1 \\ -1 & 1 \end{bmatrix} \\
\left[K^{12}\right] &= \left[K^{21}\right] = \frac{K_s AG}{l}\begin{bmatrix} -1 & -1 \\ 1 & 1 \end{bmatrix} \\
\left[K^{22}\right] &= \frac{EI}{l}\begin{bmatrix} 1 & -1 \\ -1 & 1 \end{bmatrix} + \frac{K_s AGl}{4}\begin{bmatrix} 1 & 1 \\ 1 & 1 \end{bmatrix}
\end{aligned} \tag{2.35}$$

where one-point integration is used to evaluate the second part of $\left[K^{22}\right]$.

$\left\{F^1\right\}$ and $\left\{F^2\right\}$ in Eq. (2-31) include all the forces which act on the first and second node of the beam element, respectively. These forces involve the spring forces, damping forces and the gravitational forces.

If the nodal variables are listed node by node and the equations of motion for the degrees of freedom of vehicle are added to the above equations of motion of the beam element, the total equations of motion in the coupled beam-vehicle system will become:

$$\left[M_v\right]\left\{\ddot{Q}(t)\right\} + \left[C_v(t)\right]\left\{\dot{Q}(t)\right\} + \left[K_v(t)\right]\left\{Q(t)\right\} = \left\{F_v(t)\right\} \tag{2.36}$$

where

$$\{Q(t)\} = \begin{Bmatrix} Y_1 \\ \Psi_1 \\ Y_2 \\ \Psi_2 \\ y_s \\ \theta \\ y_{p1} \\ y_{p2} \\ y_{t1} \\ y_{t2} \end{Bmatrix} \tag{2.37}$$

Also, the general mass matrix of a beam element carrying a vehicle can be written as:

$$M_v = \begin{bmatrix} \frac{\rho Al}{3} & 0 & \frac{\rho Al}{6} & 0 & 0 & 0 & 0 & 0 & 0 & 0 \\ & \frac{\rho Il}{3} & 0 & \frac{\rho Il}{6} & 0 & 0 & 0 & 0 & 0 & 0 \\ & & \frac{\rho Al}{3} & 0 & 0 & 0 & 0 & 0 & 0 & 0 \\ & & & \frac{\rho Il}{3} & 0 & 0 & 0 & 0 & 0 & 0 \\ & & & & m_s & 0 & 0 & 0 & 0 & 0 \\ & & & & & J & 0 & 0 & 0 & 0 \\ & & & & & & m_{p1} & 0 & 0 & 0 \\ & & & & & & & m_{p2} & 0 & 0 \\ & & & & & & & & m_{t1} & 0 \\ Sym. & & & & & & & & & m_{t2} \end{bmatrix} \tag{2.38}$$

The stiffness and damping matrixes of the system have also the following forms:

$$
K_v = \begin{bmatrix}
\frac{K_s AG}{l} + \alpha_1 + \alpha\alpha_1 & -\frac{1}{2}K_s AG & -\frac{K_s AG}{l} + \alpha_2 + \alpha\alpha_2 & -\frac{1}{2}K_s AG & 0 & 0 & 0 & 0 & -\alpha_4 & -\alpha\alpha_4 \\
 & \frac{1}{4}K_s AGl + \frac{EI}{l} & \frac{1}{2}K_s AG & \frac{1}{4}K_s AGl - \frac{EI}{l} & 0 & 0 & 0 & 0 & 0 & 0 \\
 & & \frac{K_s AG}{l} + \alpha_3 + \alpha\alpha_3 & \frac{1}{2}K_s AG & 0 & 0 & 0 & 0 & -\alpha_5 & -\alpha\alpha_5 \\
 & & & \frac{1}{4}K_s AGl + \frac{EI}{l} & 0 & 0 & 0 & 0 & 0 & 0 \\
 & & & & K_{p1} + K_1 + K_{p2} + K_2 & K_{p1}d_1 + K_1 b_1 - K_{p2}d_2 - K_2 b_2 & -K_{p1} & -K_{p2} & -K_1 & -K_2 \\
 & & & & & K_{p1}d_1^2 + K_1 b_1^2 + K_{p2}d_2^2 + K_2 b_2^2 & -K_{p1}d_1 & K_{p2}d_2 & -K_1 b_1 & K_2 b_2 \\
 & & & & & & K_{p1} & 0 & 0 & 0 \\
 & & & & & & & K_{p2} & 0 & 0 \\
 & & & & & & & & K_1 + K_{t1} & 0 \\
 \textit{Sym.} & & & & & & & & & K_2 + K_{t2}
\end{bmatrix} \tag{2.39}
$$

$$
C_v = \begin{bmatrix}
\frac{cl}{3} + \varepsilon_1 + \varepsilon\varepsilon_1 & 0 & \frac{cl}{6} + \varepsilon_2 + \varepsilon\varepsilon_2 & 0 & 0 & 0 & 0 & 0 & -\varepsilon_4 & -\varepsilon\varepsilon_4 \\
 & 0 & 0 & 0 & 0 & 0 & 0 & 0 & 0 & 0 \\
 & & \frac{cl}{3} + \varepsilon_3 + \varepsilon\varepsilon_3 & 0 & 0 & 0 & 0 & 0 & -\varepsilon_5 & -\varepsilon\varepsilon_5 \\
 & & & 0 & 0 & 0 & 0 & 0 & 0 & 0 \\
 & & & & C_{p1} + C_1 + C_{p2} + C_2 & C_{p1} d_1 + C_1 b_1 - C_{p2} d_2 - C_2 b_2 & -C_{p1} & -C_{p2} & -C_1 & -C_2 \\
 & & & & & C_{p1} d_1^2 + C_1 b_1^2 + C_{p2} d_2^2 + C_2 b_2^2 & -C_{p1} d_1 & C_{p2} d_2 & -C_1 b_1 & C_2 b_2 \\
 & & & & & & C_{p1} & 0 & 0 & 0 \\
 & & & & & & & C_{p2} & 0 & 0 \\
 & & & & & & & & C_1 + C_{t1} & 0 \\
\textit{Sym.} & & & & & & & & & C_2 + C_{t2}
\end{bmatrix} \tag{2.40}
$$

where in Eq. (2.39),

$$\begin{aligned}
\alpha_1 &= \int_0^l D_1 K_{t1} \varphi_1^2 \delta^*(x-\overline{\xi}_1)dx \\
\alpha_2 &= \int_0^l D_1 K_{t1} \varphi_1 \varphi_2 \delta^*(x-\overline{\xi}_1)dx \\
\alpha_3 &= \int_0^l D_1 K_{t1} \varphi_2^2 \delta^*(x-\overline{\xi}_1)dx \\
\alpha_4 &= \int_0^l D_1 K_{t1} \varphi_1 \delta^*(x-\overline{\xi}_1)dx \\
\alpha_5 &= \int_0^l D_1 K_{t1} \varphi_2 \delta^*(x-\overline{\xi}_1)dx
\end{aligned} \tag{2.41}$$

are the parameters related to the first tire, and

$$\begin{aligned}
\alpha\alpha_1 &= \int_0^l D_2 K_{t2} \varphi_1^2 \delta^*(x-\overline{\xi}_2)dx \\
\alpha\alpha_2 &= \int_0^l D_2 K_{t2} \varphi_1 \varphi_2 \delta^*(x-\overline{\xi}_2)dx \\
\alpha\alpha_3 &= \int_0^l D_2 K_{t2} \varphi_2^2 \delta^*(x-\overline{\xi}_2)dx \\
\alpha\alpha_4 &= \int_0^l D_2 K_{t2} \varphi_1 \delta^*(x-\overline{\xi}_2)dx \\
\alpha\alpha_5 &= \int_0^l D_2 K_{t2} \varphi_2 \delta^*(x-\overline{\xi}_2)dx
\end{aligned} \tag{2.42}$$

represent the parameters associated with the second tire.

Similarly, in Eq. (2.40),

$$\begin{aligned}
\varepsilon_1 &= \int_0^l D_1 C_{t1} \varphi_1^2 \delta^*(x-\overline{\xi}_1)dx \\
\varepsilon_2 &= \int_0^l D_1 C_{t1} \varphi_1 \varphi_2 \delta^*(x-\overline{\xi}_1)dx \\
\varepsilon_3 &= \int_0^l D_1 C_{t1} \varphi_2^2 \delta^*(x-\overline{\xi}_1)dx \\
\varepsilon_4 &= \int_0^l D_1 C_{t1} \varphi_1 \delta^*(x-\overline{\xi}_1)dx \\
\varepsilon_5 &= \int_0^l D_1 C_{t1} \varphi_2 \delta^*(x-\overline{\xi}_1)dx
\end{aligned} \tag{2.43}$$

correspond to the items related to the first tire and also,

$$
\begin{aligned}
\varepsilon\varepsilon_1 &= \int_0^l D_2 C_{t2} \varphi_1^2 \delta^*(x-\overline{\xi}_2)dx \\
\varepsilon\varepsilon_2 &= \int_0^l D_2 C_{t2} \varphi_1 \varphi_2 \delta^*(x-\overline{\xi}_2)dx \\
\varepsilon\varepsilon_3 &= \int_0^l D_2 C_{t2} \varphi_2^2 \delta^*(x-\overline{\xi}_2)dx \\
\varepsilon\varepsilon_4 &= \int_0^l D_2 C_{t2} \varphi_1 \delta^*(x-\overline{\xi}_2)dx \\
\varepsilon\varepsilon_5 &= \int_0^l D_2 C_{t2} \varphi_2 \delta^*(x-\overline{\xi}_2)dx
\end{aligned}
\tag{2.44}
$$

signify the parameters correlated to the second tire.

Finally, the force vector $\{F_v\}$ can be described as:

$$
F_v = \begin{Bmatrix} \varpi_1 + \varpi\varpi_1 \\ 0 \\ \varpi_2 + \varpi\varpi_2 \\ 0 \\ 0 \\ 0 \\ 0 \\ 0 \\ 0 \\ 0 \end{Bmatrix}_{10\times 1}
\tag{2.45}
$$

where ϖ_1 and ϖ_2 are the portions of the vehicle weight applied from the first tire, on the first and second nodes of the beam element respectively which can be defined as:

$$
\begin{aligned}
\varpi_1 &= \int_0^l f_{g1} \varphi_1 \delta^*(x-\overline{\xi}_1)dx \\
\varpi_2 &= \int_0^l f_{g1} \varphi_2 \delta^*(x-\overline{\xi}_1)dx
\end{aligned}
\tag{2.46}
$$

Correspondingly, $\varpi\varpi_1$ and $\varpi\varpi_2$ represent the allocation of vehicle weight applied from the second tire, on the first and second nodes of the beam, respectively:

$$\varpi\varpi_1 = \int_0^l f_{g2}\varphi_1\delta^*(x-\overline{\xi}_2)dx$$
$$\varpi\varpi_2 = \int_0^l f_{g2}\varphi_2\delta^*(x-\overline{\xi}_2)dx \tag{2.47}$$

Eq. (2.36) and the associated Eqs. (2.37-2.40) and Eq. (2-45) provide the finite element equations of motion for one beam element subjected to the both tires of the moving vehicle. It is clear that the matrix components described by Eqs. (2.41-2.47) are not constant, but changing with respect to the position of the first and second tire ($\overline{\xi}_1$ and $\overline{\xi}_2$ respectively) along the beam element.

Typically, a beam is consisted of more than one element; hence, the general equations of motion for the entire system can be obtained by assembling the matrices of all conventional beam elements and the beam element with the moving vehicle on it. It should be noted that the position of the time variable components mentioned in the previous paragraph is not fixed in damping, stiffness and force matrices of the system ($[C(t)],[K(t)]$ and $[F(t)]$), but changes depending on which element the first and the second tire is located at the time.

2.4 Solution of the Finite Element Equations of Motion

Eq. (2.36) has been solved using direct time integration technique based on unconditionally stable Newmark's β method [93,94,96]. Direct time integration involves the attempt to satisfy dynamic equilibrium at discrete points in time, after defining the solution at time zero. In Newmark β method, the following equations have been used:

$$\dot{Q}^{t+\Delta t} = \dot{Q}^t + \left[(1-\beta)\ddot{Q}^t + \beta\ddot{Q}^{t+\Delta t}\right]\Delta t \tag{2.48}$$

$$Q^{t+\Delta t} = Q^t + \dot{Q}^t \Delta t + \left[\left(\frac{1}{2} - \gamma\right)\ddot{Q}^t + \gamma \ddot{Q}^{t+\Delta t}\right]\Delta t^2 \tag{2.49}$$

In addition to these two equations, for solution of the displacements, velocities and accelerations at time $t+\Delta t$, the equation of motion (2.36) at time $t+\Delta t$ is also considered:

$$[M_v]\ddot{Q}^{t+\Delta t} + \left[C_v^{\,t+\Delta t}\right]\dot{Q}^{t+\Delta t} + \left[K_v^{\,t+\Delta t}\right]Q^{t+\Delta t} = \left\{F_v^{\,t+\Delta t}\right\} \tag{2.50}$$

Solving for $\ddot{Q}^{t+\Delta t}$ in terms of $Q^{t+\Delta t}$ in Eq. (2.49) and substituting for $\ddot{Q}^{t+\Delta t}$ into Eq. (2.48), one can obtain the equations for $\ddot{Q}^{t+\Delta t}$ and $\dot{Q}^{t+\Delta t}$ in terms of the unknown displacements $Q^{t+\Delta t}$ only. By substitution these two relations for $\ddot{Q}^{t+\Delta t}$ and $\dot{Q}^{t+\Delta t}$ into the Eq. (2.50), the unknown displacements can be calculated. Subsequently, $\ddot{Q}^{t+\Delta t}$ and $\dot{Q}^{t+\Delta t}$ can be obtained by using Eqs. (2.48) and (2.49). The complete algorithm using the Newmark integration scheme is described here:

I. Initial Calculations:

1. Initialization of $Q^{t=0}, \dot{Q}^{t=0}$ and $\ddot{Q}^{t=0}$. $(\ddot{Q}^0 = [M_v]^{-1}\left(\{F_v^{\,0}\} - \left[C_v^{\,0}\right]\dot{Q}^0 - \left[K_v^{\,0}\right]Q^0\right))$
2. Selecting time step Δt and parameters β and γ. (Here, $\beta = \frac{1}{2}, \gamma = \frac{1}{4}$ has been selected so that the equation becomes unconditionally stable.)
3. Calculation of the integration constants:

$$
\begin{aligned}
a_0 &= \frac{1}{\gamma \Delta t^2} \quad , \quad a_1 = \frac{\beta}{\gamma \Delta t} \\
a_2 &= \frac{1}{\gamma \Delta t} \quad , \quad a_3 = \frac{1}{2\gamma} - 1 \\
a_4 &= \frac{\beta}{\gamma} - 1 \quad , \quad a_5 = \frac{\Delta t}{2}\left(\frac{\beta}{\gamma} - 1\right) \\
a_6 &= \Delta t(1-\beta), \quad a_7 = \beta \Delta t
\end{aligned}
\tag{2.51}
$$

4. Establishing the effective matrix $\hat{K}^0$:

$$
\left[\hat{K}_v^{\,0}\right] = a_0\left[M_v\right] + a_1\left[C_v^{\,0}\right] + \left[K_v^{\,0}\right] \tag{2.52}
$$

II. For Each Time Step:

1. Forming the effective load at time $t + \Delta t$:

$$
\left\{\hat{F}_v^{\,t+\Delta t}\right\} = \left\{F_v^{\,t+\Delta t}\right\} + \left[M_v\right]\left(a_0 Q^t + a_2 \dot{Q}^t + a_3 \ddot{Q}^t\right) + \left[C_v^{\,t+\Delta t}\right]\left(a_1 Q^t + a_4 \dot{Q}^t + a_5 \ddot{Q}^t\right) \tag{2.53}
$$

2. Obtaining the displacement at time $t + \Delta t$:

$$
Q^{t+\Delta t} = \left[\hat{K}_v^{\,t}\right]^{-1}\left\{\hat{F}_v^{\,t+\Delta t}\right\} \tag{2.54}
$$

3. Calculation of acceleration and velocity at time $t + \Delta t$:

$$
\ddot{Q}^{t+\Delta t} = a_0\left(Q^{t+\Delta t} - Q^t\right) - a_2 \dot{Q}^t - a_3 \ddot{Q}^t \tag{2.55}
$$

$$
\dot{Q}^{t+\Delta t} = \dot{Q}^t + a_6 \ddot{Q}^t + a_7 \ddot{Q}^{t+\Delta t} \tag{2.56}
$$

2.5 Numerical Results for Half Car Model

2.5.1 Model Verification

The developed finite element model for the coupled beam-vehicle has been used to find the response of the beam and vehicle. The results are compared with those available in literature to validate the methodology. As mentioned in Chapter 1, Esmailzadeh and Jalili[58] addressed similar problem in which an Euler-Bernoulli beam traversed by a vehicle (half car model) has been studied. They used analytical approach based on mode expansion to solve the governing differential equations. Thus, this reference has been used as benchmark to validate the developed finite element formulation. In order to compare the results with those in Ref. [58] similar parameters for both beam and vehicle are used. It should be noted that in order to have fair comparison with those in Ref. [58], Euler-Bernoulli beam model has been used in the finite element formulation. The properties of the beam and the vehicle have been presented in Table 2-1 and Table 2-2, respectively. A summery of Euler-Bernoulli Finite Element formulation has been represented in Appendix A.

Table 2-1 Properties of the Euler Bernoulli Beam [58]

Elastic Modulus	207 GPa	Second Moment of Inertia (I)	0.174 m^4
Mass per Unit Length (ρ)	20000 Kg/m	Beam Structural Damping (c)	1750 Ns/m
Cross Sectional Area	4.94 m^2	Beam Length (L)	100 m

Table 2-2 Properties of the Vehicle [58]

Body mass (m_s)	$1794.4kg$
Body Rotational Mass Moment of Inertia (J)	$443.05kgm^2$
First axle mass (m_{t1})	$87.15kg$
Second axle mass (m_{t2})	$140.4kg$
Driver mass (m_{p1})	$75kg$
Passenger Mass (m_{p2})	$75kg$
First Axle Damping Ratio (C_1)	$1190Ns/m$
Second Axle Damping Ratio (C_2)	$1000Ns/m$
First Tire Damping Ratio (C_{t1})	$14.6Ns/m$
Second Tire Damping Ratio (C_{t2})	$14.6Ns/m$
Driver Damping Ratio (C_{p1})	$62.1Ns/m$
Passenger Damping Ratio (C_{p2})	$62.1Ns/m$
First Axle Stiffness (K_1)	$66824.4N/m$
Second Axle Stiffness (K_2)	$18615.0N/m$
First Tire Stiffness (K_{t1})	$01115.0N/m$
Second Tire Stiffness (K_{t2})	$01115.0N/m$
Driver Stiffness (K_{p1})	$14000.0N/m$
Passenger Stiffness (K_{p2})	$14000.0N/m$
b_1	$1.271m$
b_2	$1.716m$
d_1	$0.481m$
d_2	$1.313m$

It should be noted that the first natural frequency of the beam is equal to 1.32 rad/s. The relation between the damping coefficient and damping ratio of the beam can be defined as:[97]

$$\xi_k = \frac{c}{2\rho\omega_k} \tag{2.57}$$

where ξ_k represents the damping ratio due to kth mode of the beam, c is the damping coefficient of the beam, ρ is the linear density of the beam and ω_k is the kth natural frequency of the beam. Accordingly, the damping ratio of the beam for this situation is equal to 3.3%.

The time history for the transversal dynamic deflection of the midspan of the bridge for two different values of the vehicle speed (72 and 88 Km/h) has been shown in Figure 2-2 and Figure 2-3.

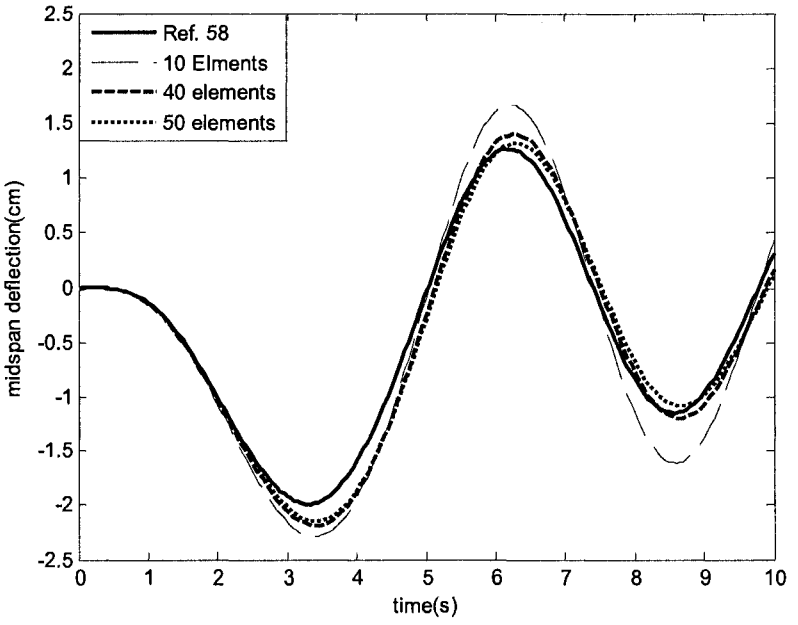

Figure 2-2 Time History of the Beam Midspan Deflection for V=72 Km/h

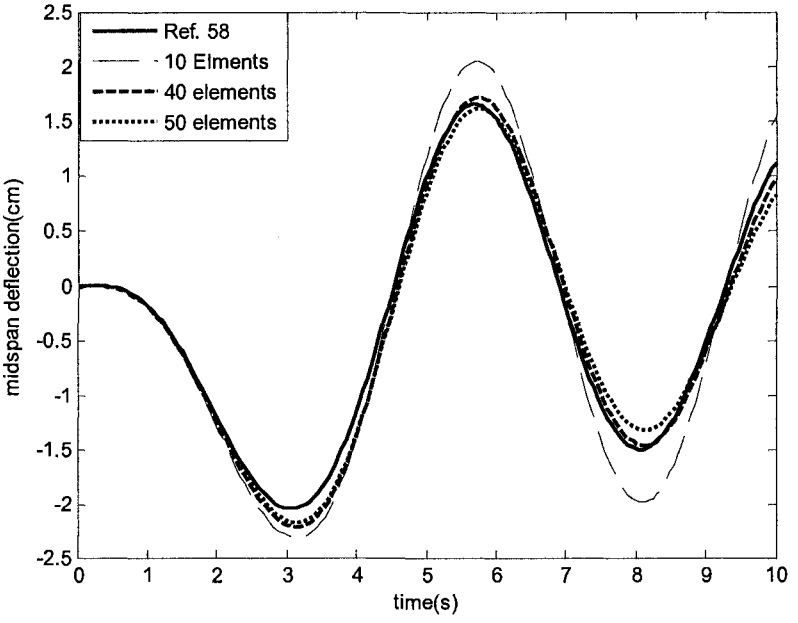

Figure 2-3 Time History of the Midspan Deflection of the Beam for V=88 Km/h

It can be realized from the figures that as the number of beam elements increases, the obtained results converge more to the analytical results. Also, the time history for the vehicle body bounce (y_s), the driver bounce (y_{p1}), the passenger bounce (y_{p2}), the front tire bounce (y_{t1}) and the rear tire bounce (y_{t2}) for V=88 km/h have been shown in Figure 2-4,Figure 2-5, Figure 2-6, Figure 2-7 and Figure 2-8, respectively. It can be seen that the results obtained from the developed finite element formulation are in very good agreement with analytical results in Ref. [58]. Also by increasing the number of elements, the finite element solution approaches the exact solution. Hereafter, considering accuracy and computational time, all the simulations will be performed using 40 beam elements.

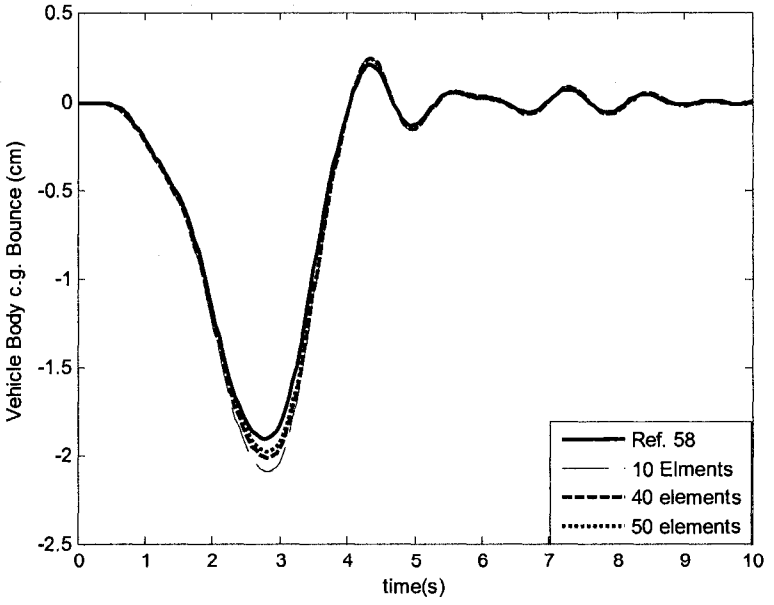

Figure 2-4 Time History of the Vehicle Body Bounce for V=88 Km/h

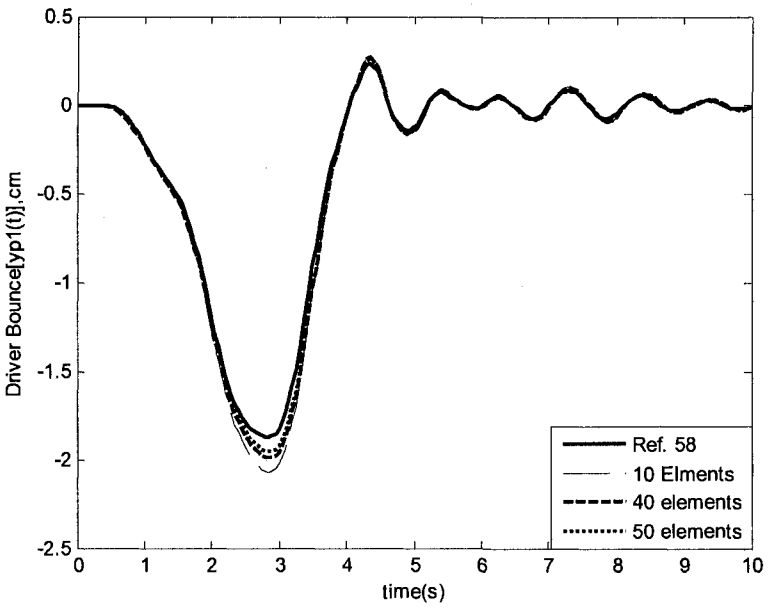

Figure 2-5 Time History of the Driver Bounce for V=88 Km/h

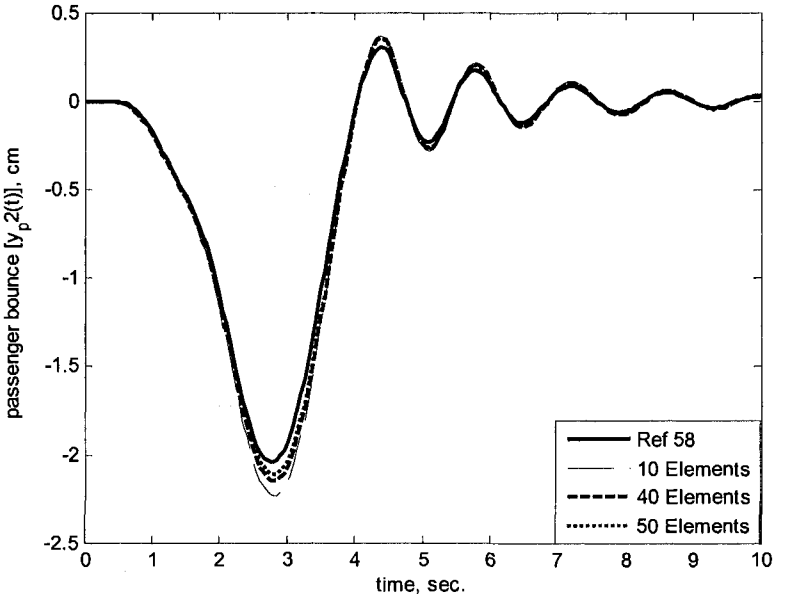

Figure 2-6 Time History of the Passenger Bounce for V=88 Km/h

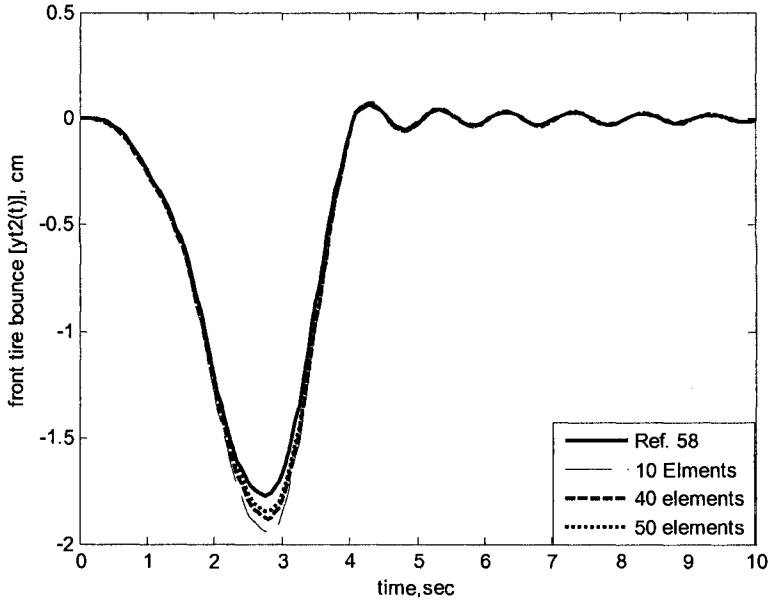

Figure 2-7 Time History of the Front Tire Bounce for V=88 Km/h

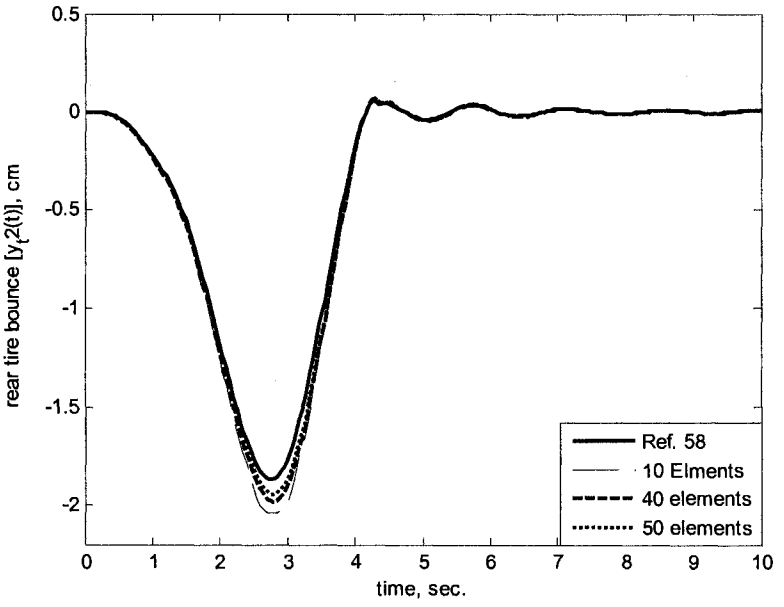

Figure 2-8 Time History of Rear Tire Bounce for V=88 Km/h

2.5.2 Numerical Results on the Behavior of the Timoshenko beam under Half Car Model

Here, the same parameters provided in previous section for the beam and vehicles have been utilized except that instead of Euler-Bernoulli beam theory, Timoshenko beam theory has been employed. It should be mentioned that the Poisson's ratio and the shear factor of the Timoshenko beam are equal to 0.3 and 5/6 respectively. Also the damping coefficient of the beam is equal to 5500 Ns/m, and according to Eq. (2.57) the damping ratio for the first mode is about 10%.

The variation of the maximum value of the transversal dynamic deflection of the Timoshenko beam, and its location along the beam with respect to the vehicle speed, has been shown in Figure 2-9 (a) and (b). It can be seen that when the vehicle travels at around the speed of 90 Km/h, the deflection of the beam attains its maximum value. This speed is referred to as the critical speed of the vehicle corresponding to the maximum transversal deflection. It is interesting to note that the maximum value of the dynamic deflection occurs around the midspan of beam (at the location of 53 m) as shown in Figure 2-9 (b).

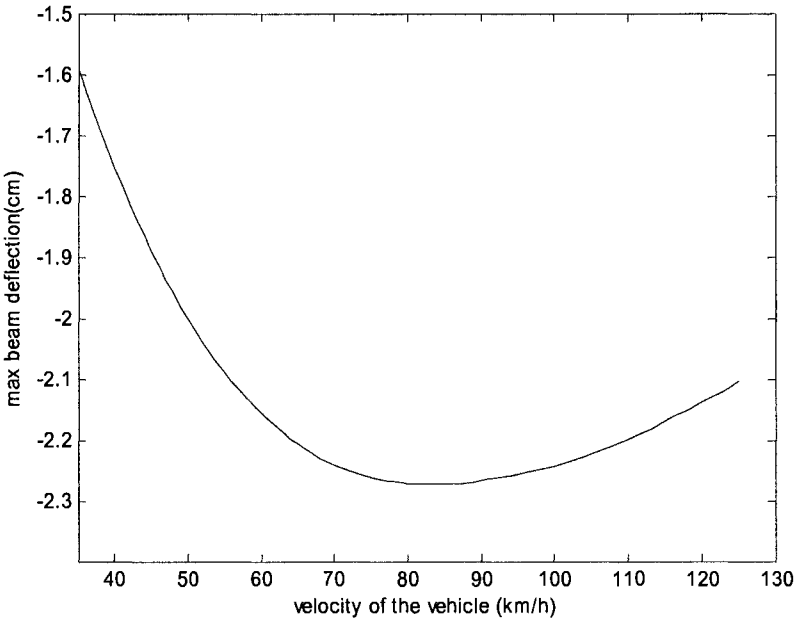

(a)

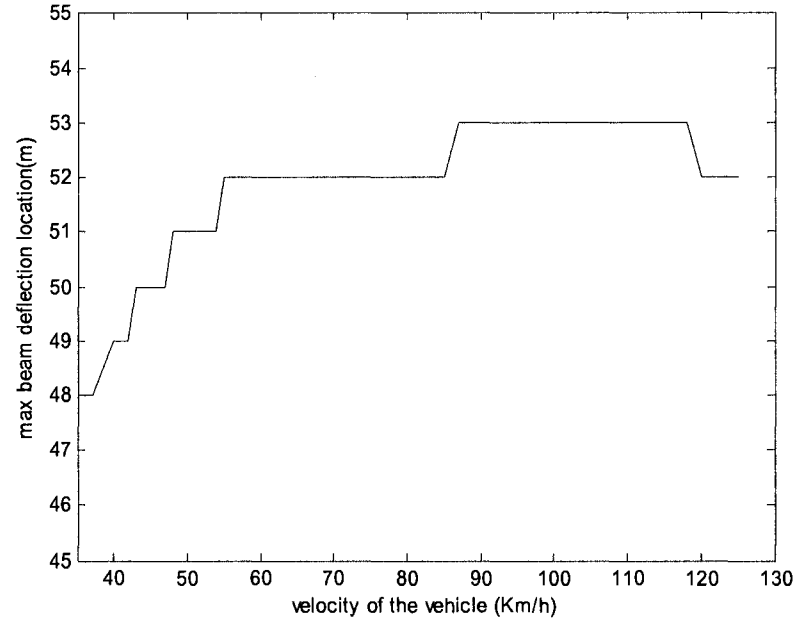

(b)

Figure 2-9 (a) Maximum Dynamic Deflection, and (b) Location versus Vehicle Velocity for the Beam 100 m Long

Similar investigation has been done on the beam with length of 70 m as shown in Figure 2-10 (a) and (b). As expected the maximum deflection for the beam with 70 m long is much less than that of 100 m long. It is interesting to note that for this case, the critical vehicle speed is 130 Km/h in which the maximum deflection of the beam reaches at its greatest value. Similarly, it can be seen that the maximum transversal deflection of the beam occurs around the midspan, at the length of 37 m.

In Figure 2-11, the configuration of the 100 m beam under the half car model moving at V=72 Km/h for the first 5 seconds has been shown. It can be observed that as the vehicle enters the beam, the deflection in the beam increases and the position of the maximum deflection moves from the left to the middle. The vehicle leaves the beam after 5 seconds. The configuration of the beam during the 5 seconds after the vehicle leaves the beam has also been illustrated in Figure 2-12. It can be seen that after the vehicle leaves the beam, the beam vibration continues and gradually dissipates due to the damping effect in the beam.

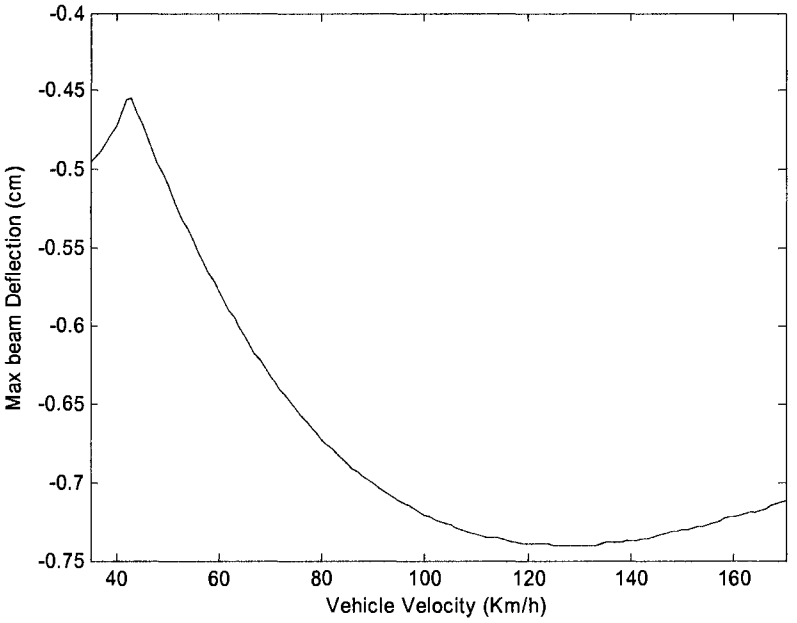

(a)

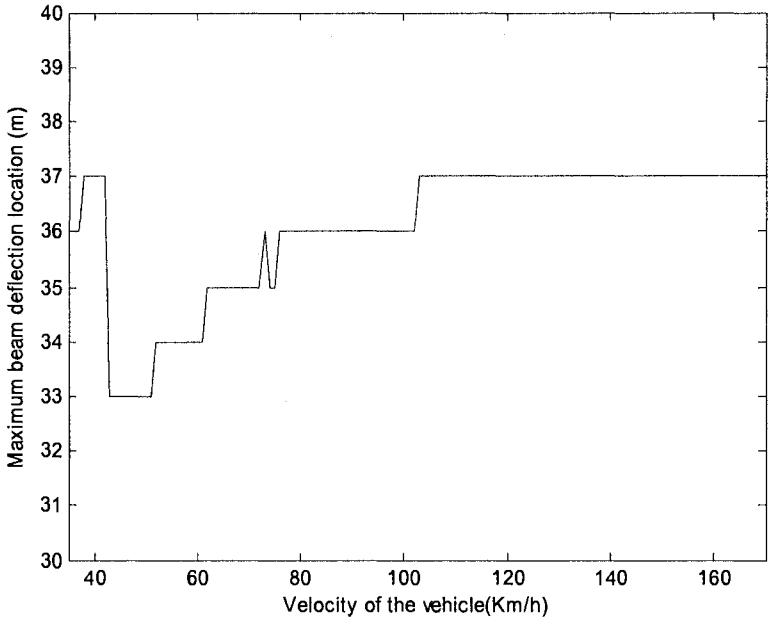

(b)

Figure 2-10 (a) The Maximum Dynamic Deflection and (b) Location versus Vehicle Velocity for the Beam 70 m Long

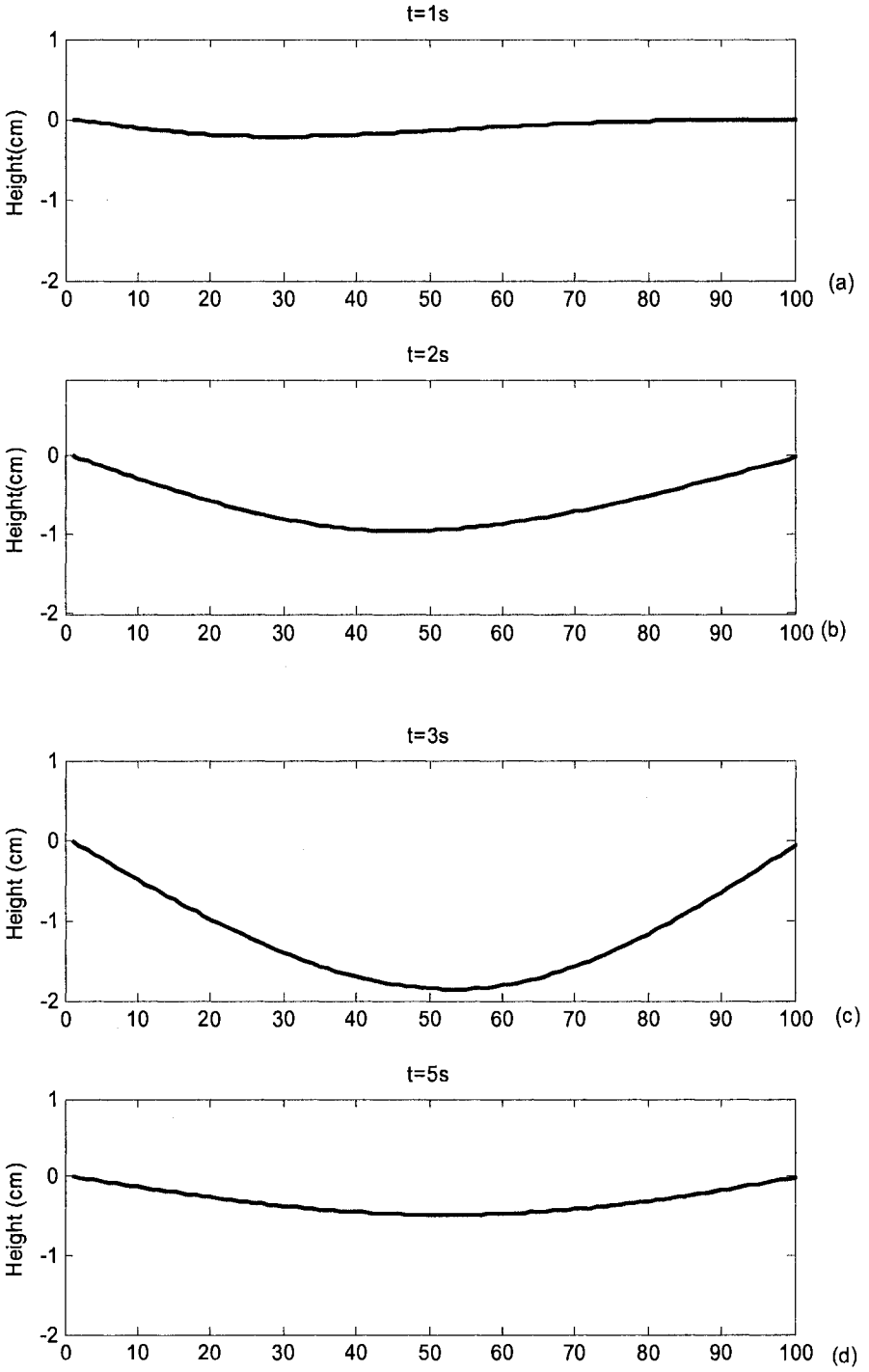

Figure 2-11 The Configuration of the Beam with L=100m under the Half Car Model Moving at V=72 Km/h for the First 5 Seconds

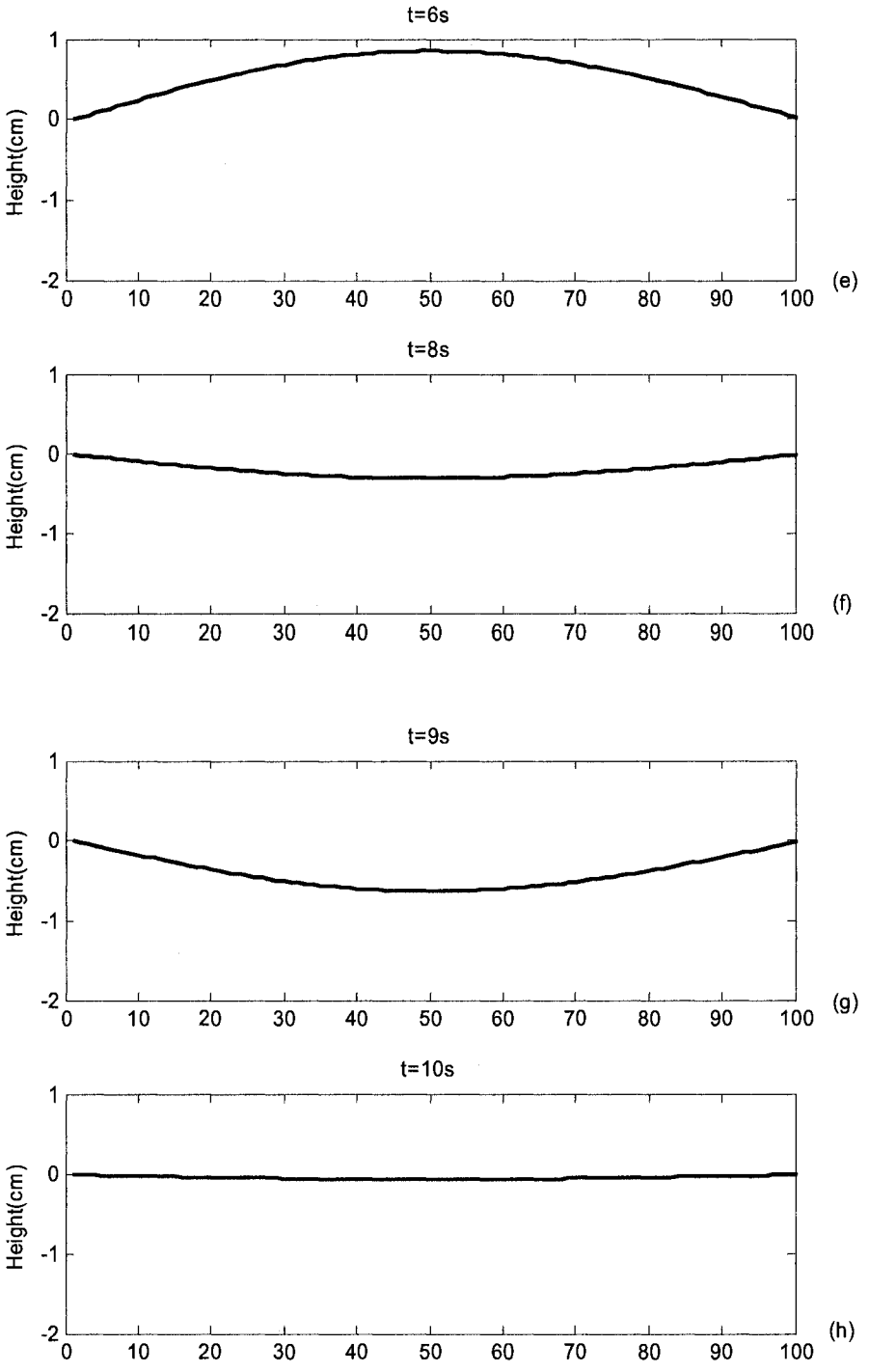

Figure 2-12 The Configuration of the Beam with L=100m under the Half Car Model Moving at V=72 Km/h for the 5 Seconds after Vehicle Leaves the Beam

2.5.3 Comparison between Euler-Bernoulli and Timoshenko Beam Models

In order to show the accuracy of the Timoshenko beam model, the maximum beam deflection versus the vehicle velocity has been plotted for both Timoshenko and Euler-Bernoulli beams at the length of 100 m in Figure 2-13. It can be observed from the diagram that the maximum beam deflection has been underestimated in Euler-Bernoulli beam model. This difference is slight in lower velocities, but as the vehicle velocity increases, the disparity between the two beam models becomes more significant. In Table 2-3 the maximum deflection for the beams obeying Timoshenko and Euler Bernoulli theories and their percentage difference have been illustrated for a few vehicle velocities.

Table 2-3 Comparison between Maximum Deflections in Timoshenko and Euler-Bernoulli Beams

Vehicle Velocity (Km/h)	35	50	70	90	120	150
Max beam deflection for Euler Bernoulli beam (cm)	1.5163	1.8180	1.9808	1.9788	1.8508	1.6761
Max beam deflection for Timoshenko beam (cm)	1.5939	2.001	2.2421	2.2677	2.1380	1.9372
Percentage difference	5.11	10.06	13.19	14.60	15.51	15.57

For more clarification, in Figure 2-14 the percentage difference between maximum deflections in Timoshenko and Euler-Bernoulli beams versus vehicle velocity has been plotted in the velocity range of 35-150 Km/h. It can be observed that the percentage difference increases by the rise of vehicle velocity and adopts an almost constant value with slight fluctuations after about V=110 Km/h.

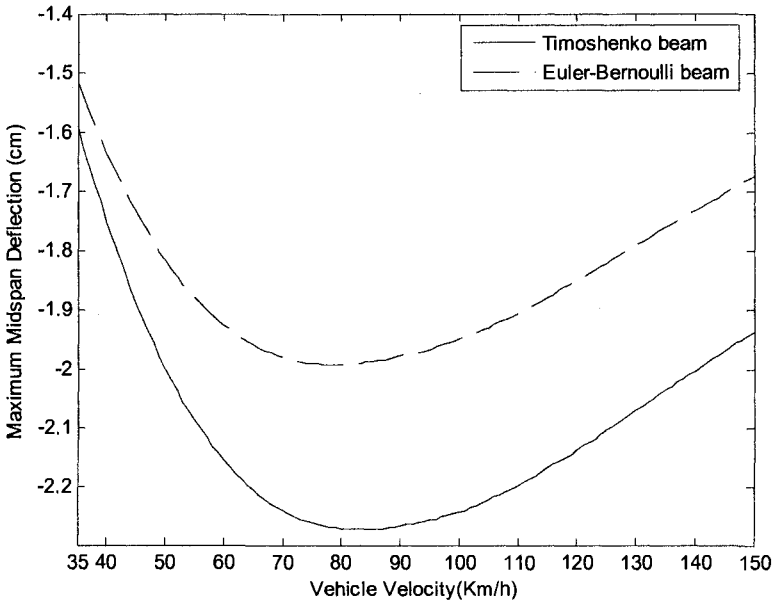

Figure 2-13 Maximum Beam Deflection versus Vehicle Velocity for Timoshenko and Euler Bernoulli Beam

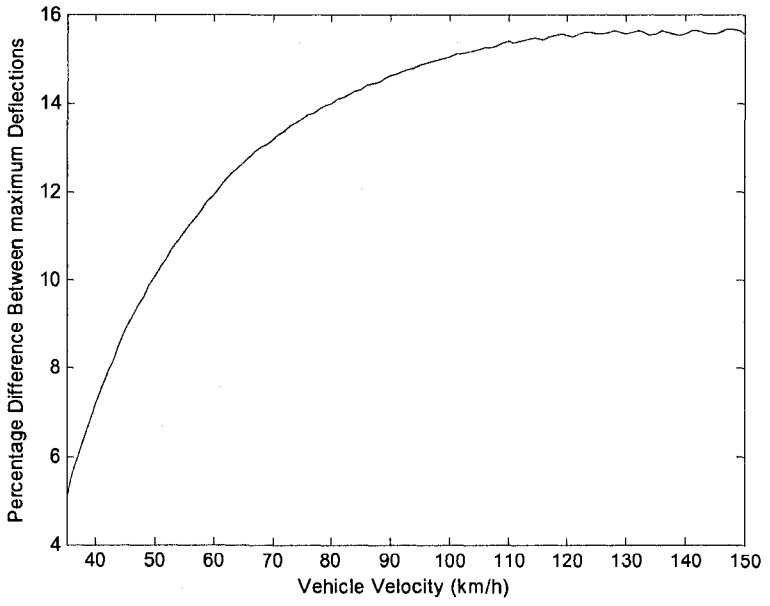

Figure 2-14 Percentage Difference between Maximum Beam Deflections in Timoshenko and Euler-Bernoulli Beam versus Vehicle Velocity

2.6 Finite Element Formulation for the Timoshenko Beam-Quarter Car Model system

In this section, the finite element formulation of the coupled bridge- moving vehicle system in which the vehicle is represented as Simple Quarter-Car (SQC) planner model as shown in Figure 2-15 is briefly described and the results are compared with those of half car model. The moving SQC model is considered as a dynamic system, with two degrees of freedom, in which M_1 and M_2 are the unsprung mass and the sprung mass of the moving vehicle respectively.

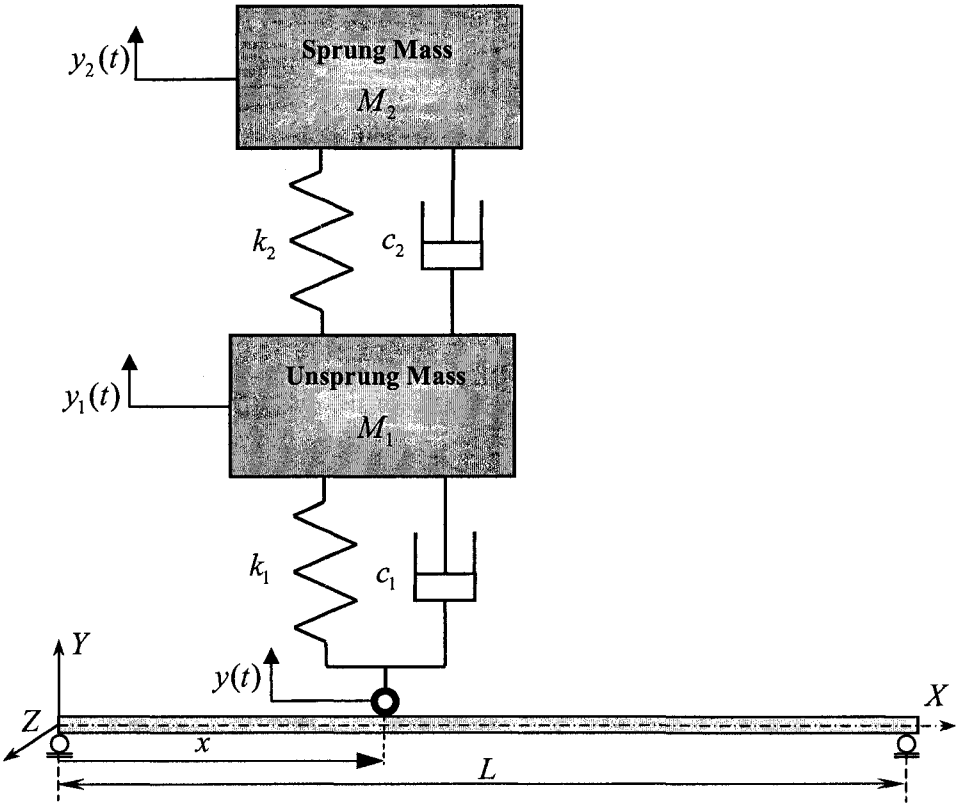

Figure 2-15 Schematic of a Bridge Traversed by a Moving Quarter Car

Similar to the half car model, the tire is assumed to be in contact with the surface of the beam at all times, and therefore the vertical displacement of the moving tire and the bridge will be the same. The vertical displacements of the unsprung mass M_1 and sprung mass M_2, related to their respective vertical equilibrium position, are $y_1(t)$ and $y_2(t)$ correspondingly. The horizontal location of the center of the mass of the moving vehicle measured from the fixed reference point, such as the left end of the bridge, is denoted by $x_v(t)$. The vehicle is moving at a constant speed v along the beam.

The governing equations of motion of the present model are obtained using the similar procedure explained in section 2.2 by utilizing Hamilton principle. The vertical motion for the unsprung mass (M_1) is governed by:

$$M_1\ddot{y}_1 + k_1(y_1 - y(x_v)) + c_1(\dot{y}_1 - \dot{y}(x_v)) + k_2(y_1 - y_2) + c_2(\dot{y}_1 - \dot{y}_2) = 0 \tag{2.58}$$

The equation of motion for the sprung mass (M_2) can be written as:

$$M_2\ddot{y}_2 + k_2(y_2 - y_1) + c_2(\dot{y}_2 - \dot{y}_1) = 0 \tag{2.59}$$

The first equation for the beam, governs the traversed deflection of the beam(y):

$$\int_0^L \rho\ddot{y}(x,t)dx - \left(\int_0^L k_s AG\left(\frac{\partial^2 y}{\partial x^2} + \frac{\partial \psi}{\partial x}\right)dx\right) + \int_0^L c\dot{y}(x,t)dx + \int_0^L k_1(y_1 - y(x,t))\delta^*(x - x_v)\,dx + \int_0^L c_1(\dot{y}_1 - \dot{y}(x,t))\delta^*(x - x_v)\,dx + \int_0^L (M_1 + M_2)g\delta^*(x - x_v)dx = 0 \tag{2.60}$$

and the orientation of the beam cross-section (ψ) around z axis can be defined as:

$$\int_0^L \rho I\ddot{\psi}(x,t)dx - \int_0^L EI\frac{\partial^2 \psi}{\partial x^2}dx + \int_0^L k_s AG\left(\psi + \frac{\partial y}{\partial x}\right)dx = 0 \tag{2.61}$$

Derivation of the finite element formulation of the governing equations is similar to the procedure described in section 2.3. The total equations of motion of the system of one beam element under the quarter car model can be described as:

$$\left[M_q\right]\left\{\ddot{Z}(t)\right\}+\left[C_q(t)\right]\left\{\dot{Z}(t)\right\}+\left[K_q(t)\right]\left\{Z(t)\right\}=\left[F_q(t)\right] \tag{2.62}$$

in which

$$\left\{Z(t)\right\}=\begin{Bmatrix} Y_1 \\ \Psi_1 \\ Y_2 \\ \Psi_2 \\ y_1 \\ y_2 \end{Bmatrix} \tag{2.63}$$

and the total mass, stiffness and damping matrices can be written as:

$$M_q=\begin{bmatrix} \frac{\rho Al}{3} & 0 & \frac{\rho Al}{6} & 0 & 0 & 0 \\ & \frac{\rho Il}{3} & 0 & \frac{\rho Il}{6} & 0 & 0 \\ & & \frac{\rho Al}{3} & 0 & 0 & 0 \\ & & & \frac{\rho Il}{3} & 0 & 0 \\ & & & & M_1 & 0 \\ Sym. & & & & & M_2 \end{bmatrix} \tag{2.64}$$

$$K_q = \begin{bmatrix} \frac{K_s AG}{l}+\kappa_1 & -\frac{1}{2}K_s AG & -\frac{K_s AG}{l}+\kappa_2 & -\frac{1}{2}K_s AG & -\kappa_4 & 0 \\ & \frac{1}{4}K_s AGl+\frac{EI}{l} & \frac{1}{2}K_s AG & \frac{1}{4}K_s AGl-\frac{EI}{l} & 0 & 0 \\ & & \frac{K_s AG}{l}+\kappa_3 & \frac{1}{2}K_s AG & -\kappa_5 & 0 \\ & & & \frac{1}{4}K_s AGl+\frac{EI}{l} & 0 & 0 \\ & & & & k_1+k_2 & -k_2 \\ \textit{Sym.} & & & & & k_2 \end{bmatrix} \quad (2.65)$$

$$C_q = \begin{bmatrix} \frac{cl}{3}+\eta_1 & 0 & \frac{cl}{6}+\eta_2 & 0 & -\eta_4 & 0 \\ & 0 & 0 & 0 & 0 & 0 \\ & & \frac{cl}{3}+\eta_3 & 0 & -\eta_5 & 0 \\ & & & 0 & 0 & 0 \\ & & & & c_1+c_2 & -c_2 \\ \textit{Sym.} & & & & & c_2 \end{bmatrix} \quad (2.66)$$

where in Eqs. (2-65) and (2-66)

$$\begin{aligned} \kappa_1 &= \int_0^l k_1 \varphi_1^2 \delta^*(x-\bar{x}_v)dx \\ \kappa_2 &= \int_0^l k_1 \varphi_1 \varphi_2 \delta^*(x-\bar{x}_v)dx \\ \kappa_3 &= \int_0^l k_1 \varphi_2^2 \delta^*(x-\bar{x}_v)dx \\ \kappa_4 &= \int_0^l k_1 \varphi_1 \delta^*(x-\bar{x}_v)dx \\ \kappa_5 &= \int_0^l k_1 \varphi_2 \delta^*(x-\bar{x}_v)dx \end{aligned} \quad (2.67)$$

$$\eta_1 = \int_0^l c_1 \varphi_1^2 \delta^*(x-\bar{x}_v)dx$$
$$\eta_2 = \int_0^l c_1 \varphi_1 \varphi_2 \delta^*(x-\bar{x}_v)dx$$
$$\eta_3 = \int_0^l c_1 \varphi_2^2 \delta^*(x-\bar{x}_v)dx \qquad (2.68)$$
$$\eta_4 = \int_0^l c_1 \varphi_1 \delta^*(x-\bar{x}_v)dx$$
$$\eta_5 = \int_0^l c_1 \varphi_2 \delta^*(x-\bar{x}_v)dx$$

The general force vector in right hand side of Eq. (2.62) can also be written as:

$$F_q = \begin{bmatrix} \int_0^l (M_1+M_2) g \varphi_1 \delta^*(x-\bar{x}_v)dx \\ 0 \\ \int_0^l (M_1+M_2) g \varphi_2 \delta^*(x-\bar{x}_v)dx \\ 0 \\ 0 \\ 0 \end{bmatrix} \qquad (2.69)$$

The general equations of motion for the entire system can be obtained by assembling the matrices of all conventional beam elements and the beam element on which the moving vehicle is attached. Eq. (2.62) can be solved by the direct time integration Newmark β method as explained in section 2.4

2.6.1 Comparison between the Half Car Model and Quarter Car Model

Here the midspan deflection of the Timoshenko beam at length 100 m with the properties mentioned in section 2.5.2 traversed by a moving vehicle simulated as half car and quarter car models have been compared for the critical car velocity (V=90 Km/h). The properties of the half car model are the same as mentioned in Table 2-2. For the sake

of comparison, the equivalent properties for the quarter car model have been selected as follows:

$$M_1 = m_{t1} + m_{t2}\ ,\ M_2 = m_s + m_{p1} + m_{p2}\ ,\ f_g = -(M_1 + M_2)H(x - \xi(t))$$
$$k_1 = K_{t1} + K_{t2}\ ,\ k_2 = K_1 + K_2\ ,\ c_1 = C_{t1} + C_{t2}\ ,\ c_2 = C_1 + C_2$$

Figure 2-16 shows the midspan deflection for both car models at velocity of 90 Km/h.

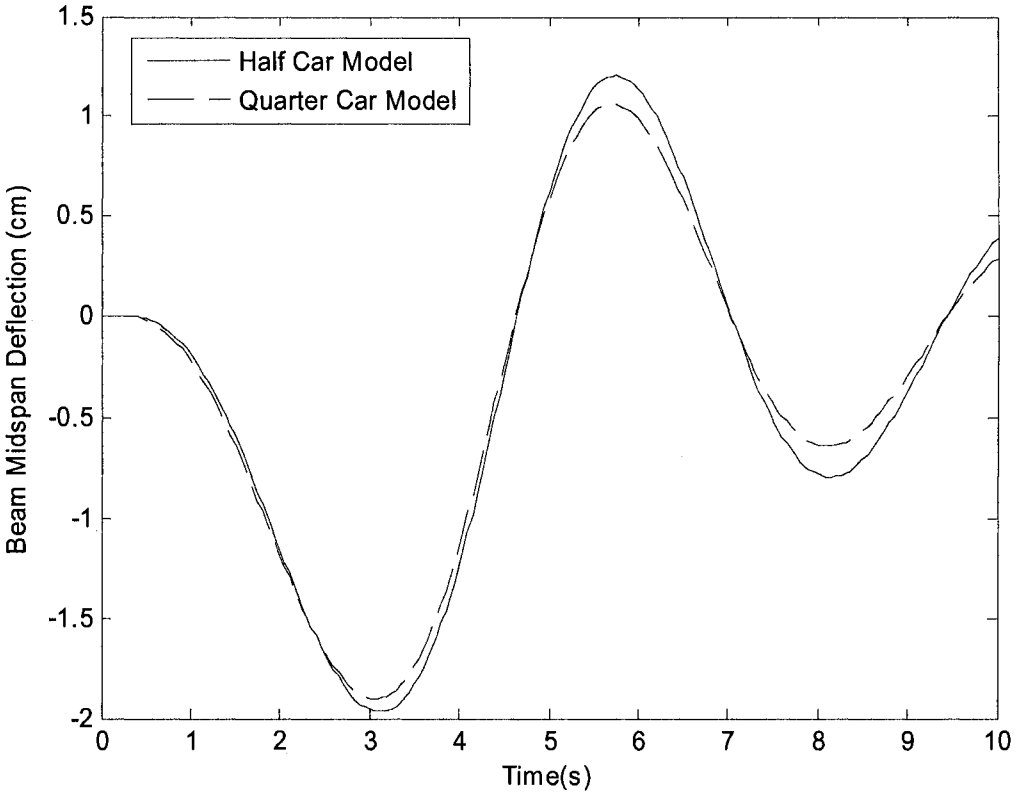

Figure 2-16 Time History of Midspan Deflection at V=90 Km/h for Half and Quarter Car Model

The beam midspan deflections for three consecutive peaks of the response have been shown in Table 2-4. It can be realized that generally the quarter car model underestimates

the deflection. Although at the first peak the difference is not significant (3.74%), as the time passes, the difference become more considerable.

Table 2-4 Beam Midspan Deflection Comparison between Half car and Quarter car model

Time (s)	3.15	5.75	8.15
Maximum deflection for half car model (cm)	-1.968	1.204	-0.7927
Maximum deflection for quarter car model (cm)	-1.897	1.061	-.06372
Percentage difference	3.74	13.48	24.4

2.7 Conclusion

The finite element formulation of a bridge type structure, modeled as a simply supported Timoshenko beam, under a moving vehicle considered either as a half car or a quarter car model, have been presented. The problem is solved by direct time integration technique based on the Newmark's β method. The obtained results for the half car model have been validated with those reported in literature. The maximum deflections of the beam based on the Euler-Bernoulli and the Timoshenko models were compared and it was observed that, as the vehicle velocity increases, the difference between the results in the two models becomes more significant. The beam midspan defections for the beam under a quarter car model and a half car model have been compared.

Chapter 3: FINITE ELEMENT FORMULATION OF THE TIMOSHENKO BEAM WITH ATTACHED TMDs TRAVERSED BY A MOVING VEHICLE

3.1 Introduction

In this chapter the finite element formulation of a simply supported Timoshenko beam with n attached TMDs under a half car model is presented. Initially, the finite element formulation for a Timoshenko beam with the attached TMDs is obtained, and then by superposition the derived equations are combined with the equations of the beam under the moving vehicle presented in Chapter 2 in order to obtain the governing equations of motion for the total system.

3.2 Formulation of the Timoshenko Beam with Attached TMDs

A simply supported beam with n TMDs as shown in Figure 3-1 is utilized to set up the equations of motion for the general case. $x_h, M_{TMD_h}, C_{TMD_h}$ and K_{TMD_h} are defined as the position, mass, damping and stiffness of the hth TMD respectively.

Further to Chapter 2, the Hamilton's principle is employed to obtain the governing equations of motion of the model.

The total kinetic energy of the system can be defined as:

$$T = \frac{1}{2}\{\int_0^L \rho \dot{y}^2(x,t)dx + \int_0^L \rho I(x)\dot{\psi}^2(x,t)dx + M_{TMD_1}\dot{z}_1^2 + ... + M_{TMD_n}\dot{z}_n^2\} \tag{3.1}$$

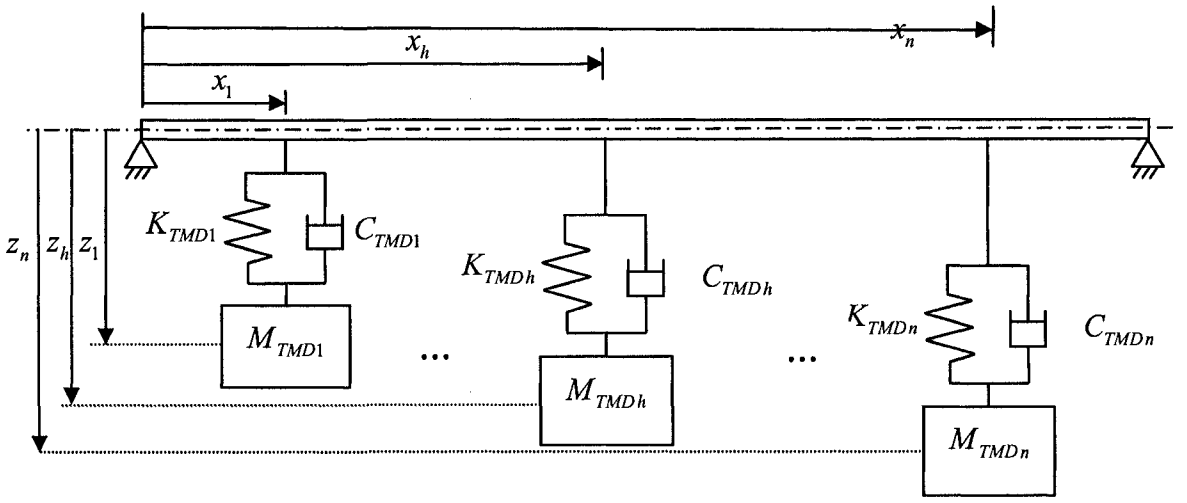

Figure 3-1 Simply Supported Beam with *n* Attached TMDs

Therefore, the virtual kinetic energy of the system is described as:

$$\delta T = \int_0^L \rho \dot{y}(x,t)\frac{\partial \delta y}{\partial t}dx + \int_0^L \rho I(x)\dot{\psi}(x,t)\frac{\partial \delta \psi}{\partial t}dx + M_{TMD_1}\dot{z}_1(t)\frac{d\delta z_1}{dt} + \ldots + M_{TMD_n}\dot{z}_n(t)\frac{d\delta z_n}{dt} \tag{3.2}$$

Consequently, one can write:

$$\int_{t1}^{2} \delta T dt = -\int_{t_1}^{t_2}\{\int_0^L \rho \ddot{y}(x,t)dx\delta y + \int_0^L \rho I\ddot{\psi}(x,t)dx\delta\psi + M_{TMD_1}\ddot{z}_1\delta z_1 + \ldots + M_{TMD_n}\ddot{z}_n\delta z_n\}dt \tag{3.3}$$

The total potential energy of the system can also be written as:

$$U = \frac{1}{2}\{\int_0^L EI\left(\frac{\partial \psi}{\delta x}\right)^2 dx + \int_0^L k_s AG\left(\frac{\partial y}{\partial x}+\psi\right)^2 dx + K_{TMD_1}\left(y(TMD_1,t)-z_1\right)^2 K_{TMD_n}\left(y(TMD_n,t)-z_n\right)^2\} \tag{3.4}$$

Thus, the virtual potential energy of the system is given by:

$$\delta U = \int_0^L EI\frac{\partial\psi}{\partial x}\frac{\partial\delta\psi}{\partial x}dx + \int_0^L k_s AG\psi\delta\psi\,dx + \int_0^L k_s AG\frac{\partial y}{\partial x}\delta\psi\,dx + \int_0^L k_s AG\frac{\partial\delta y}{\partial x}\psi\,dx +$$
$$\int_0^L k_s AG\frac{\partial y}{\partial x}\frac{\partial\delta y}{\partial x}dx + K_{TMD_1}\left(y_{TMD_1} - z_1\right)(\delta y_{TMD_1} - \delta z_1) + \ldots + \tag{3.5}$$
$$K_{TMD_n}\left(y_{TMD_n} - z_n\right)(\delta y_{TMD_n} - \delta z_n)$$

Intergrading from both sides of Eq. (3.5) will yield:

$$\int_{t1}^{t2}\delta U dt = \int_{t1}^{t2}\{\left(\int_0^L -EI\frac{\partial^2\psi}{\partial x^2}dx + \int_0^L k_s AG\left(\psi + \frac{\partial y}{\partial x}\right)dx\right)\delta\psi$$
$$-\left(\int_0^L k_s AG\left(\frac{\partial^2 y}{\partial x^2} + \frac{\partial\psi}{\partial x}\right)dx\right)\delta y + K_{TMD_1}\left(y_{TMD_1} - z_1\right)(\delta y_{TMD_1} - \delta z_1) \tag{3.6}$$
$$+\ldots + K_{TMD_n}\left(y_{TMD_n} - z_n\right)(\delta y_{TMD_n} - \delta z_n)\}dt$$

Also, the non conservative virtual work in the system can be expressed as

$$\int_{t_1}^{t_2}\delta W_{nc}dt = \int_{t_1}^{t_2}\{-\int_0^L c\dot{y}dx\delta y - C_{TMD_1}(\dot{y}_{TMD_1} - \dot{z}_1)\delta(y_{TMD_1} - z_1)$$
$$-\ldots - C_{TMD_n}(\dot{y}_{TMD_n} - \dot{z}_n)\delta(y_{TMD_n} - z_n)\}dt \tag{3.7}$$

Substituting Eqs. (3.3), (3.6) and (3.7) in the Hamilton principle will yield:

$$0 = \int_{t_1}^{t_2}\{-\int_0^L \rho\ddot{y}(x,t)dx\delta y - \int_0^L \rho I\ddot{\psi}(x,t)dx\,\delta\psi - M_{TMD_1}\ddot{z}_1\delta z_1 - \ldots - M_{TMD_n}\ddot{z}_n\delta z_n$$
$$+\left(\int_0^L EI\frac{\partial^2\psi}{\partial x^2}dx - \int_0^L k_s AG\left(\psi + \frac{\partial y}{\partial x}\right)dx\right)\delta\psi + \left(\int_0^L k_s AG\left(\frac{\partial^2 y}{\partial x^2} + \frac{\partial\psi}{\partial x}\right)dx\right)\delta y$$
$$-\int_0^L K_{TMD_1}(y - z_1)\delta^*(y - y_{TMD_1})dx\delta y + \int_0^L K_{TMD_1}(y - z_1)\delta^*(y - y_{TMD_1})dx\delta z_1 - \ldots \tag{3.8}$$
$$+\ldots - \int_0^L K_{TMD_n}(y - z_n)\delta^*(y - y_{TMD_n})dx\delta y + \int_0^L K_{TMD_n}(y - z_n)\delta^*(y - y_{TMD_n})dx\delta z_n$$
$$-\int_0^L C_{TMD_1}(\dot{y} - \dot{z}_1)\delta^*(y - y_{TMD_1})dx\delta y + \int_0^L C_{TMD_1}(\dot{y} - \dot{z}_1)\delta^*(y - y_{TMD_1})dx\delta z_1 - \ldots$$
$$+\ldots - \int_0^L C_{TMD_n}(\dot{y} - \dot{z}_n)\delta^*(y - y_{TMD_n})dx\delta y + \int_0^L C_{TMD_n}(\dot{y} - \dot{z}_n)\delta^*(y - y_{TMD_n})dx\delta z_n\}dt$$

Subsequently, the dynamics of the system can be described by n+2 second order differential equations obtained by setting the coefficients of deltas ($\delta y, \delta\psi, \delta y_{TMD_1}, \ldots$ and δy_{TMD_n}) to zero.

The vertical deflection of the beam is given by:

$$\begin{aligned}&\int_0^L \rho\ddot{y}(x,t)dx - \left(\int_0^L k_s AG\left(\frac{\partial^2 y}{\partial x^2}+\frac{\partial\psi}{\partial x}\right)dx\right)+\int_0^L c\dot{y}(x,t)dx \\ &+\int_0^L C_{TMD_1}(\dot{y}-\dot{z}_1)\delta^*(x-x_1)\,dx+\ldots+\int_0^L C_{TMD_n}(\dot{y}-\dot{z}_n)\delta^*(x-x_n)\,dx \\ &+\int_0^L K_{TMD1}(y-z_1)\delta^*(x-x_1)\,dx+\ldots+\int_0^L K_{TMD_n}(y-z_n)\delta^*(x-x_n)\,dx=0\end{aligned} \tag{3.9}$$

The orientation of the beam cross-section (ψ) around Z axis is defined by:

$$\int_0^L \rho I\ddot{\psi}(x,t)dx-\int_0^L EI\frac{\partial^2\psi}{\partial x^2}dx+\int_0^L k_s AG\left(\psi+\frac{\partial y}{\partial x}\right)dx=0 \tag{3.10}$$

and finally the equation of motion for the hth attached TMD is given as:

$$M_{TMD_h}\ddot{z}_h+\int_0^L C_{TMD_h}(\dot{z}_h-\dot{y})\delta^*(x-x_h)dx+\int_0^L K_{TMD_h}(z_h-y)\delta^*(x-x_h)dx=0 \tag{3.11}$$

3.3 Finite Element Formulation of the Timoshenko Beam with Attached TMDs

In order to derive the finite element formulation of the system, the same procedure as described in section 2.3 will be implemented. The Galerkin weak form of Eqs. (3.10) and (3.11) over an element of the length l can be applied to develop the finite element formulation. The same linear interpolation given in Eqs. (2.27) and (2.28) for the vertical deflection of the beam (y) and the rotation of it about Z axis (ψ) is considered.

Since the properties of the beam and the interpolation functions are the same as those used in Chapter 2, the equations of motion and the basic matrices for the beam element will be the same as those presented in Eqs. (2.31) to (2.35).

Identifying the nodal variables and combining the equations of motion for the vertical position of the connected TMDs, the total equations of motion for a beam element with n attached TMDs can be described into the following finite element form:

$$[M_T]\{\ddot{\Lambda}(t)\}+[C_T]\{\dot{\Lambda}(t)\}+[K_T]\{\Lambda(t)\}=[F_T] \tag{3.12}$$

where $\Lambda(t)$ is the nodal displacement vector written as:

$$\{\Lambda(t)\}=\begin{Bmatrix} Y_1 \\ \Psi_1 \\ Y_2 \\ \Psi_2 \\ z_1 \\ \vdots \\ z_n \end{Bmatrix} \tag{3.13}$$

and $[M_T]$, $[K_T]$ and $[K_T]$ are the mass, the stiffness and the damping matrices of the beam element with n attached TMDs and have the following forms:

$$M_T = \begin{bmatrix} \frac{\rho Al}{3} & 0 & \frac{\rho Al}{6} & 0 & 0 & \cdots & 0 \\ & \frac{\rho Il}{3} & 0 & \frac{\rho Il}{6} & 0 & \cdots & 0 \\ & & \frac{\rho Al}{3} & 0 & 0 & \cdots & 0 \\ & & & \frac{\rho Il}{3} & 0 & \cdots & 0 \\ & & & & M_{TMD_1} & \cdots & 0 \\ & & & & & \ddots & \vdots \\ Sym. & & & & & & M_{TMD_n} \end{bmatrix} \tag{3.14}$$

$$K_T = \begin{bmatrix} \frac{K_s AG}{l} + \vartheta_{1_1} + \ldots + \vartheta_{n_1} & -\frac{1}{2}K_s AG & -\frac{K_s AG}{l} + \vartheta_{1_2} + \ldots + \vartheta_{n_2} & -\frac{1}{2}K_s AG & -\vartheta_{1_4} & \cdots & -\vartheta_{n_4} \\ & \frac{1}{4}K_s AGl + \frac{EI}{l} & \frac{1}{2}K_s AG & \frac{1}{4}K_s AGl - \frac{EI}{l} & 0 & \cdots & 0 \\ & & \frac{K_s AG}{l} + \vartheta_{1_3} + \ldots + \vartheta_{n_3} & \frac{1}{2}K_s AG & -\vartheta_{1_5} & \cdots & -\vartheta_{n_5} \\ & & & \frac{1}{4}K_s AGl + \frac{EI}{l} & 0 & \cdots & 0 \\ & & & & K_{TMD_1} & & \vdots \\ & & & & & \ddots & 0 \\ Sym. & & & & & & K_{TMD_n} \end{bmatrix} \tag{3.15}$$

$$C_T = \begin{bmatrix} \frac{cl}{3} + \varsigma_{1_1} & 0 & \frac{cl}{6} + \varsigma_{1_2} & 0 & -\varsigma_{1_4} & \cdots & -\varsigma_{n_4} \\ +\ldots+\varsigma_{n_1} & & +\ldots+\varsigma_{n_2} & & & & \\ & 0 & 0 & 0 & 0 & \cdots & 0 \\ & & \frac{cl}{3} + \varsigma_{1_3} & 0 & -\varsigma_{1_5} & \cdots & -\varsigma_{n_5} \\ & & +\ldots+\varsigma_{n_3} & & & & \\ & & & 0 & 0 & \cdots & 0 \\ & & & & C_{TMD_1} & & \vdots \\ & & & & & \ddots & 0 \\ Sym. & & & & & & C_{TMD_n} \end{bmatrix} \tag{3.16}$$

where for the *h*th TMD,

$$\begin{aligned} \vartheta_{h_1} &= \int_0^l K_{TMD_h} \varphi_1^2 \delta^*(x - \overline{x}_h) dx \\ \vartheta_{h_2} &= \int_0^l K_{TMD_h} \varphi_1 \varphi_2 \delta^*(x - \overline{x}_h) dx \\ \vartheta_{h_3} &= \int_0^l K_{TMD_h} \varphi_2^2 \delta^*(x - \overline{x}_h) dx \\ \vartheta_{h_4} &= \int_0^l K_{TMD_h} \varphi_1 \delta^*(x - \overline{x}_h) dx \\ \vartheta_{h_5} &= \int_0^l K_{TMD_h} \varphi_2 \delta^*(x - \overline{x}_h) dx \end{aligned} \tag{3.17}$$

and

$$
\begin{aligned}
\varsigma_{h_1} &= \int_0^l C_{TMD_h} \varphi_1^2 \delta^*(x-\overline{x}_h)dx \\
\varsigma_{h_2} &= \int_0^l C_{TMD_h} \varphi_1 \varphi_2 \delta^*(x-\overline{x}_h)dx \\
\varsigma_{h_3} &= \int_0^l C_{TMD_h} \varphi_2^2 \delta^*(x-\overline{x}_h)dx \\
\varsigma_{h_4} &= \int_0^l C_{TMD_h} \varphi_1 \delta^*(x-\overline{x}_h)dx \\
\varsigma_{h_5} &= \int_0^l C_{TMD_h} \varphi_2 \delta^*(x-\overline{x}_h)dx
\end{aligned}
\tag{3.18}
$$

Since there are no external forces, the force vector is zero:

$$
F_T = \begin{bmatrix} 0 \\ \vdots \\ 0 \end{bmatrix}_{n+2\times 1} \tag{3.19}
$$

Assembling the matrices of all conventional beam elements and the beam elements with the attached TMDs will result in the general equations of motion for the entire system.

3.4 Finite Element Formulation of the Timoshenko Beam with Attached TMDs under the Half Car Model

In order to obtain the finite element formulation of a beam element with *n* attached TMDs under a half car model, the superposition principle has been used where the equations of motion of a beam element under the half car model developed in Chapter 2 are combined with the equations of motion related to a beam element with *n* attached TMDs derived in the previous section. The final equations of motion for the system of

beam with the attached TMDs under moving vehicle can be described the by following finite element form:

$$[M]\{\ddot{\chi}(t)\}+[C(t)]\{\dot{\chi}(t)\}+[K(t)]\{\chi(t)\}=\{F(t)\} \tag{3.20}$$

where $\chi(t)$ is the nodal displacement vector described as:

$$\{\chi(t)\}=\begin{Bmatrix} Y_1 \\ \Psi_1 \\ Y_2 \\ \Psi_2 \\ y_s \\ J \\ y_{p1} \\ y_{p2} \\ y_{t1} \\ y_{t2} \\ z_1 \\ \vdots \\ z_n \end{Bmatrix}_{n+10\times 1} \tag{3.21}$$

and $[M],[K]$ and $[K]$ are the mass, the stiffness and the damping matrices of the beam element with n attached TMDs traversed by a moving half car model and have the following forms:

$$M = \begin{bmatrix} \frac{\rho Al}{3} & 0 & \frac{\rho Al}{6} & 0 & 0 & 0 & 0 & 0 & 0 & 0 & 0 & \cdots & 0 \\ & \frac{\rho Il}{3} & 0 & \frac{\rho Il}{6} & 0 & 0 & 0 & 0 & 0 & 0 & 0 & \cdots & 0 \\ & & \frac{\rho Al}{3} & 0 & 0 & 0 & 0 & 0 & 0 & 0 & 0 & \cdots & 0 \\ & & & \frac{\rho Il}{3} & 0 & 0 & 0 & 0 & 0 & 0 & 0 & \cdots & 0 \\ & & & & m_s & 0 & 0 & 0 & 0 & 0 & 0 & \cdots & 0 \\ & & & & & J & 0 & 0 & 0 & 0 & 0 & \cdots & 0 \\ & & & & & & m_{p1} & 0 & 0 & 0 & 0 & \cdots & 0 \\ & & & & & & & m_{p2} & 0 & 0 & 0 & \cdots & 0 \\ & & & & & & & & m_{t1} & 0 & 0 & \cdots & 0 \\ & & & & & & & & & m_{t2} & 0 & \cdots & 0 \\ & & & & & & & & & & M_{TMD_1} & \cdots & 0 \\ & & & & & & & & & & & \ddots & \vdots \\ Sym. & & & & & & & & & & & & M_{TMD_n} \end{bmatrix} \quad (3.22)$$

$$
K = \begin{bmatrix}
\frac{K_s AG}{l}+\alpha_1 & & -\frac{K_s AG}{l}+\alpha_2 & & & & & & & & & & \\
+\alpha\alpha_1+\vartheta_{1_1} & -\frac{1}{2}K_s AG & +\alpha\alpha_2+\vartheta_{1_2} & -\frac{1}{2}K_s AG & 0 & 0 & 0 & 0 & -\alpha_4 & -\alpha\alpha_4 & -\vartheta_{1_4} & \cdots & -\vartheta_{n_4} \\
+\ldots+\vartheta_{n_1} & & +\ldots+\vartheta_{n_2} & & & & & & & & & & \\
 & \frac{1}{4}K_s AGl+\frac{EI}{l} & \frac{1}{2}K_s AG & \frac{1}{4}K_s AGl-\frac{EI}{l} & 0 & 0 & 0 & 0 & 0 & 0 & 0 & \cdots & 0 \\
 & & \frac{K_s AG}{l}+\alpha_3 & & & & & & & & & & \\
 & & +\alpha\alpha_3+\vartheta_{1_3} & \frac{1}{2}K_s AG & 0 & 0 & 0 & 0 & -\alpha_5 & -\alpha\alpha_5 & -\vartheta_{1_5} & \cdots & -\vartheta_{n_5} \\
 & & +\ldots+\vartheta_{n_3} & & & & & & & & & & \\
 & & & \frac{1}{4}K_s AGl+\frac{EI}{l} & 0 & 0 & 0 & 0 & 0 & 0 & 0 & \cdots & 0 \\
 & & & & K_{p1}+K_1 & K_{p1}d_1+K_1 b_1 & & & & & & & \\
 & & & & +K_{p2}+K_2 & -K_{p2}d_2-K_2 b_2 & -K_{p1} & -K_{p2} & -K_1 & -K_2 & 0 & \cdots & 0 \\
 & & & & & K_{p1}d_1^2+K_1 b_1^2 & & & & & & & \\
 & & & & & +K_{p2}d_2^2+K_2 b_2^2 & -K_{p1}d_1 & K_{p2}d_2 & -K_1 b_1 & K_2 b_2 & 0 & \cdots & 0 \\
 & & & & & & K_{p1} & 0 & 0 & 0 & 0 & \cdots & 0 \\
 & & & & & & & K_{p2} & 0 & 0 & 0 & \cdots & 0 \\
 & & & & & & & & K_1+K_{t1} & 0 & 0 & \cdots & 0 \\
 & & & & & & & & & K_2+K_{t2} & 0 & \cdots & 0 \\
 & & & & & & & & & & K_{TMD_1} & & \vdots \\
 & & & & & & & & & & & \ddots & 0 \\
\textit{Sym.} & & & & & & & & & & & & K_{TMD_n}
\end{bmatrix} \tag{3.23}
$$

$$
C = \begin{bmatrix}
\frac{cl}{3}+\varepsilon_1 & & \frac{cl}{6}+\varepsilon_2 & & & & & & & & & & \\
+\varepsilon\varepsilon_1+\varsigma_{1_1} & 0 & +\varepsilon\varepsilon_2+\varsigma_{1_2} & 0 & 0 & 0 & 0 & 0 & -\varepsilon_4 & -\varepsilon\varepsilon_4 & -\varsigma_{1_4} & \cdots & -\varsigma_{n_4} \\
+\ldots+\varsigma_{n_1} & & +\ldots+\varsigma_{n_2} & & & & & & & & & & \\
 & 0 & 0 & 0 & 0 & 0 & 0 & 0 & 0 & 0 & 0 & \cdots & 0 \\
 & & \frac{cl}{3}+\varepsilon_3 & & & & & & & & & & \\
 & & +\varepsilon\varepsilon_3+\varsigma_{1_3} & 0 & 0 & 0 & 0 & 0 & -\varepsilon_5 & -\varepsilon\varepsilon_5 & -\varsigma_{1_5} & \cdots & -\varsigma_{n_5} \\
 & & +\ldots+\varsigma_{n_3} & & & & & & & & & & \\
 & & & 0 & 0 & 0 & 0 & 0 & 0 & 0 & 0 & \cdots & 0 \\
 & & & & C_{p1}+C_1 & C_{p1}d_1+C_1b_1 & & & & & & & \\
 & & & & +C_{p2}+C_2 & -C_{p2}d_2-C_2b_2 & -C_{p1} & -C_{p2} & -C_1 & -C_2 & 0 & \cdots & 0 \\
 & & & & & C_{p1}d_1^2+C_1b_1^2 & & & & & & & \\
 & & & & & +C_{p2}d_2^2+C_2b_2^2 & -C_{p1}d_1 & C_{p2}d_2 & -C_1b_1 & C_2b_2 & 0 & \cdots & 0 \\
 & & & & & & C_{p1} & 0 & 0 & 0 & 0 & \cdots & 0 \\
 & & & & & & & C_{p2} & 0 & 0 & 0 & \cdots & 0 \\
 & & & & & & & & C_1+C_{t1} & 0 & 0 & \cdots & 0 \\
 & & & & & & & & & C_2+C_{t2} & 0 & \cdots & 0 \\
 & & & & & & & & & & C_{TMD_1} & & \vdots \\
 & & & & & & & & & & & \ddots & 0 \\
\textit{Sym.} & & & & & & & & & & & & C_{TMD_n}
\end{bmatrix}
$$

(3.24)

where $\alpha_{1-5}, \alpha\alpha_{1-5}, \varepsilon_{1-5}, \varepsilon\varepsilon_{1-5}, \vartheta_{h_{1-5}}$ and $\varsigma_{h_{1-5}}$ have been introduced before in Eqs. (2.41)-(2.44), (3.17) and (3.18), respectively.

Finally, the force vector can be written as:

$$F = \begin{Bmatrix} \varpi_1 + \varpi\varpi_1 \\ 0 \\ \varpi_2 + \varpi\varpi_2 \\ 0 \\ 0 \\ 0 \\ 0 \\ 0 \\ 0 \\ 0 \\ 0 \\ 0 \\ \vdots \\ 0 \end{Bmatrix}_{n+10\times 1} \tag{3.25}$$

where ϖ_1 and ϖ_2 as well as $\varpi\varpi_1$ and $\varpi\varpi_2$ are the portions of vehicle weight applied from the first and second tire on the first and second nodes of the beam respectively, which are defined in Eqs. (2.46) and (2.47), correspondingly.

The general equations of motion for the entire beam-TMD-vehicle system can be obtained by assembling the matrices of all conventional beam elements, beam elements with attached TMDs, and the beam element with the moving vehicle and attached TMDs.

Eq. (3.20) can be solved by utilizing direct time integration using the Newmark's β method. Similar to the procedure described in section 2.3, after the solution is defined at time zero, the dynamic equilibrium at discrete points in time should be satisfied.

3.5 Conclusion

The governing equations of motion of a system of Timoshenko beam with n attached TMDs have been derived and then transformed into the finite element form using the Galerkin weak form approximation. Subsequently, using the superposition principle, the derived finite element equations of motion for the beam element with the attached TMDs are combined with the finite element equations of motion for the beam element under the moving half car model derived in Chapter 2. This is to obtain the total governing equations of motion of a Timoshenko beam element with n attached TMDs subjected to a moving half car model.

Chapter 4: OPTIMAL DESIGN OF TUNED MASS DAMPER

4.1 Introduction

In this chapter an optimal design strategy has been presented to obtain the optimal parameters (frequency and damping ratios) of a single TMD for which, the deflection at the mid-span of the Timoshenko beam traversed by a moving vehicle (half car model) is minimized. The design optimization methodology combines the developed finite element analysis with the optimization algorithm based on the Sequential Quadratic Programming (SQP) technique.

4.1.1 Optimization

Optimization is one of the most significant aspects of design in almost all disciplines. In today's competitive market the importance of increasing the performance in every product, through design and manufacturing process, has been accentuated since it can serve directly to make more efficient, accurate, environmental-friendly products with lower costs and a reduction of energy consumption. Due to the revolution in computer technology and numerical computations in the recent past, today's computers can perform complex calculations and process large amounts of data rapidly. The engineering design and optimization processes benefit greatly from this revolution because they require a large number of calculations. Better systems can now be designed by analyzing and optimizing various options in a short time with less cost and more capability.

Structural Optimization is one of the necessary features in the structural design procedures to improve the behavior of a mechanical structure while keeping its structural

properties. This aspect has matured to the point that it can be routinely applied to a wide range of real design tasks.

As mentioned earlier, by implementing a tuned mass damper on a primary structure, a large reduction in its dynamic responses can be achieved. Although the basic design concept of the TMD is simple, the parameters of the TMD system must be obtained through optimal design procedures to attain the best performance of the tuned mass damper. In this regard, this section is allocated to acquisition of the optimal parameters of a TMD to control the vibration of the Timoshenko beam subjected to a moving vehicle, which its finite element formulation was developed in the previous chapter.

4.1.2 Optimization Fundamentals

Generally, the most important terminologies in optimization can be represented as followed:

Design variables: Design variables are entities that identify a particular design. These entities will change over a prescribed range in the search for the optimal design. In applied mathematical terminology, design variables are the unknown of the problem being solved. The set of design variables is identified as the design vector.

Objective function: Design optimization problem is defined by an objective function which usually has to be minimized or maximized. The objective function must depend, explicitly or implicitly, on the design variables.

Constraint functions: As design functions, these will be influenced by the design variables. The format of these functions requires them to be compared to some

numerically limiting values set up by the design requirements, or the designer. These limiting values stay constant during the optimization. The constraint functions can be classified as equality constraints or inequality constraints.

Problems without constraints are called unconstrained problems. If constraints present, then meeting them is more necessary than the optimum. Constraint satisfaction is crucial before the design established by the current value of the design variables is considered valid and acceptable. If constraints are not satisfied, also called "Violated", then there is no solution.

Side constraints: The range for the design variables are expressed by side constraints. Each design variable must be bounded by numerical values for its lower and upper limit.

The standard format for an optimization problem can be expressed as:

Minimize	$f(x_1, x_2, ..., x_n)$	(Objective function)
Subject to	$g_i(x_1, x_2, ..., x_n) = 0 \;,\; i = 1, 2, ..., m_e$	(Equality constraints)
	$g_i(x_1, x_2, ..., x_n) \le 0 \;,\; i = m_e + 1, ..., m$	(Inequality constraints)
	$x_j^l \le x_j \le x_j^u \;,\; j = 1, 2, ..., n$	(Side constraints)

Based on the above mentioned definition, an optimal solution is one that has met the design objective while it remains in the feasible domain (satisfies all the constraints).

4.1.3 Optimization Technique

Here, the Sequential Quadratic Programming (SQP)[98], which is one of the most powerful methods among the mathematical nonlinear programming techniques, has been employed to solve the design optimization problem regarding TMD. The computer implementation of the algorithm has been performed in MATLAB© environment. This method allows Newton's method for the constrained optimization to be closely mimicked just like that of unconstrained optimization. Using the quasi-Newton updating method, the Hessian of the Lagrangian function has to be approximated for every iteration to create a Quadratic Programming (QP) sub-problem. The solution of the QP sub-problem is used to form a search direction for a line search procedure.

The general problem can be written as:

Minimize $f(x)$ with respect to $x \in \Omega$,

Where $\Omega = \left\{ x \in R^n / g_i(x) = 0, i \in (1,\ldots,m_e),\ g_i(x) \le 0, i \in (m_e+1,\ldots,m) \right\}$

The main idea is to generate a QP problem based on a quadratic approximation of the Lagrangian function described as:

$$L(x,\lambda) = f(x) + \sum_{i=1}^{m} \lambda_i g_i(x) \tag{4.1}$$

where *f(x)* denotes the objective function and the equality and inequality constraints are given by $g_i(x) = 0$ and $g_i(x) \le 0$ respectively. i is an index for variables and functions associated with a particular constraint, i. For λ without a subscript indicates the vector with elements λ_i, which are taken to be independent variables.

The SQP implementation in MATLAB© consists of three main stages:

(I) Quadratic programming problem solution

(II) Line search and calculation of the merit function

(III) Update the Hessian matrix of the Lagrangian function

At each major iteration, a QP sub-problem of the following form is solved:

Minimize J_k (with respect to d):

$$\begin{aligned} J_k &= \frac{1}{2} d^T H_k d + \nabla f(x_k)^T d && d \in R^n \\ \nabla g_i(x_k)^T d + g_i(x) &= 0 && i \in \{1,\ldots,m_e\} \\ \nabla g_i(x_k)^T d + g_i(x) &\le 0 && i \in \{me+1,\ldots,m\} \end{aligned} \tag{4.2}$$

where H is the Hessian of the Lagrangian, denoted by

$$H(x,\lambda) := \nabla^2_{xx} L(x,\lambda) \tag{4.3}$$

H_k indicates the approximate Hessian of L at the current iteration x_k.

The solution is used to form a new iterate:

$$x_{k+1} = x_k + \alpha_k d_k \tag{4.4}$$

The step length parameter α_k should be determined by using an appropriate line search technique (one-dimensional minimizations) in order to produce a sufficient decrease in the merit function. At the end of the one-dimensional minimization, the Hessian of the Lagrangian, required for the solution of the next positive definitive quadratic programming problem, is updated using the Broyden-Fletcher-Goldfarb-Shanno (BFGS) updating formula as:

$$H_{k+1} = H_k + \frac{q_k q_k^T}{q_k^T s_k} - \frac{H_k^T s_k s_k^T H_k}{d_k^T H_k d_k} \tag{4.5}$$

where

$$s_k = x_{k+1} - x_k \tag{4.6}$$

$$q_k = \nabla f(x_{k+1}) + \sum_{i=1}^{m} \lambda_i . \nabla g_i(x_{k+1}) - \left(\nabla f(x_k) + \sum_{i=1}^{m} \lambda_i . \nabla g_i(x_k) \right) \tag{4.7}$$

and H_{k+1} is the approximated Hessian of L at x_{k+1}.

A complete overview of the SQP can be found in the work by Nocedal and Wright[98], Arora[99] and Fletcher[100]

4.2 Optimization Procedure

4.2.1 Preliminaries

The formulation of a Timoshenko beam traversed by a moving vehicle with n attached TMDs has been presented in Chapter 2. Here, the aim is to suppress the vibration of this beam by optimal designing of the attached single TMD. As stated earlier, the natural frequency of TMD is usually tuned in resonance with the one of the modes of the beam, so that a large amount of the structural vibrating energy is transferred to the TMD and then dispersed by the damping as the primary structure is subjected to external disturbances.

In order to attain the best performance of the TMD, it is necessary to optimize the parameters of the TMD system to make the beam vibration as small as possible. The TMD parameters include its number, mass, stiffness, damping and its location on the beam. In this thesis, the optimization is performed using one TMD and since the fundamental vibration mode of the beam is dominant in the dynamic behavior of the beam (since the maximum deflection of the beam typically takes place around the midspan, as shown in Figures 2-9 and 2-10) the TMD system is designed to be tuned at the first mode of the beam and therefore, it is placed at the beam mid-point. Due to practical implementation, the mass of the TMD is usually assumed to be a known parameter. As a result, the stiffness and damping of the TMD are considered as the design variables to be optimized.

For the sake of numerical simplicity, all the design variables and the mass of TMD are transformed into dimensionless parameters as:

$$\mu = \frac{M_{TMD}}{M_{structure}}, f_{TMD} = \frac{\omega_{TMD}}{\omega_n}, \xi_{TMD} = \frac{C_{TMD}}{2\sqrt{K_{TMD} M_{TMD}}} \tag{4.8}$$

where ω_n is the nth natural frequency of the beam without TMD, $\omega_{TMD} = \sqrt{K_{TMD} / M_{TMD}}$ and $M_{structure}$ is the total mass of the beam. It should be noted that in practice, the mass ratio of the TMD to the beam is greater than 10%.

Now, the optimization problem for the Timoshenko beam with the attached TMD and known mass ratio (μ), under the moving half car model can be described as:

Find the design variables:	$\{X\} = \{\xi_{TMD}, f_{TMD}\}$
to minimize:	*Max Amplitude in frequency response of midspan* (4.9)
with the constraints:	$0 \le \xi_{TMD} \le 1, 0 \le f_{TMD} \le 2.5$

The SQP method, as described in Section 4.1.3, has been used to solve the above design optimization problem. The computer implementation of the algorithm has been performed in MATLAB© environment. As mentioned before, due to the fact that the dynamic responses of a beam system without a TMD are mostly dominated by the first mode, the design of the TMD is based on this mode, and the maximum displacement at the beam mid-point is considered as the vibration control criterion.

4.2.2 Numerical Results

The properties of the beam are presented in Table 4-1. The finite element formulation, developed in Chapter 2, is used to find the response of the beam.

Table 4-1 Properties of the Timoshenko Beam

Beam Length	70 (m)	Shear Coefficient (K_s)	0.83
Elastic Modulus	207 (GPa)	Beam Structural Damping	7000 (Ns/m)
Poisson's Ratio	0.3	Cross Sectional Area	4.94 (m^2)
Mass per Unit Length (ρ)	20000 (Kg/m)	Second Moment of Inertia	0.174 (m^4)

It should be noted that, according to Eq. 2.57, the damping ratio for the first mode of the beam is 6.5%. The first 3 natural frequencies of the beam obtained by the finite element method are compiled in Table 4-2.

Table 4-2 The First Three Natural Frequencies of the Tmishenko Beam by FEM Method

ω_1 (Hz)	ω_2 (Hz)	ω_3 (Hz)
0.4304	1.7251	3.8936

The properties of the half car model are the same as described in Table 2-2. As the maximum displacement of the beam midspan is the decisive factor, it has been plotted versus different vehicle speeds in Figure 4-1. The result shows that when the vehicle travels at 130 Km/h, the maximum traversal deflection at the midspan attains its highest value. Thus it can be considered as the critical speed of the vehicle. Here, the parameters of TMD are optimally designed for this critical speed.

As pointed out in Eq. 4.9, the objective function is the response due to the first vibration mode in the midspan. For this purpose, it is required to convert the displacement from the time domain to the frequency domain. This conversion can be performed by the Fast Fourier Transform (FFT)[101] of the response at the beam midspan[102].

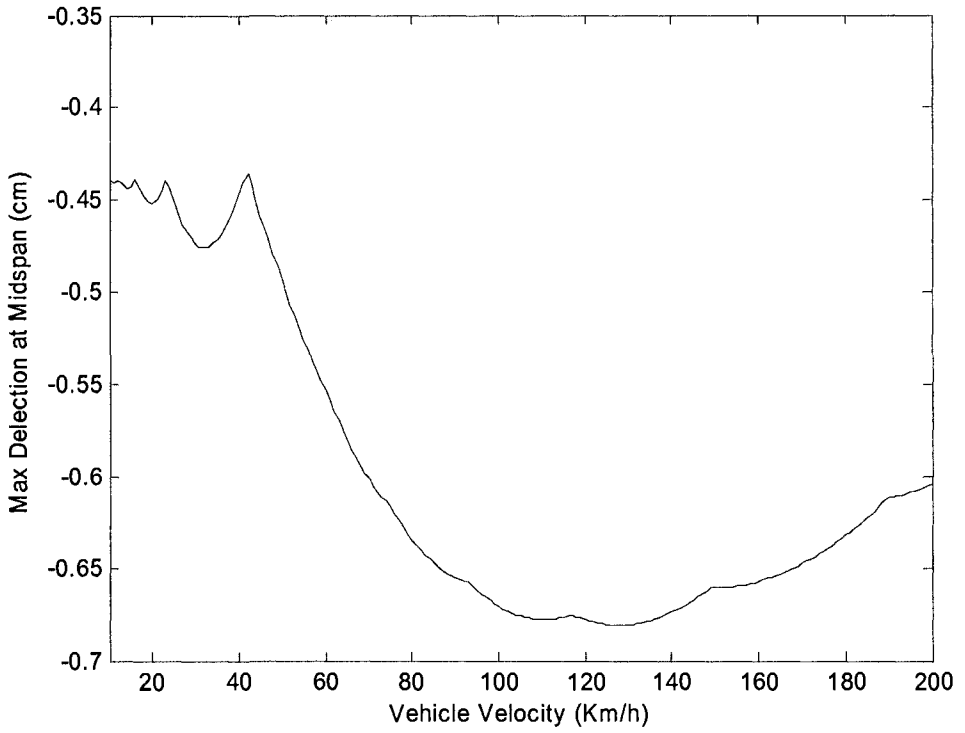

Figure 4-1 Max Beam Midspan Deflection versus Vehicle Velocity

As the Fast Fourier Transform is discrete, the number of sampling has been increased (2^{20} points in the frequency range of 0-10 Hz), so that the transform becomes almost close to the continuous Fourier transform. In other words, the objective can now be defined as the minimization of the maximum point in the FFT of the beam mid-point response versus frequency diagram, which actually is located close to the first natural frequency of the beam.

The variation of the optimum frequency ratio of the TMD (f_{TMD}) with respect to the TMD mass ratio (μ) is illustrated in Figure 4-2. It can be observed that as the mass ratio increases, the optimum frequency ratio will decrease.

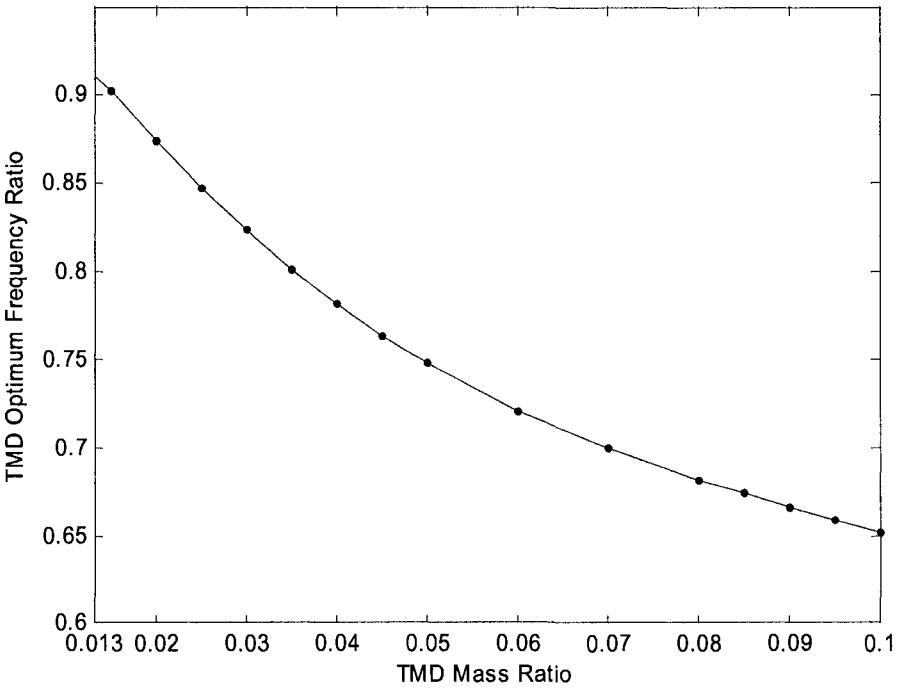

Figure 4-2 The Optimum TMD Frequency Ratio versus TMD Mass Ratio for V=130 Km/h

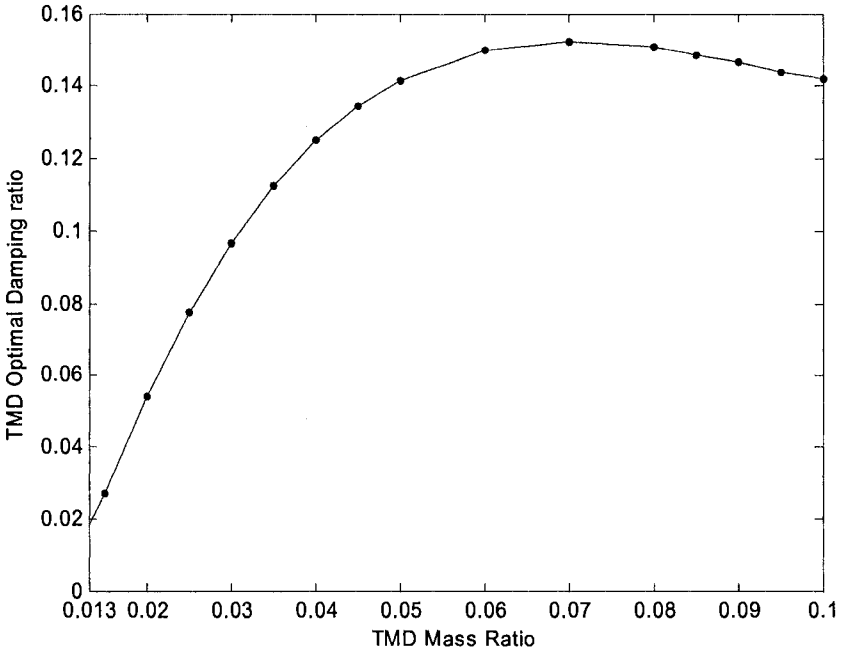

Figure 4-3 The Optimum TMD Damping Ratio versus TMD Mass Ratio for V=130 km/h

The optimal damping factor of the TMD (ξ_{TMD}) versus the TMD mass ratio is plotted in Figure 4-3. It can be noticed that by increasing the mass ratio, the optimum damping ratio of the TMD levitates. However, after the mass ratio reaches to around 7%, the optimum damping ratio adopts an almost constant amount with small decrease.

The minimized objective function versus the TMD mass ratio has been plotted in Figure 4-4. The results indicate that the increase of the mass ratio enhances the aptitude of minimization of the objective function. However, it should be noted that although the increase of TMD mass ratio can achieve higher vibration control efficiency, it brings about much more static deflections at the same time. Therefore, the mass ratio should be such chosen by considering all aspects of the bridge design.

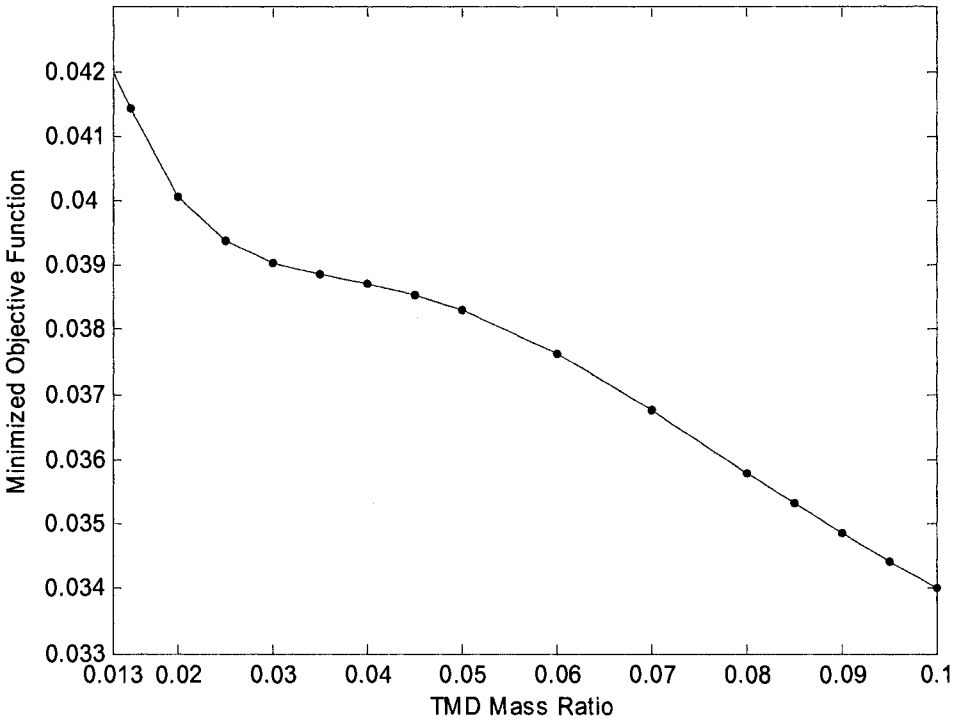

Figure 4-4 TMD Minimized Objective Function versus the TMD Mass Ratio for V=130 Km/h

The optimum design parameters of a TMD with the mass ratio of 5% have been presented in Table 4-3. The FFT diagram of the beam midspan response versus the frequency has been presented in Figure 4-5 for this optimum configuration.

Table 4-3 Optimal Results for the Mass Ratio of 5%

	TMD Optimal Frequency	
TMD Mass Ratio	Ratio	TMD Optimal Damping Ratio
0.05	0.747553	0.141695

It can be observe that in the case of no TMD, the peak value of the graph is located around the fundamental frequency of the beam which represents the first resonant frequency. The effect of the tuned damping induced by the optimal TMD is noticeable in the diagram. The combined system in this case encounters two resonant frequencies around the relative tuned frequency with significantly minor responses due to the optimal TMD.

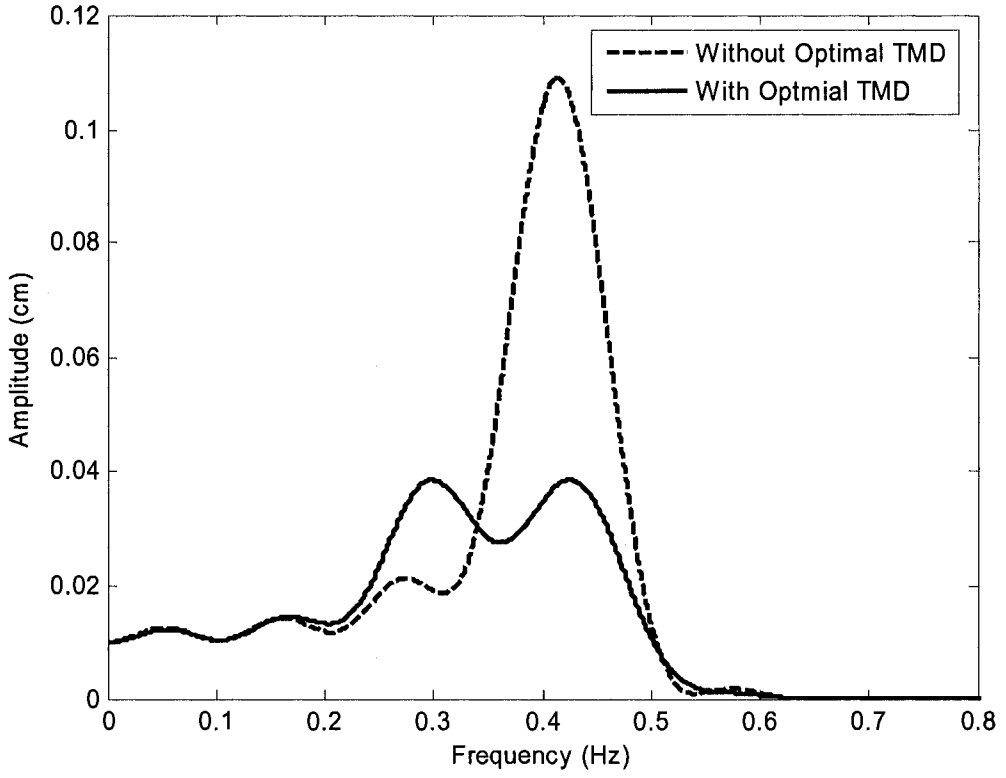

Figure 4-5 FFT for Beam midspan response with and without TMD

Moreover, to exemplify the efficiency of the optimal frequency ratio of the TMD, the robustness test has been carried out. The FFT of the beam mid-point response with respect to 20% deviation of the optimal TMD frequency is illustrated in Figure 4-6. The consequence of the deviation of the frequency ratio from its optimal value is found to be remarkable. That is to say that a small deviation of the frequency ratio may cause off-tuning and hence, results into large changes in the system performance.

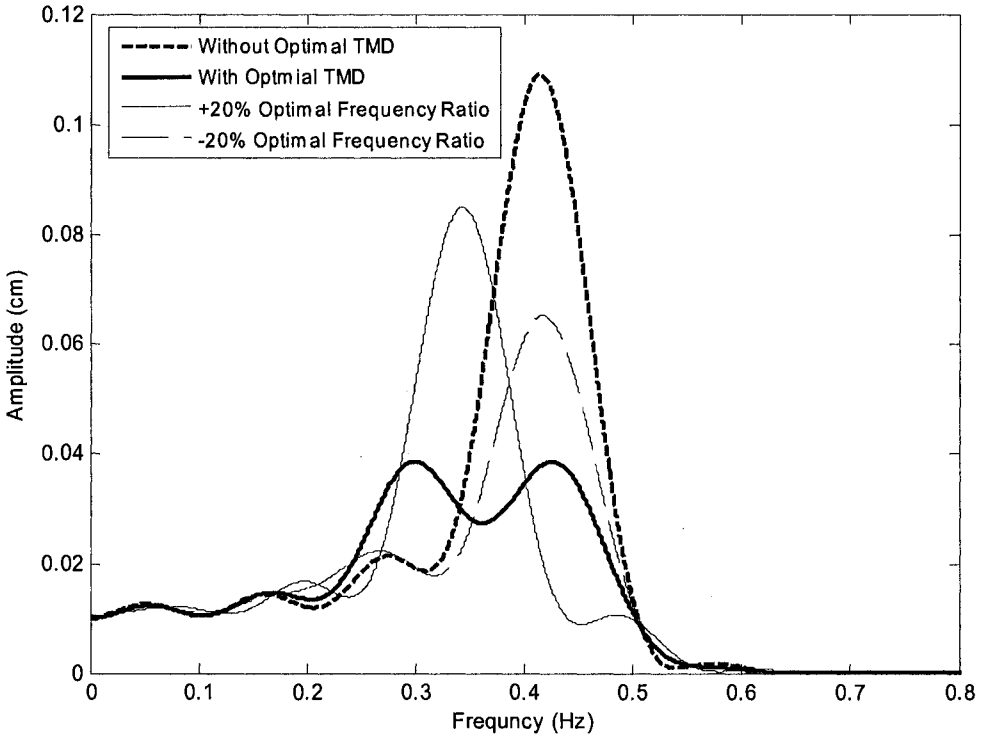

Figure 4-6 The Robustness Test for Optimal Frequency Ratio of TMD

A similar diagram has been plotted in Figure 4-7, where the robustness test has been performed for the optimal TMD damping ratio. The effect of divergence from the optimal value of the damping ratio can be observed from the diagram. It can be seen that the

effect of deviations from the optimal value of damping ratio is smaller than the effect of the variation in the optimal frequency ratio. However, this deviation is also capable of changing the maximum amplitude of the frequency response.

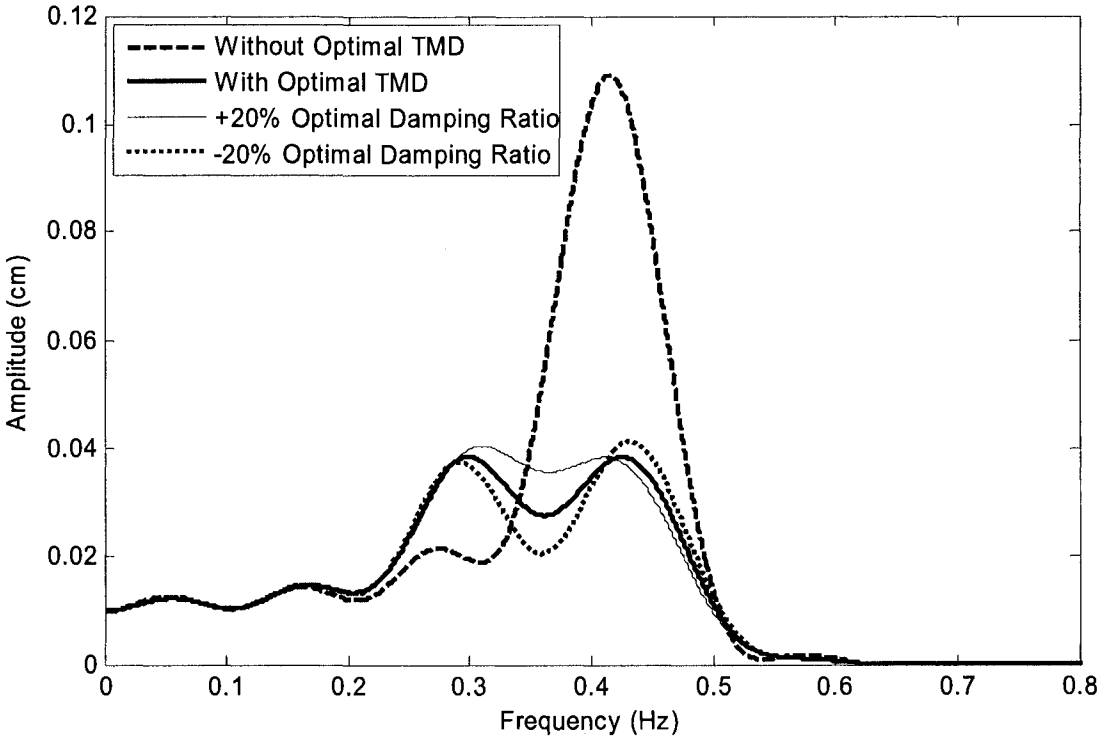

Figure 4-7 The Robustness Test for Optimal Damping ratio of TMD

After acquisition of the optimal TMD parameters, the effect of the optimal TMD should be studied on the beam response in the time domain. Figure 4-8 shows the beam mid-point deflection both before and after attaching the optimal TMD to the system. The beam midspan deflections, for four consecutive peaks of the response have been compiled in Table 4-4. It is interesting to see that by adding the optimal TMD a significant faster damping can be achieved. This is to say, as time passes, the effect of the

optimal TMD in the vibration dissipation becomes more significant, and hence, the difference from 3.28% at the first peak (t = 1.5 s) will become 77.81% at the fourth peak (t = 5.1 s).

Table 4-4 Beam Midspan Deflection with and without Optimal TMD

Time(s)	1.5	2.8	4	5.1
Midspan deflection without TMD (cm)	-0.6858	0.5165	-0.4198	0.3443
Midspan deflection with TMD (cm)	-0.6633	0.4179	-0.2228	0.0764
Percentage difference (%)	3.28	19.09	46.92	77.81

In order to investigate the effectiveness of TMD to suppress vibration more inclusively, an energy performance index evaluated at the beam mid-point can be defines as[103]:

$$e = \frac{1}{2}[Q]^T_{midspan}\left[\bar{K}\right][Q]_{midspan} \tag{4.10}$$

where $[Q]_{midspan}$ is the midspan response vector and $\left[\bar{K}\right]$ can be an arbitrary weighting matrix, here chosen as an identity matrix. The values of this index for the case with and without TMD are provided in Table 4-5. It can be observed that the optimal TMD was capable of reducing the midspan response energy by 87.91% during 20 seconds.

Table 4-5 Beam midspan energy with and without Optimal TMD

Energy without optimal TMD	Energy with optimal TMD	Percentage difference (%)
21.3891	2.5860	87.91

These results show that by adding the optimal TMD one can effectively reduce the vibration of the beam due to passage of the vehicle.

4.3 Conclusion

A design optimization method has been developed in which, the previously derived finite element model of a Timoshenko beam, with an attached TMD at its mid-point, traversed by moving vehicle has been combined with the Sequential Quadratic Programming (SQP) technique in order to obtain the optimal design parameters of the TMD to efficiently attenuate the vibration amplitude of the beam caused by the passage of vehicle.

Subsequently, the effect of the mass ratio of the TMD on the optimal frequency and damping ratio of the TMD and the minimization of the objective function has been studied. Finally, the effect of adding an optimal TMD with the mass ratio of 5% on the beam midspan deflection has been investigated.

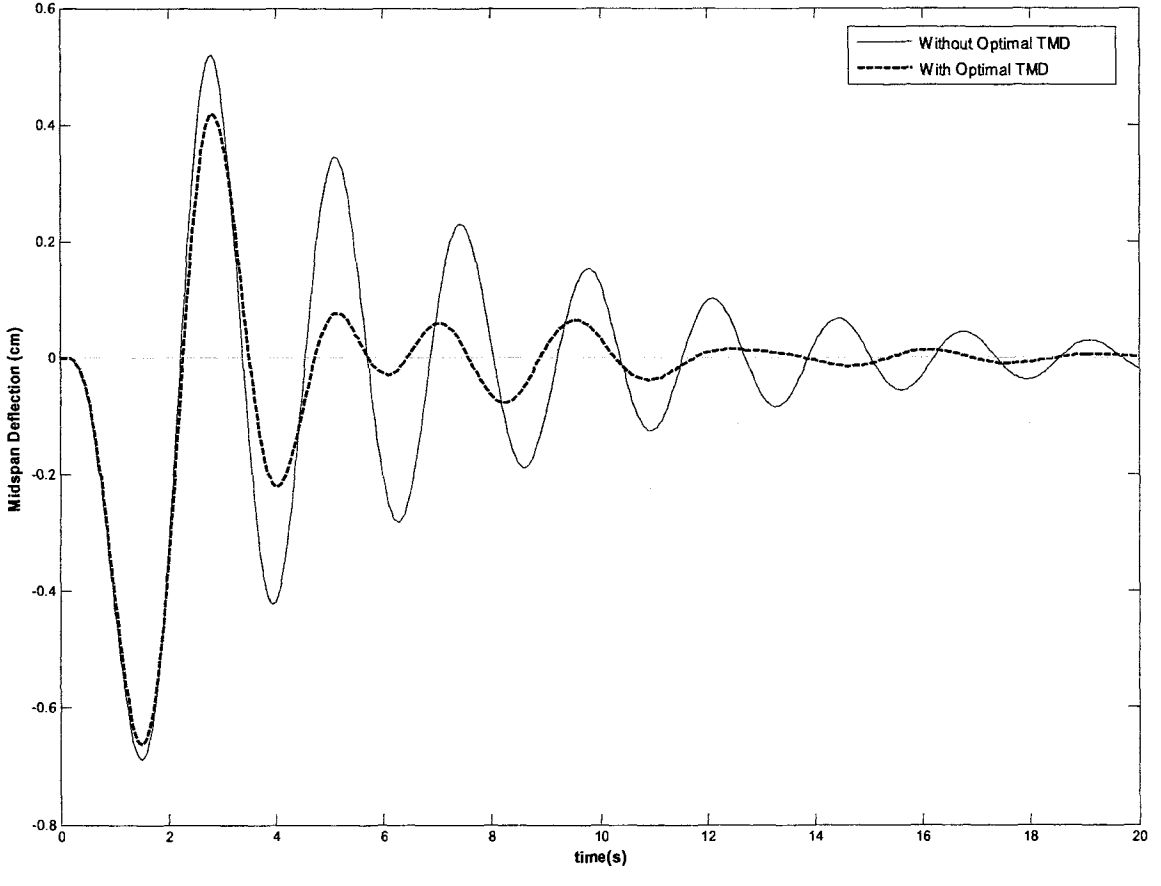

Figure 4-8 Beam Midspan deflection with and without Optimal TMD

Chapter 5: CONCLUSIONS AND FUTURE WORKS

5.1 Introduction

In this study a comprehensive finite element model has been developed to investigate the dynamic behavior of a Timoshenko beam subjected to a moving vehicle in the form of a half car model. The model has been validated by comparing the results with those reported in literature. The results for the beam deflections obeying the Euler-Bernoulli beam and the Timoshenko beam theories have been compared. Moreover, further comparison was performed between the results obtained for the systems including the half car model and a simple quarter car model.

The finite element formulation for a Timoshenko beam with n attached TMDs has been derived, and then combined with the governing equations of the beam vibration traversed by the moving half car model in the finite element form, in order to obtain the total finite element equations of motion for the combined system of Beam-Vehicle-TMD.

Finally, the developed formulations have been utilized to conduct the design optimization procedure using the Sequential Quadratic Programming (SQP) technique. The optimization has been performed to suppress the vibration of the beam under moving vehicle by attaching a single TMD to the beam midspan. The maximum amplitude of the frequency response of the beam has been minimized while the mass and the location of the TMD have been considered as the known parameters and the TMD frequency and damping ratios have been chosen as the design variables.

5.2 Contributions and Conclusions

The most important contributions of the current work can be described as:

- Development of a comprehensive finite element model in order to simulate the behavior of a Timoshenko beam traversed by a half car model having six degree-of-freedom, with and without the attached TMDs.
- Establishment of a design optimization scheme in which, the developed finite element model is combined with the formal gradient based optimization technique to determine the optimal parameters of the TMD with the purpose of efficiently suppressing the vibration of the beam traversed by moving vehicle.

The most significant conclusions of this study can be summarized as:

- The Euler-Bernoulli beam theory generally underestimates the beam response due to moving vehicles. Although the difference is not much in the nominal vehicle velocities, the error becomes more significant as the vehicle velocity increases.
- The half car model provides a more exact model when compared to the quarter car model. As time passes, the difference in the beam response becomes more considerable. However, the quarter car model is capable of predicting the beam response to some extent.
- By utilizing the design optimization method the optimal parameters of a TMD can be determined from which, the vibration of the beam due to the moving vehicle is suppressed. The results show that by increasing the mass ratio of the TMD the optimal frequency ratio decreases; however the optimal damping ratio has an escalating pattern.

- Results obtained for the optimal tuned mass dampers also show that as the mass of the TMD increases, higher vibration control efficiency can be achieved. However, as the enhancement of the TMD mass causes more static deflection and also can change the dynamic properties of the main system, the value of the TMD mass ratio should be chosen considering all aspects of the structure design and should not be greater than 10%.
- The results illustrate that compared with the uncontrolled structure the optimal TMD can considerably decrease the structural frequency response at its tuned frequency. The combined system in this case exhibit two natural frequencies around the tuned frequency with notably smaller responses owing to the optimal TMD.
- Based on the obtained results, the effect of the deviation in the optimal frequency ratio in the system behavior is much more substantial than the optimal damping factor for a designed optimal TMD.
- The results indicate that adding an optimal TMD to the system will lead to a faster vibration suppression of the system and can effectively reduce the amplitude in the time domain.

5.3 Future works

Although important contributions towards the finite element analysis of a Timoshenko beam subjected to a moving vehicle and the design optimization of a TMD to passively control the vibration have been accomplished in this thesis, other important and interesting subjects for future works are identified as:

- The vehicle in this study has been considered as a half car model with six degrees of freedom. The three-dimensional car model can be considered to present a more inclusive model.
- The analysis has been performed for a single vehicle traveling on the bridge. It would be interesting to increase the number of moving vehicles to provide a more realistic case study.
- In this work, the vehicle velocity is assumed to be constant. The natural extension to this work is to obtain the response and optimal parameters of TMD due to variable vehicle speed.
- The surface of the bridge has been assumed to be completely smooth and without irregularities. It would be more practical to consider the surface roughness and study its effect on the vehicle-bridge interaction.
- It would be interesting to utilize several tuned mass dampers attached at different beam locations to be tuned to different vibration modes and study their performance.
- The developed finite element equations can easily be extended to plate-type structures under moving vehicles.

References

1. E. P. Popov, Mechanics of Materials (2nd edition), Prentice Hall, Englewood Cliffs, N. J., 1976.

2. S. P. Timoshenko, History of Strength of Materials, McGraw Hill, 1953.

3. J. W. S. Baron Rayleigh, The Theory of sound (2nd edition), Macmillan, London, 1894 (republished by: Dover Publications, New York, N.Y., 1945)

4. S.M. Han, H. Benaroya and T. Wei, "Dynamics of Transversely Vibrating Beams Using Four Engineering Theories", *Journal of Sound and Vibration*, **225**(5), 1999, pp. 935-988.

5. N. Challamel, "On the Comparison of Timoshenko and Shear Models in beam Dynamics", *Journal of Engineering Mechanics*, **132**(10), 2006, pp. 1141-1145.

6. S. P. Timoshenko, "On the Correction for Shear of the Differential Equations for Transverse Vibrations of Bars of Uniform Cross-Section", *Philosophical Magazine,* **41**, 1921, pp. 744-746.

7. J. Sutherland and L. Goodman, "Vibration of Prismatic Bars Including Rotary Inertia and Shear Corrections", *Report No. N6-ORI-71 T06*, 1951, Department of Civil Engineering, University of Illinois, Urbana, Illinois.

8. P. A. A. Laura, M. J. Maurizi and R. E. Rossi, "A Survey of Studies Dealing With Timoshenko Beams", *The Shock and Vibration Digest*, **22** (11), 1990, pp. 3-10.

9. T. C. Huang, "Effect of Rotary Inertia and Shear on the Vibrations of Beams Treated by the Approximate Methods of Ritz and Galerkin", *Proceeding of the 3rd U.S. National Congress of Applied Mechanics*, 1958, pp. 189-194.

10. R. Anderson, "Flexural Vibrations in Uniform Beams According to the Timoshenko Theory", *Journal of applied Mechanics, Transaction of the American Society of Mechanical Engineers*, **20**, 1953, pp. 504-510.

11. C. Dolph, "On the Timoshenko Theory of Transverse Beam Vibrations", "*Quarterly of Applied Mathematics*", **12**, 1954, pp. 175-178.

12. T. C. Huang, "The Effect of Rotary Inertia and of Shear Deformation on the Frequency and Normal Mode Equations of Uniform Beams with Simple End Conditions", *Journal of Applied Mechanics, Transaction of the American Society of Mechanical Engineering,* **83**, 1961, pp. 579-584.

13. D. L. Thomas, J. M. Wilson and R. R. Wilson, "Timoshenko Beam Finite Elements", *Journal of Sound and Vibration*, **31**(3), 1973, pp. 315-330.

14. R. B. McCalley, "Rotary Inertia Correction for Mass Matrices", *General Electric Knolls Atomic Power Laboratory*, 1963, Report DIG/SA 63-73, Schenectady, New York.

15. J. S. Archer, "Consistent Matrix Formulations for Structural Analysis Using Finite Element Techniques", *American Institute of Aeronautics and Astronautics Journal*, **3**,1965, pp. 1910-1918

16. J. S. Przemieniecki, Theory of Matrix Structural Analysis, McGraw Hill, 1968 (republished by Dover Publication, 1985).

17. K. K. Kapur, "Vibrations of a Timoshenko Beam Using Finite Element Approach", *Journal of the acoustical Society of America*, **40**, 1966, pp. 1058-1063.

18. W. Carnegie, J. Thomas and E. Dokumaci, "An Improved Method of Matrix displacement Analysis in Vibration Problems", *The Aeronautical Quarterly*, **20**, 1969, pp. 321-332.

19. J. Thomas and B. A. H. Abbas, "Finite Element Model for dynamic Analysis of Timoshenko Beam", *Journal of Sound and Vibration*, **41**(3), 1975, pp. 291-299.

20. D. J. Dawe, "A Finite Element for the Vibration Analysis of Timoshenko Beams", *Journal of Sound and Vibration*, **60**(1), 1978, pp. 11-20.

21. A. E. Lees and D. L. Thomas, "Unified Timoshenko Beam Finite Element", *Journal of Sound and Vibration*, **80**(3), 1982, pp. 355-366.

22. G. Prathap and G. R. Bhashyam, "Reduced Integration and the Shear Flexible Beam Element", *International Journal of Numerical Method in Engineering* **18**(2), 1982, pp. 195-210.

23. J. N. Reddy, An Introduction to the Finite Element Method, McGraw Hill, 1984, 1993, 2005.

24. O. C. Zienkiewicz, R.L. Taylor and J.M. Too, "Reduced Integration Technique in General Analysis of Plates and Shells", *International Journal of Numerical Methods in Engineering* **3**(2), 1971, pp. 275-290.

25. T. J. R. Hughes, R. L. Taylor and W. Kanoknukulchai, "A Simple and Efficient Finite Element for Plate Bending", *International Journal of Numerical Methods in Engineering*, **11**(10), 1977, pp. 1529-1543.

26. E. D. L. Pugh, E. Hinton and O. C. Zienkiewicz, "A Study of Quadrilateral Plate Bending Elements With Reduced Integration, *International Journal of Numerical Methods in Engineering*, **12**(5), 1978, pp. 1059-1079.

27. H. Stolarski, N. Carpenter and T. Belytschko, "A Kirchoff-mode Method for c^0 Bilinear and Serendipity Plate Elements", *Journal of Computer Methods in Applied Mechanics and Engineering*, **50**(2), 1985, pp. 121-145.

28. I. Fried, "Shear in c^0 and c^1 Bending Finite Elements", *International Journal of Solids and Structures* **9**(4), 1973, pp. 449-460.

29. D. J. Dawe and S. Wang, "Vibration of Shear-Deformable Beams Using a Spline-Function Approach", *International Journal of Numerical Methods in Engineering*. **33**(4), 1992, pp. 819-844.

30. F. T. K. Au , Y. S. Cheng and Y. K. Cheung, "Vibration Analysis of Bridges under Moving Vehicles and Trains: An Overview", *Progress in Structural Engineering and Materials* **3**(3), 2001, pp. 299-304

31. G. G. Stokes, Discussion of a Differential Equation Relating to the Breaking of Railway Bridges, *Transaction of the Cambridge Philosophical Society*, Part 5-85, 1849, pp. 707-735.

32. R. Willis, Appendix to the Report of the Commissioners Appointed to Inquire into Application of Iron to Railway Structures, London H. M. Stationary, 1849.

33. S. P. Timoshenko, "Forced Vibration of Prismatic Bars", *Izvestiya Kievskogo politekhnicheskogo instituta* (1908) (In Russian).

34. S. P. Timoshenko, "On Forced Vibration of a Bridges", *Philosophical Magazine Series*, 6 (43), 1922, pp. 1018-1019.

35. A. N. Krylov, *Mathematical Collection of Papers of the Academy of Science, (Matematischeskii sbornik Akademii Nauk)* **61**, Petersburg, 1905.

36. C. E. Inglis, A Mathematical Treatise on Vibration in Railway Bridges, Cambridge University Press, 1934.

37. L. Frýba, Vibration of Solid and Structures under Moving Loads, Telford Books, Prague, 1972, 1989, 1999.

38. S. P. Timoshenko, D. H. Young and W. Weaver, Vibration Problems in Engineering, John Wiley and Sons, New York, 1974.

39. G. B. Warburton, The Dynamic Behavior of Structures, Pergamon Press, Oxford, 1976.

40. S. H. Crandall, "The Timoshenko Beam on an Elastic Foundation", *Proceeding of the Third Midwestern Conference on Solid Mechanics*, Ann Arbor, Michigan, 1957, pp. 146-159.

41. A. L. Florence, "Traveling Force on a Timoshenko Beam", *Journal of Applied Mechanics, Transaction of the American Society of Mechanical Engineering* **32**, 1965, pp. 351-358.

42. C. R. Steele, "The Timoshenko Beam With a Moving Load", *Journal of Applied Mechanics, Transaction of the American Society of Mechanical Engineering* **35**, 1968, pp. 481-488.

43. C. C. Huang, "Traveling Loads on a Viscoelastic Timoshenko Beam", *Journal of Applied Mechanics, Transaction of the American Society of Mechanical Engineering* **44**, 1977, pp. 183-184.

44. S. Mackertich, "Moving Load on a Timoshenko Beam", *Journal of acoustical Society of America*, **88**(2), 1990, pp. 1175-1178

45. H. H. Jeffcott, "On the Vibration of Beams under the Action of Moving Loads", *Philosophical Magazine, Series* 7 (8), 1922, pp. 66-97

46. V. V. Bolotin, The Dynamic Stability of Elastic Systems, Holden-Day Press, San Francisco, 1964.

47. M. M. Stanišić and J. C. Hardin, "On the Response of Beams to an Arbitrary Number of Concentrated Moving Masses", *Journal of the Franklin Institute* **287**(2), 1969, pp. 115-123.

48. C. M. Leach and B. Tabarrok, "The Timoshenko Beam under the Influence of a Traveling Mass", *Proceeding of the Symposium on Structural Dynamics* **2**, 1970, pp. 1-27.

49. S. Sadiku and H. H. E. Leipholz, "On the Dynamics of Elastic Systems with Moving Concentrated Masses", *Ingenieur Archiv* **57**, 1987, pp. 223-242.

50. J. E. Akin and M. Mofid, "Numerical Solution for Response of Beams With Moving Mass", *Journal of Structural Engineering, ASCE* **115**(1), 1989, pp. 120–131

51. E. Esmailzadeh and M. Ghorashi, "Vibration Analysis of Beams Traversed by Uniform Partially Distributed Moving Masses", *Journal of Sound and Vibrations* **184**(1), 1995, pp. 9-17

52. E. Esmailzadeh and M. Ghorashi, "Vibration Analysis of a Timoshenko Beam Subjected to Traveling Mass", *Journal of Sound and Vibrations* **199**(4), 1997, pp. 615-628

53. R. K. Wen, "Dynamic Response of Beams Traversed by Two-Axle Loads", *Journal of the Engineering Mechanics Division, ASCE* **86**(5), 1960, pp. 91-111.

54. K. T. Sundara and K. S. Jagadish, "Dynamic Response of Highway Bridges to Moving Loads", *International Association for Bridge and Structures Engineering (IABSE)* **20**(2), 1970, pp. 57-76.

55. E. S. Hwang and A. S. Nowak, "Simulation of Dynamic Load for Bridges", *Journal of Structural Engineering (ASCE)* **117**(5), 1991, pp. 1413-1434.

56. Y. B. Yang, S. S. Liao and B. H. Lin, "Impact Formulas For Vehicle Moving Over Simple and Continuous Beams", *Journal of Structural Engineering (ASCE)* **121**(11), 1995, pp. 1644-1650.

57. K. Henchi, M. Fafard, M. Talbot and G. Dhatt, "An Efficient Algorithm for Dynamic Analysis of Bridges under Moving Vehicles Using a Coupled Modal and Physical Components Approach", *Journal of Sound and Vibration* **212**(4), 1998, pp. 663-683

58. E. Esmailzadeh and N. Jalili, "vehicle-passenger-Structure Interaction of Uniform Bridges Traversed by Moving Vehicles, *Journal of Sound and Vibration* **260**(4), 2003, pp. 611-635

59. D. M. Yoshida and W. Weaver, "Finite Element Analysis of Beams and Plates with Moving Loads", *International Association for Bridge and Structures Engineering (IABSE)* **31**(1), 1971, pp. 179-195

60. F. V. Filho, "Finite Element Analysis of Structures under Moving Loads", *Shock and Vibration Digest*, **10**(8), 1978, pp .27–35.

61. J. Hino, T. Yoshimura, K. Konishi and N. Ananthanarayana, "A Finite Element Method Prediction of the Vibration of a Bridge Subjected to a Moving Vehicle Load", *Journal of Sound and Vibrations* **96**(1), 1984, pp. 45–53.

62. J. Hino, T. Yoshimura and N. Ananthanarayana, "Vibration Analysis of Non-linear Beams Subjected to a Moving Load Using the Finite Element Method. *Journal of Sound and Vibrations* **100**(4), 1985, pp. 477–491

63. M. Olsson, Finite element, modal co-ordinate analysis of structures subjected to moving loads. *Journal of Sound and Vibrations* **99**(1), 1985, pp. 1–12.

64. J. S. Wu, M. L. Lee and T. S. Lai, "The dynamic Analysis of a Flat Plate under a Moving Load by the Finite Element Method", *International Journal of Numerical Methods in Engineering* **24**(4), 1987, pp. 743-762

65. Y. H. Lin and M. W. Trethewey, "Finite Element Analysis of Elastic Beams Subjected to Moving Dynamic Loads, *Journal of Sound and Vibrations* **136**(2), 1990, pp. 323–342

66. L. Frýba, S. Nakagiri, and N. Yoshikawa, " Stochastic Finite Elements for a Beam on Random Foundation with Uncertain Damping under a Moving Force", *Journal of Sound and Vibrations* **163**(1), 1993, pp. 31–45.

67. Y. B. Yang and B. H. Lin, "Vehicle-Bridge Interaction Analysis by Dynamic Condensation Method", *Journal of Structural Engineering (ASCE)* **121**(11), 1995, pp. 1636-1643.

68. Y. B. Yang and J. D. Yau, "Vehicle-Bridge Interaction Element for Dynamic Analysis", *Journal of Structural Engineering (ASCE)* **123**(11), 1997, pp. 1512-1518.

69. Y. B. Yang, C. H. Chang and J. D. Yau, "An Element for Analyzing Vehicle-Bridge Systems Considering Vehicle's Pitching Effect", *International Journal of Numerical Methods in Engineering* **46**(7), 1999, pp. 1031-1047.

70. Y.S. Cheng, F.T.K. Au and Y.K. Cheung, " Vibration of Railway Bridges under a Moving Train by Using Bridge Track-Vehicle Element", *Engineering structures* **23**(12), 2001, pp. 1597-1606.

71. C. G Koh, J. S. Y. Ong, D. K. H., Chua and J. Feng, "Moving Element Method for Train-Track Dynamics." *International Journal of Numerical Methods in Engineering* **56**(11), 2003, pp. 1549–1567.

72. K. Hou, J. Kalousek and R. Dong, "A Dynamic Model for an Asymmetrical Vehicle–Track System" *Journal of Sound and Vibrations* **267**(3), 2003, pp. 591–604.

73. T. H. Young and C. Y. Li, "Vertical Vibration Analysis of Vehicle – Imperfect Track Systems" *Vehicle System Dynamics* **40**(5), 2003, pp. 329–349.

74. P. Lou and Q. Y. Zeng, "Formulation of equations of motion of finite element form for vehicle–track–bridge interaction system with two types of vehicle model", *International Journal of Numerical Methods in Engineering* **62**(3), 2005, pp. 435-474.

75. P. Lou and Q. Y. Zeng, "Vertical Vehicle-Track coupling Element", *Proceedings of the Institution of Mechanical Engineers, Part F (Journal of Rail and Rapid Transit)* **220**(F3), 2006, pp. 293-304.

76. S. H. Ju, H. T. Lin, C. C. Hsueh and S. L. Wang, "A Simple Finite Element Model for Vibration Analyses Induced by Moving Vehicles", *International Journal of Numerical Methods in Engineering* **68**(12), 2006 pp. 1232-1256.

77. H. Frahm, "Device for Damped Vibration of Bodies", *US Patent No. 989958*, Oct 1909.

78. J. P. Den Hartog and J. Ormondroyd, "The Theory of the Dynamic Vibration Absorber", *Transaction of the American Society of Mechanical Engineering* **50**, 1928, pp. 9-22.

79. J. E. Brock, "A Note on the Damped Vibration Absorber", *Journal of Applied Mechanics, Transaction of the American Society of Mechanical Engineering,* **13**, 1946, p. A284.

80. J. P. Den Hartog, Mechanical Vibrations, McGraw Hill, New York, 1956 (reprinted by Dover Publications, New York 1985).

81. D. Young, "Theory of Dynamic Absorbers for beams", *Proceedings of First US National Congress of Applied Mechanics*, 1952, pp. 91-96.

82. V. H. Neubert, "Dynamic Absorbers Applied to a Bar That Has Solid Damping", *Journal of Acoustic Society of America*, **36**, 1964, pp. 673-680.

83. J. C. Snowdon, Vibration and Shock in Damped Mechanical Systems, John Wiley and Sons, New York, 1968.

84. R. G. Jacquot, "Optimal Vibration Absorbers for General beam system" *Journal of Sound and Vibration* **60**(4), 1978, pp. 535-542.

85. B. Candir, H. N. Ozguven, "Dynamic Vibration Absorbers for Reducing Resonance Amplitudes of Hysterically Damped Beams", *Proceedings of the Fourth International Model Analysis Conference*, 1986, pp. 1628-1635.

86. E. Esmailzadeh and N. Jalili, "Optimal Design of Vibration Absorbers for Structurally Damped Timoshenko Beams", *Journal of Vibration and Acoustics* **120**(4), 1998, pp. 833-841.

87. D. Younesian, E. Esmailzadeh and R. Sedaghati, "Passive Control of Vibration of Beams Subjected to Random Excitation with Peaked PSD", *Journal of Vibration and Control* **12**(9), 2006, pp. 941-953.

88. Y. Kajikawa, M. Okino, S. Uto, Y. Matsuura and J. Iseki, "Control of traffic Vibration on Urban Viaduct with Tuned Mass Dampers", *Journal of Structural Engineering (JSCE)* 35A, 1989, pp. 585-595.

89. H. C. kwon, M. C. Kim and I. W. Lee, "Vibration Control of Bridges under Moving Loads", *Journal of Computer and Structures* **66**(4),1998, pp. 473-480.

90. T. H. Chen and D. S. Chen, "Timoshenko Beam with Tuned Mass Dampers to Moving Loads", *Journal of Bridge Engineering* **9**(2), 2004, pp. 167-177.

91. J. F. Wang, C. C. Lin and B. L. Chen, "Vibration Suppression for High-speed Railway Bridges Using Tuned Massed Dampers", *International journal of Solids and Structures* **40**(24-25), 2003, pp. 456-491.

92. C. C. Lin, J. F. Wang and B. L. Chen, "Train-Induced Vibration Control of High-Speed Railway

Bridges Equipped with Multiple Tuned Mass Dampers", *Journal of Bridge Engineering* **10**(4), 2005, pp. 398-414.

93. K.J. Bathe and E. L. Wilson, Numerical Methods in Finite Element Analysis, Prentice Hall, Englewood Cliffs, N.J., 1976.

94. N. M. Newmark, "A Method of Computation for Structural Dynamics", *Journal of Engineering Mechanics (ASCE)* **85**(3), 1959, pp. 67–94.

95. C. Lanczos, The Variational Principles of Mechanics, Dover Publications, New York, N.Y., 1986.

96. K. J. Bathe, Finite Element Procedures in Engineering Analysis, Prentice Hall, Englewood Cliffs, N.J., 1982.

97. B. Yang, Stress, Strain and Structural Dynamics, Butterworth-Heinemann, Elsevier Academic Press, 2005.

98. J. Nocedal and S.J. Wright, Numerical Optimization, (2nd Edition), Springer, New York, 2006.

99. J. S. Arora, Introduction to Optimum Design, (2nd Edition) Elsevier Academic Press, San Diego, CA, 2004.

100. R. Fletcher, Practical Methods of Optimization, (2nd Edition) John Wiley & Sons, New York, 1987.

101. W. T. Cochran, J. W. Cooley, D. L. Favin, H. D. Helms and P. D. Welch, "What is the Fast Fourier Transform?", *Proceedings of IEEE* **55**(10), 1967, pp. 1664-1674.

102. C. Bingham, M. D. Godfrey and J. W. Tukey, "Modern Techniques of Power Spectrum Estimation", *IEEE Transaction on Audio and Electro Acoustics* **15**(2), 1967, pp. 56-66.

103. M. Petyt, Introduction to Finite Element Vibration Analysis, Cambridge University Press, 1990.

Appendix A

The Euler-Bernoulli Beam Finite Element Formulation [23]

In the Euler-Bernoulli beam theory, it is assumed that plane cross-sections perpendicular to the axis of the beam remain plane and perpendicular to the axis after deformation. The equation of motion of the Euler-Bernoulli beam can be defined as:

$$\rho A\frac{\partial^2 y}{\partial t^2}+\frac{\partial^2}{\partial x^2}\left(EI\frac{\partial^2 y}{\partial x^2}\right)=F(x) \qquad \text{for } 0<x<L \tag{A.1}$$

Where ρ denotes the linear density, A shows the cross-sectional area, EI is the modulus of elasticity E and the moment of inertial I of the beam, F is the transversely load, and y is the traversed deflection of the beam. The beam damping effect has been neglected.

Using the Galerkin weak formulation, in order to derive of the form of a linear Euler-Bernoulli element including two nodes with two degrees of freedom, yields

$$y^e(x)=u_1^e\varphi_1^e+u_2^e\varphi_2^e+u_3^e\varphi_3^e+u_4^e\varphi_4^e=\sum_{j=1}^{4}u_j^e\varphi_j^e \tag{A.2}$$

where u_i^e are the nodal variables of a typical beam element defined as:

$$\begin{aligned} u_1^e &= y(x_e) & u_2^e &= \left(-\frac{dy}{dx}\right)\Big|_{x=x_e} \\ u_x^e &= y(x_{e+1}) & u_4^e &= \left(-\frac{dy}{dx}\right)\Big|_{x=x_{e+1}} \end{aligned} \tag{A.3}$$

and φ_i^e denote the Hermite cubic interpolation functions as:

$$
\begin{aligned}
\varphi_1^e &= 1-3\left(\frac{x-x_e}{l}\right)^2+2\left(\frac{x-x_e}{l}\right)^3 \\
\varphi_2^e &= -(x-x_e)\left(1-\frac{x-x_e}{l}\right)^2 \\
\varphi_3^e &= 3\left(\frac{x-x_e}{l}\right)^2-2\left(\frac{x-x_e}{l}\right)^3 \\
\varphi_2^e &= -(x-x_e)\left[\left(\frac{x-x_e}{l}\right)^2-\frac{x-x_e}{l}\right]
\end{aligned}
\tag{A.4}
$$

in which x_e and x_{e+1} represent the global coordinate of first and second nodes respectively. The cubic interpolation functions in Eq. (A.4) are derived by interpolating y and its derivatives at the nodes.

The equation of motion of a beam element can be generally defined as:

$$
[M]\{\ddot{U}\}+[K]\{U\}=\{Q\}+\{f\} \tag{A.5}
$$

where

$$
\begin{aligned}
M_{ij}^e &= \int_{x_e}^{x_{e+1}} \rho A \varphi_i^e \varphi_j^e dx \\
K_{ij}^e &= \int_{x_e}^{x_{e+1}} EI \frac{d^2\varphi_i^e}{\partial x^2}\frac{d^2\varphi_j^e}{\partial x^2} dx
\end{aligned}
\tag{A.6}
$$

$\{U\}$ denotes the nodal variable vector as:

$$
\{U\}=\begin{Bmatrix} u_1^e \\ u_2^e \\ u_3^e \\ u_4^e \end{Bmatrix} \tag{A.7}
$$

and $\{Q\}$ and $\{f\}$ are the nodal and distributed force vectors respectively.